USSR

TRANSLATION

STRUCTURAL STRENGTH OF AIRCRAFT
(Prochnost' Samoleta)

STAT

By S. N. Kan

STATE PUBLISHING HOUSE FOR THE DEFENSE INDUSTRY, MOSCOW
1955

STAT

Pages 155 - 208, 217 - 264

PREPARED BY
TECHNICAL DOCUMENTS LIAISON OFFICE
MCLTD
WRIGHT-PATTERSON AIR FORCE BASE, OHIO

STAT

Table of Contents

STAT

STAT

CHAPTER VIII

THE CONTROLS

The controls* of aircraft consist of mechanisms, rockers, push-and-pull rods, etc., by which the pilot controls the rudder, ailerons, trim tabs, flaps, wing flaps, brakes, the raising and lowering of the landing gear, the propulsive units, etc.

The entire complex of aircraft controls is easily divided into two groups. The first group includes the control by ailerons, elevator, and rudder. This control is called "basic control". The second group includes the remaining controls, i.e., control of the trim tabs, wing flaps, flaps, etc. which is called "supplementary or auxiliary control".

In this way, using basic control, the pilot has the possibility of generating or eliminating the moment of the airplane relative to its three axes in space. The pilot himself is in a position to maintain or change the flight path.

Basic control, in turn, takes the form of "manual control" which is carried out by manual action and "foot control", carried out by foot action.

Hand control includes control of ailerons and elevators, and foot control covers control of the control surfaces.

The concentration of control of the ailerons and elevators in one unit, as is done in all modern aircraft, has been in effect throughout the history of aviation.

---

* According to the writings in the contemporary chapters of the widely used book by L.I.Sutugin. "Design of Aircraft Parts", Oborongiz, 1947.

STAT

This system of control was worked out by the Russian inventor, Ul'yaninyi in 1906.

To simplify control of the aircraft, the direction in which the hands and feet are moved is coordinated with the instinctive motions of man. Thus, creating a diving moment of the aircraft, the pilot instinctively strives to move his entire body forward. Therefore, his stick (column) is also moved forward, which deflects the elevator downward. This leads to the obtainment of additional lift on the horizontal tail surface; the lift produces a diving moment along the arm leading to the CG of the aircraft and reduced the angle of attack of the wing.

If it is required to bank or turn the aircraft, the pilot pushes the stick sideways or turns the control wheel. This action leads to lowering of the aileron on one wing and raising on the other wing, thus producing the necessary banking moment of the aircraft.

The action of the rudders, i.e., a turning of the aircraft relative to the vertical axis, is accomplished by leg control. If the aircraft is to turn to the right, the pilot depresses the right pedal with the foot. This causes the rudder to deflect to the right, which leads to a generation of lifting force on the vertical tail surfaces, effective toward the left. This force creates a moment relative to the vertical central axis of the aircraft, which turns the aircraft to the right.

The quality of this or any other system of control is determined primarily by the rapidity of action and ease with which the pilot is able to maneuver the aircraft relative to any spatial axis. Controls which meet these requirements will reduce pilot fatigue and give him an opportunity to devote his entire attention to fulfilling the basic mission. From the above, however, it does not follow necessarily that control of the aircraft requires only a minor effort. The pilot, carrying out basic control, must sense this control and must smoothly increase the pressure proportionally to the deflection of the control surfaces from the neutral position, in a direction opposite to that of the deflection. For this, the controls must have a tendency to return to the neutral position under the action of aerodynamic for-

STAT

The ease of control depends greatly on the friction in the control-cable hinges. In order to reduce this friction, the control mechanisms in modern aircraft are fitted with ball bearings. Friction in hinges, backlash, and deformation in the controls produce a retardation effect. This effect results in the fact that between the moment of application of pressure to the controls and the incipient deflection of the control surfaces, a certain time will elapse, a measurable part of a second. It is obvious that the occurence of this lag is harmful, especially in flight close to the ground or in flight in bumpy air.

The design of the basic controls must meet certain requirements. These demands are common to all types of aircraft and include: sufficient mechanical strength and rigidity, light weight and resistance of projecting parts in contact with the air flow, convenience of use and long life, simplicity of production and repair, etc.

Concerning specific requirements, in relation to controls, the following basic specifications should be mentioned:

1. The control rods must have such geometric dimensions that the frequency of their vibration is outside the sphere of the revolutions and even double the rpm of the propulsive unit (propeller, turbines, etc.) i.e., they must be out of the way of resonant vibrations. The determination of the frequency of free vibration of the control rods is described in Chapter XIV.

2. The design must guarantee the independence of action of the ailerons and elevators, i.e., the operation of the control stick in the longitudinal direction must not cause deflection of the ailerons and an inclination of the stick to the side must not deflect the elevators.

3. Possible deformations of the wing or the fuselage must not lead to fouling of the lines or control mechanisms.

4. The design of the foot controls must allow for the regulation of the position of the pedals at the level of the pilot.

5. The angles of inclination of the control mechanisms, the angles of inclina-

STAT

tion of the controls, the loads on the control levers and control pedals, and the ruggedness of the control lines etc. must satisfy the strength standards.

Section 31. Principal Systems of Basic Control

All modern aircraft have two accepted systems, differing only in the method of controlling the ailerons. In one system, control of the ailerons is achieved by inclination of the lever (the stick) to the sides, and in the other control systems, the ailerons are actuated by the rotation of the control wheel relative to the axis which is applied to the column. For accomplishing this, the column can be displaced only in the plane of symmetry of the aircraft.

The first as well as the second control system may be either single or dual. In the dual system there may be two sticks, two wheels, or a combination of a stick and a wheel. Often the second stick is removable so as to relieve the copilot when he is performing duties not immediately connected with piloting the aircraft.

The individual control mechanisms, levers, and tubes usually are installed underneath the pilot's seat, in order not to impede the work of the pilot in the cabin. This also protects ball bearings and hinges from damage.

The selection of the type of mechanism and distribution of control levers relative to the stick depends on the layout of the cabin and wings. In a cabin placed rearward relative to the wing, the aileron control levers are placed in front of the stick. If the cabin is located ahead of the wing, the aileron control levers and the elevator control levers are placed in back of the stick. For circumventing various obstacles, the elevator control levers sometimes are installed at the side of the fuselage as are all other control cables.

Control by the Stick

In the case of a cabin located behind the wing, the ailerons are controlled by a torque tube (1) (Fig.171a) having an axis of rotation ab with one radial and another radially resisting ball bearing. On the tube a lever (2) is mounted, to which a rod (3) for aileron control is attached. The stick (4) rotates in a longitudinal

STAT

direction relative to the axis cd and in a lateral direction, together with the tube (1), relative to the axis ab. The front of the rod (5) for elevator control is attached to the stick, and the rear to the rocker (6).

The independence of action of the rudders and ailerons is obtained by placing the upper end of the rocker (6) on the extended axis ab. On deflecting the stick sideways (for aileron control) the tube (5) describes the exterior of a cone so that the cable to the elevator (7) is not displaced in a longitudinal direction. Moving

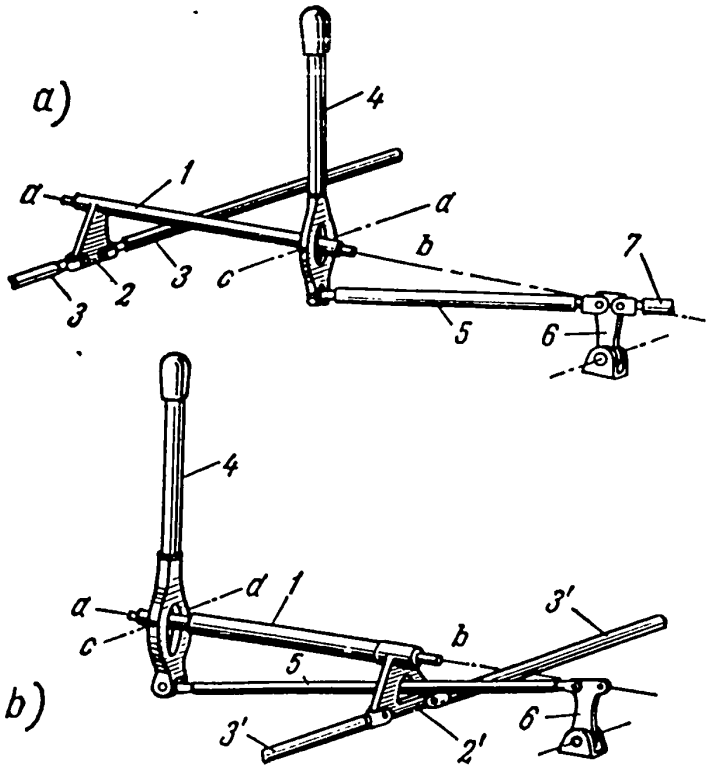

Fig.171 - Stick Control

a - Cabin located behind the wing; b - Cabin located in front of the wing

the stick only in longitudinal direction does not produce a rotation of the tube (1) so that the aileron cable does not function.

If the cabin is located in front of the wing or directly below it (Fig.171b), the aileron control lever is shifted toward the rear, behind the stick. The rod (3) to the ailerons is underneath the rod (5) going to the elevators. To ensure inde-

STAT

pendence of function of the ailerons and rudders in cabins placed far ahead of the wing, the control lever is designed in the form of a small triangle (21) with connecting hinges on the aileron control rods.

The rod (5), at the connection point with the stick (4) and the rocker (6), is provided with spherical joints or universal joints. For lower angles of deviation, double-aligning ball bearings are used.

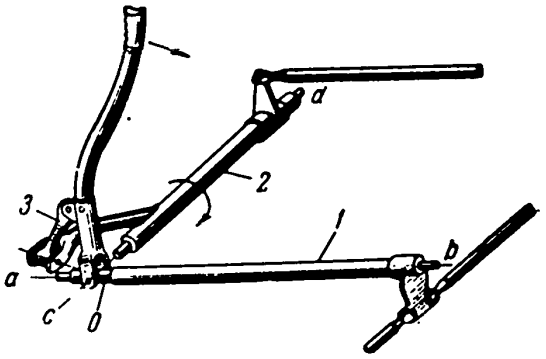

Fig.172 - Stick Control with Torque Tubes

a) To elevator; b) To aileron

In cases when the control cables to the elevators do not pass through the plane of symmetry (Fig.172), control is transmitted by means of a torque tube, for control of both ailerons (tube 1) and elevators (tube 2). Independence of action of the rudders and ailerons is achieved if the rotation of the rod (3) is laid through the axis Oa and the rotation of the rod (2) and the stick through the axis cd.

In some aircraft (Fig.173) the axes of rotation of the stick in longitudinal and lateral directions cd and ab are manipulated by elevation. In the longitudinal direction, the stick is rotated in relative to the axis cd and in a transverse direction, together with the tube (1) or the aileron control, relative to the axis ab. The bracket (2) to which the stick is mounted, compensates through the cut-out in the tube (1), for the gap in the lower end of the stick. The forward end of the tube (1) carries the lever (3) of the aileron control. The independence of action of the rudders and ailerons is achieved by placing the axis of the attachment joints of the rod (4) to the lever (5) of the elevator control, on the axis ab or on its extension.

Wheel Control

The control wheel (1) shown in Fig.1 is located on the upper part of the column

STAT

(3) and is rotatable. The wheel is rigidly coupled to the cogwheel (2) which carries a bicycle-type chain. To the chain are attached two cables (5) which, by turning the wheel and thus passing the chains over the cogwheel, actuate the rods (or cables) going to the ailerons. The column may be swung forward or backward on ball bearings

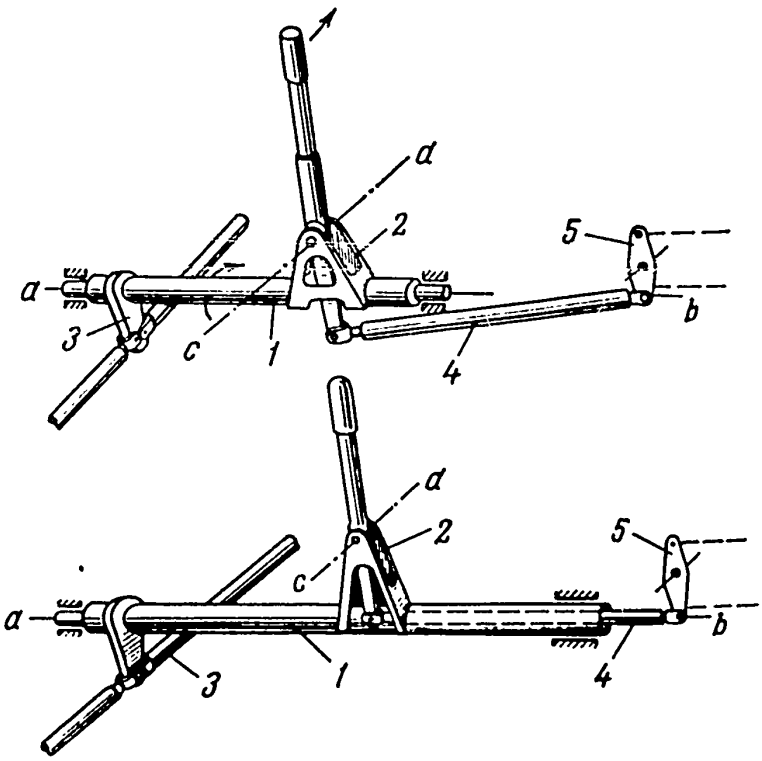

Fig.173 - Stick Control with Transmission by Raising the Axes of Rotation

(4) thus actuating the system of rods (or cables) of the elevator control.

In this mechanism, full independence of action of the rudder and ailerons is maintained.

Foot Control

The basic elements of foot control are pedals and mechanisms, which connect with the rudder control cables.

The dimensions of the pedals are determined by convenience of foot placement, these dimensions usually being about 140 mm width and 280 mm length.

STAT

The feet of the pilot move together with the pedals, through which action forces are exerted both in the horizontal and vertical planes. For ease in operating the pedals, the distance between them must be minimal. In different aircraft, this spacing varies between 250 and 500 mm and is determined by the type of manual controls and the design of the pedal mechanisms.

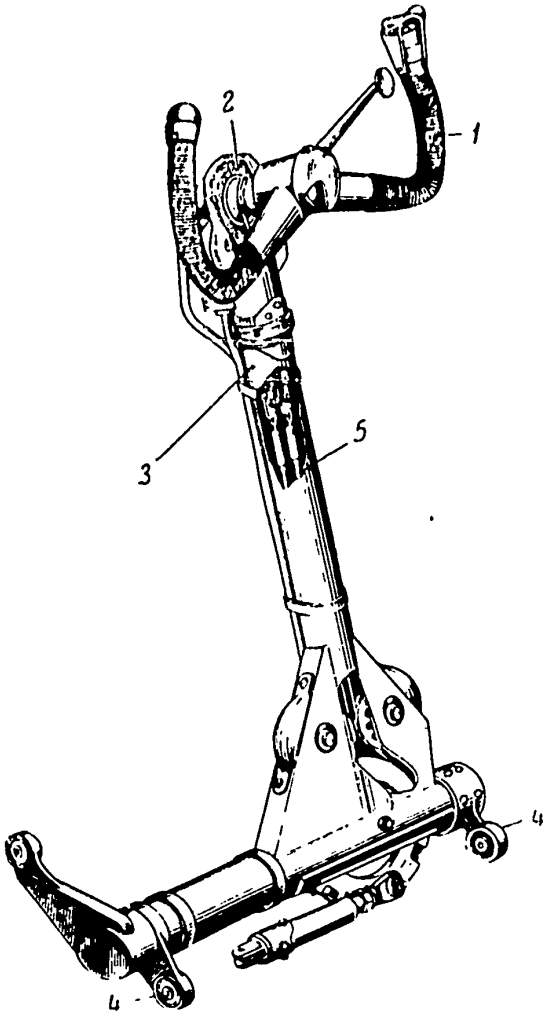

Fig.174 - Wheel Control

Displacement of the pedals in the horizontal plane is achieved by means of a hinged parallelogram (Fig.175) or by linear float guides (Fig.176).

The hinged parallelogram is simple in design. It consists of two cross bars (1) and (2) which are attached over hinges (Fig.175) to the longitudinal elements (3). This hinge mechanism is actuated over the pedals (4), attached to the longitudinal elements (3).

The pedals can be regulated underneath the pilot's seat.

The fixed points of the entire mechanism are the hinges (5) and (6) and the cross bars (1) and (2).

To the cross bar (1), the bracket (7) is welded. To this a sectional cable guide (8) is mounted, for controlling the rudders. The strap (9) serves for attaching the feet of the pilot to the pedals.

Because of the design of the front sections of the hinged parallelogram, the pedals are shifted gradually without turning. This in itself facilitates the control and prevents the feet of the pilot from slipping off the pedals.

STAT

The design of the linear float guides (Fig.176) for progressive shifting of the pedals can be obtained by the following system: The pedals are attached to the bracket (1) and, by means of the adjusting sliders (2), can be shifted freely along the

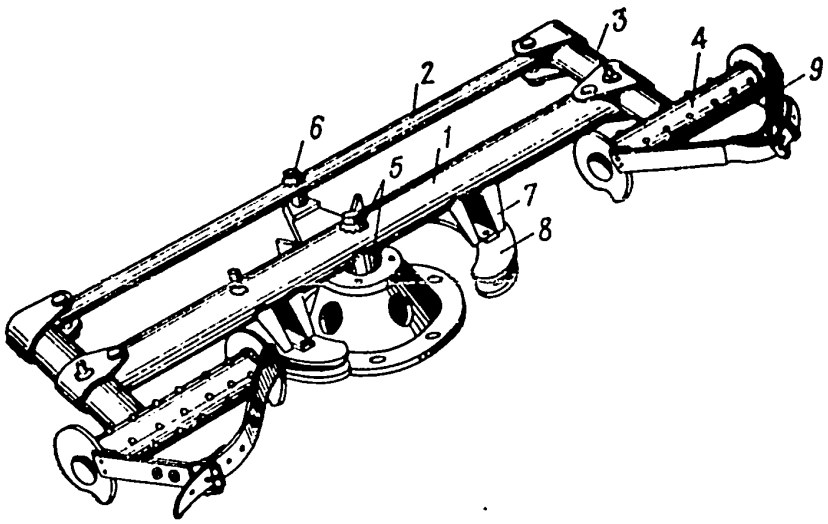

Fig.175 - Foot Control over a Hinged Parallelogram

linear guides (3). The pedals, over the bracket (1) and the sliders (2) connected with the cable (4), control the deflection of the control surfaces. The sliders (2) are interconnected by the cable (5) over the pulley (6) to achieve an integral cable line.

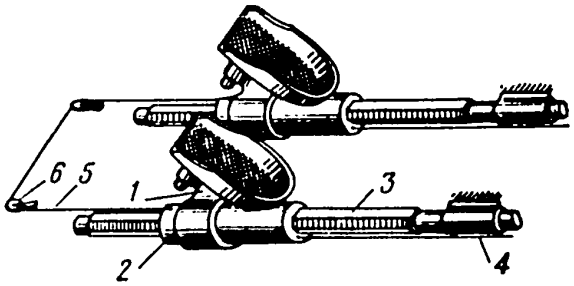

Fig.176 - Foot Control by Linear Float Guides

The displacement of the pedals in the vertical plane is usually accomplished with the help of rocking levers. In this, the pedals attached to the levers describe an arc of a circle, which changes their inclination. In some aircraft, the pedals are connected to hinges or joints forming a sort of parallelogram, which permits a displacement of the pedals without changing their inclination.

Figure 177 shows a system of lever attachment to the upper and lower grouping

STAT

of the pedals. Here, the pedals are hinged to the levers, which are able to rock relative to the fixed axis ab. Tne motion of the pedals is further transmitted over the sector (1) to the cable (2). The sector (1) is connected to the cable (3) over the pulley (4).

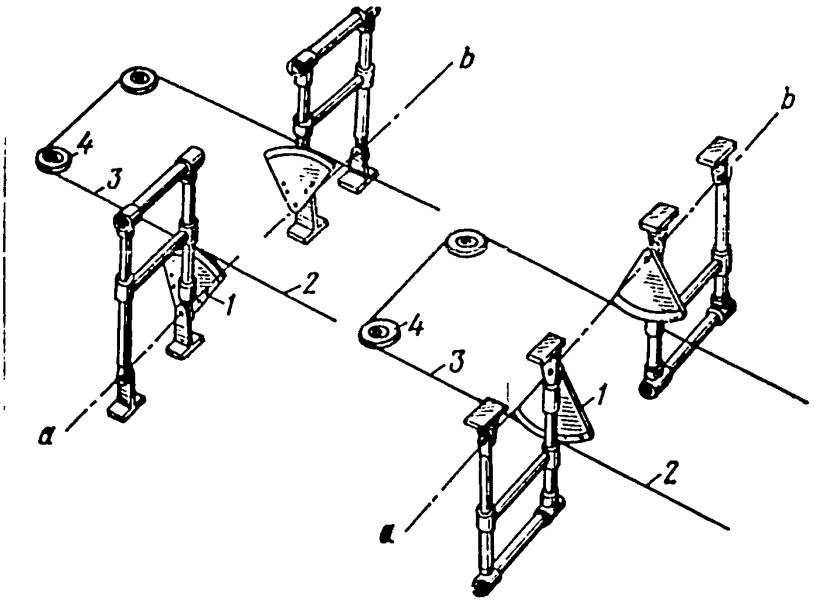

Fig.177 - Foot Control with Levers, Swinging in a Vertical Plane

Section 32. The Principal Systems of Control Cables

The cables of both hand control and foot control may be rigid, flexible, or mixed. In rigid control cables, the forces are transmitted by means of tubes which work by extension and contraction. Flexible control lines consist of cables, wires, or belts which transmit forces only by extension. Finally, mixed control lines comprise portions of both rigid and flexible types.

The rigid cables (tubes) have the following advantages: Tubes, working with little stress under compression, deform less and for that reason are more advantageous; in addition, they do not contribute to the generation of self-oscillations (flutter) of the wing or tail group (see Chapter XIV). Here, friction in the control lines can be reduced to a minimum by having all joints work on ball bearings, which in addition prevent backlash. Rigid control lines result in longer life of the c

With respect to elevator control, separate rods located in the wing can be used with the possibility of controlling the aircraft by only one aileron.

In listing the drawbacks of rigid control cables, the difficulty of "by-passing" equipment, complexity of design due to the great number of joints, and excessive weight of the entire control system. In addition, it is of importance that no resonance of the tubes with the power plant occurs.

Flexible control lines, due to their design, have small dimensions, light weight, and readily permit "by-passing" installations.

One drawback of flexible control lines to be mentioned is a low mechanical strength, leading to deformations of the cables which are harmful since they may generate self-oscillations (flutter) of the wing or tail unit. In actual operation, despite the fact that they are pre-stretched when being installed, flexible control lines are less long-lived, and considerable friction occurs in the transmission. Because of their constant bending on the pulleys, the cables wear out rapidly.

The possible systems of transmission of manual stick control are presented in Fig.178. The control stick (1) (Fig.178a) in its function as a fixed point has a horizontal joint (3) attached to the fork of the horizontal tube (2). This tube (2) is supported by the radial bearing (4) and by the radial thrust bearing (5). Pushing the stick (1) forward and rotating the tube (2) actuates the aileron control levers (6). Through this action the elevators remain in neutral, so that the upper joint of the first rocker (11) coincides with the longitudinal axis of the tube (2).

Consequently, pushing the stick (1) forward causes the rod (7) to describe a cone and the elevator to remain stationary. Deflection of the elevator is achieved by pushing the stick (1) toward or away from the pilot. This produces a displacement of the lower end of the stick either forward or backward and causes a displacement of the rods (7), (8), (9), and (10) or (10') as well as of the lever (14) attached directly to the elevator. These rods rest on the rockers (11), (12), and (13). In presence of the control lever (14) below the rudder (dotted lines) the

STAT

rocket (13) is replaced by an intermediate double-arm lever (15) in the control system.

In some instances of control transmission, the rocker (Fig.178b) is replaced by guides (11). When using guides, the transmission system has less clearance.

The deflection of the ailerons (Fig.178c), as shown above, is achieved by pushing the control stick (6) forward together with the rods (17), (18), (19), and (20)

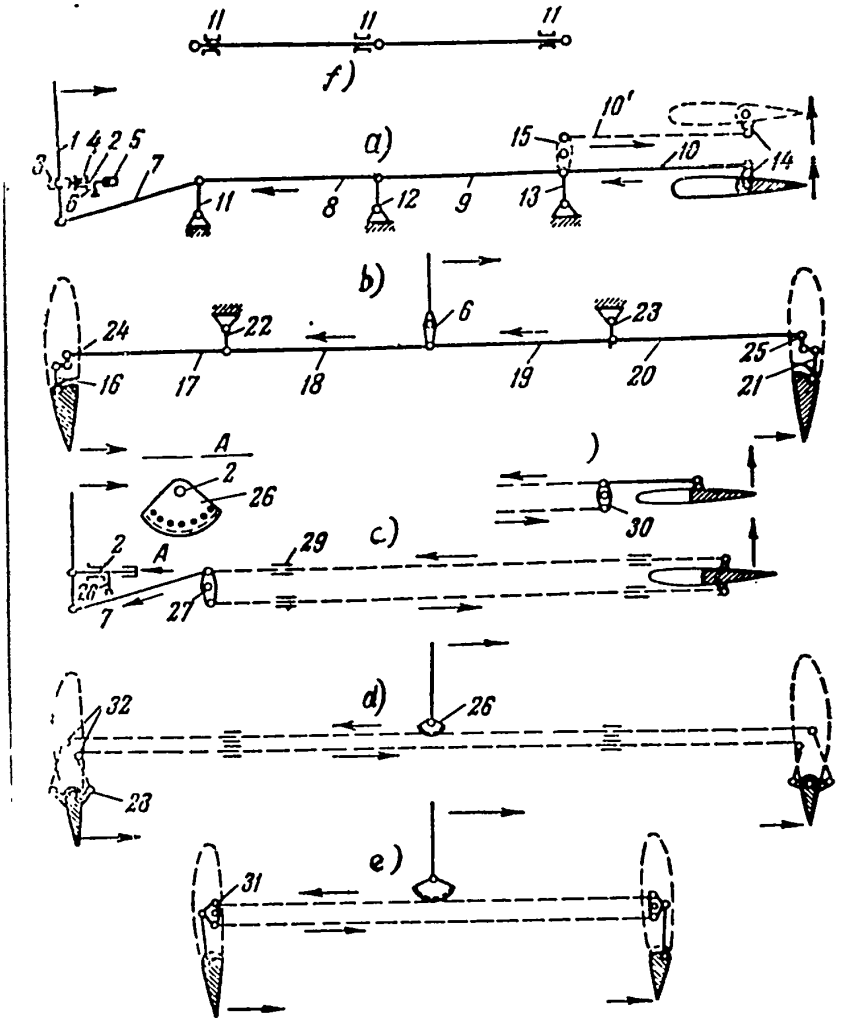

Fig.178 - Control Lines for Manual Stick Control

which rest on the rockers (22) and (23). The forward shift of the rods causes rotation of the double-arm levers (24) and (25) which are connected to the rods (16) and (21) which, in turn, are directly attached to the ailerons.

STAT

The above is a consideration of the system with rigid controls. If the controls are flexible (Fig.178d), the rod (7) is mounted to the double-arm lever (27), to which cables, lines or, belts going to the elevators are attached. These are supported along their length by guides (29). Turning the control lines is done with the help of the pulleys (32) (Fig.178c) but only in the case of cables. For deflecting

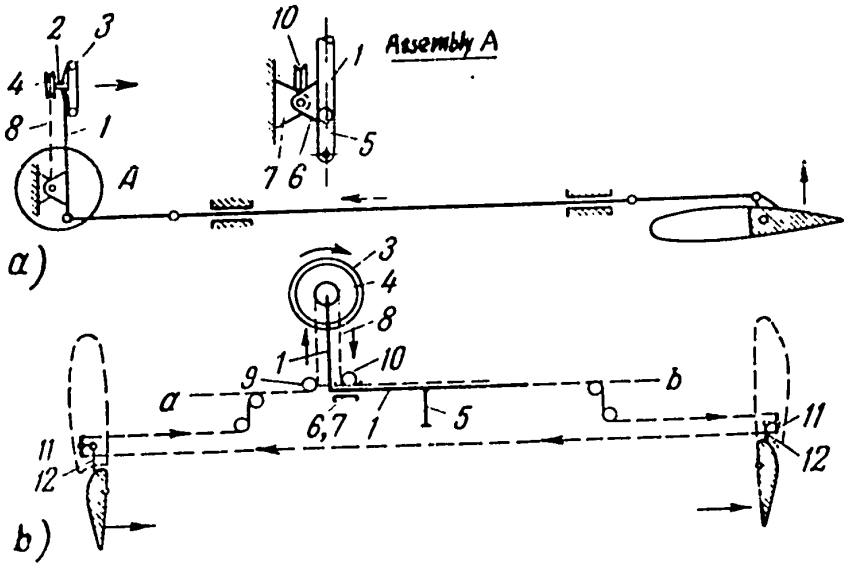

Fig.179 - Control Cables for Manual Wheel Control

the ailerons (Fig.178c), the sector (26) is used instead of the lever (6). Since the cables in flexible control lines work only by traction, double-arm levers (27) and (28), forming a locking chain, are attached to the elevators (Fig.178d) and the ailerons (Fig.178f). In Figs.178e and 178g, a mixed system of control lines is shown. In this, auxiliary elements are the double-arm lever (30) and the triple-arm lever (31).

Control cables controlled by a wheel considerably reduce the stress on the ailerons, thus increasing the rpm of the wheel. In this case, full deflection of the ailerons requires more time than does stick control. For this reason, wheel control is not used in manuvering aircraft. The advantage of this type of control lies only in the transfer of stress from the wheel to the aileron control cables. The

STAT

central control mechanism (Fig.179a and b) consists of an articulated tube (1) to which the wheel (3) and the cogwheel (4) rotating relative to the axis (2) are attached. Control of the elevators is carried out by the lever (5) attached to the horizontal part of the tube (1). The tube (1) can be turned only relative to the joints attached to the brackets (6) with the brackets (7). Aileron control here is also carried out by cables attached to the column by a chain (8) placed over the cogwheel. Turning the wheel (3) rotates the cogwheel (4), thus actuating the cable which, over a system of pulleys (9) and (10) (Fig.179b), goes to the ailerons. The

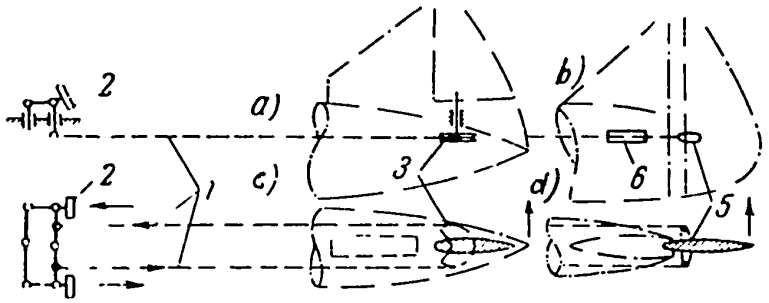

Fig.180 - Foot Control Cables of the Hinged Parallelogram Varient

a - From the side; b - From above

pulleys (9) and (10) is so arranged that the cables pass through them along the axis ab, which is the pivot of the column. This ensures independence of action of the rudders and ailerons. The three-arm lever (11) ensures the transmission of stresses from the cables to the rods (12) which are directly attached to the ailerons.

The control cables of the foot control can be rigid, flexible, or mixed. Flexible and mixed cables are more common since they have less weight, require less space, and permit easier installation and fitting. As described earlier, the pedals of the centrol foot-control mechanism may be in the form of a horizontal parallelogram (Fig.180) or may be displaced forward (Fig.181) along guides (2). In the first instance, for reducing the load on the feet, the cables (1) (Fig.180) are attached less to the lever arms than to the pedals (2). The rudder control cables are con-

STAT

nected directly to the two levers (5) (Fig.180b,d) or to the sector (3) (Fig.180a,b), independent of the position of the rudder with respect to the fuselage.

In the second variant, the pedals (Fig.181) are connected to a lug (5) over a cable (3) which turns on pulleys (4). Direct control of the rudder is achieved over the double-arm rocker (8), which is turned by the cables (7). The levers (10) of the rudder control are connected to the rocker (8) by rods. The kinematics of the rudder control are satisfied by only one rod (9).

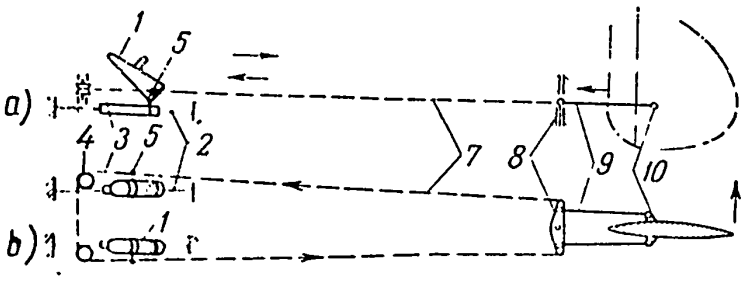

Fig.181 - Foot Control Cables of the Guide Variant

Section 33. Hydraulic Aids

Hydraulic aids or boosters take the form of special mechanisms which relieve the pilot from excessive burdens of control. However, this does not eliminate the feeling of controlling the aircraft.

The necessity of hydraulic boosters in aircraft control systems is explained in the following. Through the control elements, the pilot controls the hinge moment of the rudders (ailerons) M_h which is well defined by the equation

$$M_h = c_h S_p \frac{V^2}{2} b_p$$

where c_h = coefficient of hinge moment of the rudder or aileron;

s_p = area of the rudder surface;

STAT

p = air density;

v = flying speed;

b_p = chord of the rudder or aileron.

At low speeds, the hinge moment Mh is lowered by changing the coefficient c_h by producing aerodynamic balance of the rudders or ailerons (cf. Section 18). For example, in axial aerodynamic balance, the hinge moment is reduced by displacing the axis of rotation of the rudder along the chord backward, nearer to the center of pressure. In heavier aircraft (increased S_p and b_p) and in high-speed aircraft (increased V), it is impossible to facilitate control by aerodynamic compensation since undesirable overcompensation might occur. In addition, in flights approaching the speed of sound, a sharp increase in the hinge moment might take place, due to significant change in the position of pressure of the control surfaces.

Hydraulic boosters in the control system permit meeting the requirements for sensing and control at times when the pilot has to apply only slight pressure to the controls.

Such boosters also make it possible to eliminate aerodynamic compensation, including internal compensation, which is very important for high-speed airplanes with thin airfoils.

It should be mentioned that hydraulic boosters also act as dampers for quenching oscillations generated by rudder flutter.

In modern aircraft, an attempt is made to place the hydraulic boosters as near the rudders and ailerons as possible so that the greater part of the control cables can be relieved. This leads to a lowering of structural weight and a decrease in friction on the joints and pulleys of the control lines. To ensure independence of function of the controls a self-supporting hydraulic system is usually installed. The hydraulic boosters are applied easily and quickly according to the wishes of the pilot, resulting in direct control of the aircraft. The presence of hydraulic boosters does not disrupt control and does not cause a lag in the deflection of the rud-

STAT

ders, which is done by the stick.

Hydraulic boosters of two types exist: reversible and nonreversible.

In the reversible system of hydraulic boosters, the deflection of the control surfaces, basically, is produced by the hydro-system; a small portion (from 1/30 to 1/6) is accomplished with the help of pilot's forces which constitute the constant percentage of the full necessary stress. The more common tractive forces for rudder deflection and the portion contributed by the pilot, can be coupled by means of levers or special pistons of the hydraulic system. In the first case a hydro-system with mechanical coupling and in the second case one with hydraulic coupling is involved.

The nonreversible system of hydraulic boosters is characterized by the fact that the entire hinge moment is compensated by the hydro-system. Here, the sensing of control is ensured by a spring, whose tension increases on deflection of the stick. Hence, independently of the flying speed, the pilot must apply the same pressure to the control stick, which can change only with respect to the angle of deflection of the rudder.

Booster Diagrams

The principal diagram of a reversible hydraulic booster system with hydraulic coupling is shown in Fig.182. The control system includes: the slide valve (3), the booster (4), induction pipe and exhaust manifold, and the piping (9) and (10) with the cock (11).

The diagram shows the system in the neutral position, when the fluid from the induction pipe flows back freely to the tank through the central groove in the center piston of the slide valve, the piping (10), and the exhaust manifold.

In the working position, for example, while pushing the control stick (1) (forward), three slide-valve pistons, rigidly interconnected, are shifted forward with the help of the control rod (2). This causes displacement of the fluid from the induction pipe through the piping (9) and the cock (11) into the right half STAT

the booster cylinder (4) and into the left part of the cock of the slide-valve cylinder (3). By this action, the pipe (12), over the slide valve, connects the

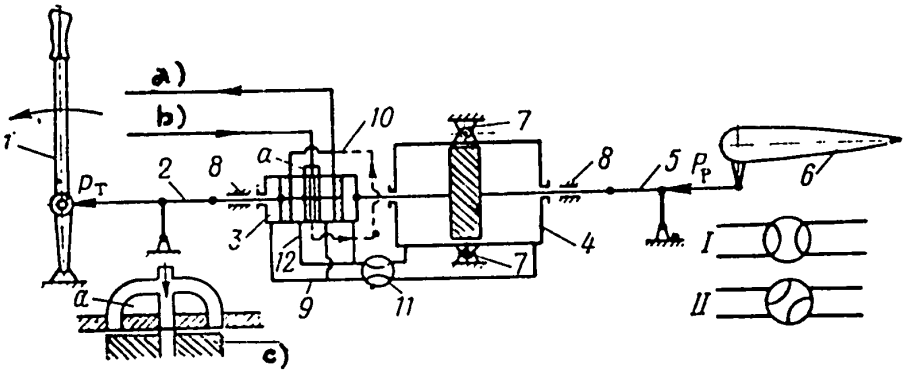

Fig.182 - Reversible Hydraulic Booster System, with Hydraulic Connection

a) Exhaust; b) Induction pipe; c) Center piston of valve

left part of the booster cylinder with the exhaust manifold. Consequently, the force P_p transmitted through the rod (5) to the control surface (6) will produce pressure to the right on the booster piston (4) and pressure to the left on the cylinder bottom of the slide valve.

$$P_p = p(S_y + S_z), \tag{87}$$

where p is the pressure of the fluid into the induction pipe, in kg/cm^2;

S_y is the area of the booster cylinder;

S_z is the area of the slide valve.

The control rod (2), tightly connected with the slide-valve cylinder (3), will measure the force of pressure on the left cylinder.

$$P_T = pS_z. \tag{88}$$

On dividing the left and right-hand sides of eqs.(87) and (88), the following relationship is obtained.

STAT

$$\frac{P_p}{P_T} = \frac{S_y + S_z}{S_z}, \qquad (89)$$

which shows that the greater the force exerted on the rod P_p the greater will be the force P_T on the hydraulic booster.

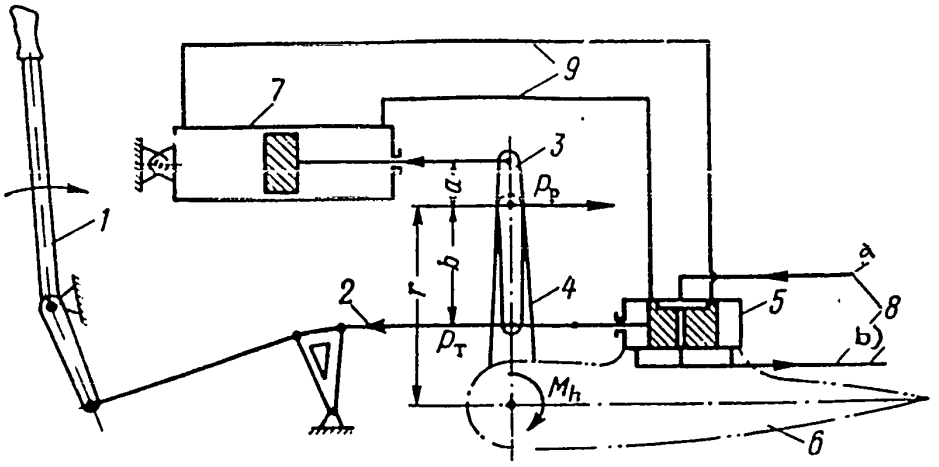

Fig.183 - Reversible System of Hydraulic Booster, with Mechanical Connections

a) Induction pipe; b) Exhaust

The force exerted on the control rod P_p overcomes the hinge moment of the control surface, deflecting the latter through some angle. This deflection ceases as soon as the control stick is shifted.

In the same way, the actuation of the rod (2) and the slide-valve piston (3) is stopped. The booster cylinder (4), actuating the slide-valve cylinder, closes the induction pipe and thus stops the boosting.

By turning the cock (11) to the position (I), it is possible to control the rudder without boosting. By turning the cock to position (II) it can be used for locking the control surfaces, thereby preventing displacement of the booster piston (4).

The slide-valve piston (3) and the booster piston (4) are connected by rods which slide along the guides (8).

STAT

The booster cylinder (4) is rigidly attached by means of bolts (7).

Figure 183 presents the reversible system of hydraulic boosters with mechanical connections. The auxiliary elements here are: the double-arm rocker (3), the hinge attachment to the control lever (4) of the servorudder, the slide valve (5), the cylinder which is rigidly attached to the rudder (6), the booster (7), the cylinder which is hinged to the body of the aircraft, the pipeline system (9) and the induction and exhaust pipes of the hydraulic-booster system (8) with flexible hose. The hydraulic-booster system is illustrated in the neutral position, in which the fluid from the induction pipe flows freely back into the tank through the central groove of the slide-valve piston and the exhaust manifolds.

In the working position, for example, on pulling the control stick (backward), the control rod (2) displaces the slide-valve piston (5) to the left. By this, the exhaust line is separated from the induction lines and the latter will dispense fluid under pressure into the right part of the booster cylinder (7) which causes its piston to be displaced to the left. The fluid from the left part of the booster cylinder will flow freely into the exhaust manifold through the pipe (9) and the slide valve (5).

From the condition of equilibrium of the double-arm rocker (3) with the arms (a) and (b) it follows that

$$\frac{P_p}{P_T} = \frac{b + a}{a}. \qquad (90)$$

Consequently: $P_p = P_T \frac{b + a}{a}$ and $P_T = P_p \frac{a}{b + a}$.

If the pilot stops pulling the stick, the slide-valve piston (5) will become stationary and its cylinder, connected rigidly with the rudders, will shift to the left and thus disconnect the induction pipe from the booster cylinder (7).

A consideration of the system of hydraulic boosters with mechanical connection shows that it starts operating immediately, without jars, and has several advantages

STAT

over a system of hydraulic boosters with hydraulic connections. One of these is the relative ease of changing the arms of the double-arm rocker (3), giving the possibility of changing the ratio (90). In the latter system (Fig.183), friction on the booster cylinder (7) does not influence the force P_T on the control lines. Besides this, in operation of the aircraft, less rigid requirements as to tightening of the slide valve (5) are possible.

The systems of nonreversible hydraulic boosters are shown in Figs.184 and 185, resembling the systems shown in Figs.182 and 183. In Fig.184, a displacement of the stick (1) causes a displacement of the rod (2) and of the pistons of the slide valve (3). As a result of this, the fluid from the induction pipe flows into the booster cylinder (4) through the pipe (9) and the cock (11) where (in the booster cylinder) the force P_p from the piston is exerted on the rod (5) going to the rudder. At this time, the other cavity of the booster cylinder, through the cock (11), the pipe (9) and the slide valve, connects with the exhaust manifold. The coordination of deflection of the rudder (6) by working the stick (1) is achieved by connection of the booster cylinder (4) with the cylinder of the slide valve (3).

The pilot senses the force P_p exerted on the control stick by the springs (10).

The piston rods of the slide valve (3) and the booster cylinder (4) slide along the guides (8).

The booster (4) is connected to the body of the aircraft by bolts (7).

A study of this system shows that shifting into the neutral position is accomplished by moving the control stick (1). In the same way, if the stick (1) is moved, the springs (10) will tend to bring it into a neutral position. This will be accompanied by a displacement of the slide-valve piston (3), and the fluid from the corresponding part of the booster cylinder will flow into the exhaust manifold.

In the system pictured in Fig.185, moving the stick (1) causes displacement of the rod (2) and of the pistons of the slide valve (5). This causes the fluid from the induction pipe to pass along the pipe (9) into the booster cylinder (7) where

STAT

pressure by the piston P_p is transferred to the control rods (4). At this time, the other cavity of the booster cylinder, through the pipe (9) and the cylinder of the

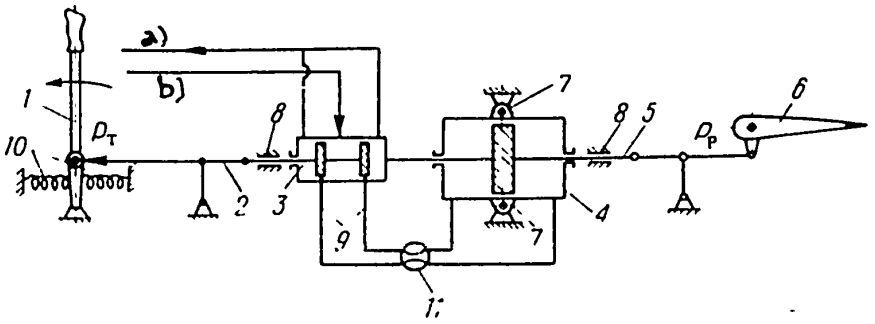

Fig.184 - Nonreversible System of Hydraulic Booster, with Hydraulic Connection

a) Exhause; b) Induction pipe

slide valve (5), is connected with the exhaust manifold (8).

On the rod (2), leading to the slide-valve piston (5), no force or sensing by means of the springs (3) is present. Here, as in the system in Fig.184, return to

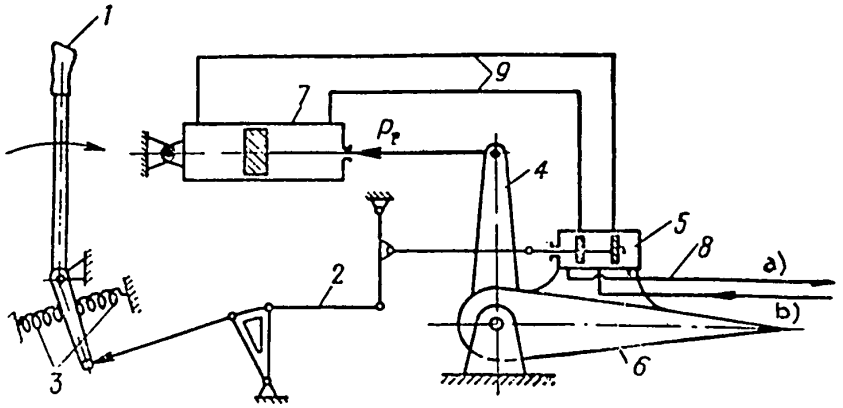

Fig.185 - Nonreversible System of Hydraulic Booster, with Mechanical Connection

a) Exhaust; b) Induction pipe

the neutral position is ensured by moving the control stick (1) and also by the presence of proportionality of the travel of the stick with the angle of deflection of the rudder (6).

STAT

CHAPTER IX

THE FUSELAGE

The fuselage is usually the base of support for many parts of the airplane: the wing, the tail group, the engine nacelle, and the landing gear. Besides this,

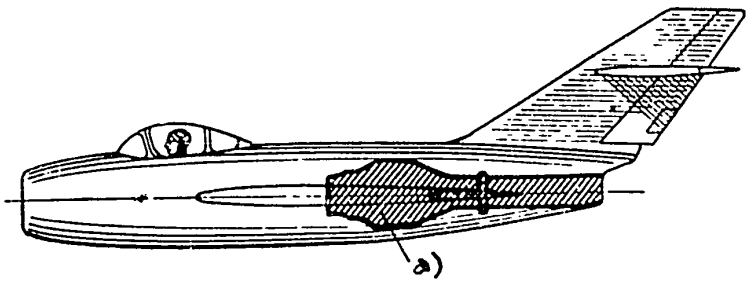

Fig.186 - Fuselage with Internal Power Plant

The construction is extended and thus absorbs the fuselage loading

a) Engine

the fuselage houses the crew, the fuel, armament, the power plant, equipment, and other loads. Hence, the exterior loads of the fuselage are determined primarily by the forces of mass action of parts within it and by the forces exerted by the individual parts of the airplane.

From an aerodynamic point of view, the fuselage is the parasite part of the airplane, since it does not accomplish a lifting force and actually produces drag. For this reason, the overall size of the fuselage must be minimal and its form streamlined. In smaller machines, the overall size of the fuselage is determined by

STAT

the size of the engine, the dimensions of the cabin, or the bulk of the armament. In larger machines, the overall size of the fuselage is determined by the dimensions of the cargo space, and the crew quarters. Practically speaking, the range of transverse dimensions is 1 - 3 m or larger.

The installation of jet engines in the fuselage outside of its body raises the question: should the engine be located within the power system of the fuselage (Fig.186) or outside it (Fig.187). In the first instance, the fuselage is more satisfactory from an aerodynamic and mechanical strength viewpoint. The rationality of arrangement within the power system is demonstrated by the fact that, in the power system in Fig.186, the structure of the fuselage is larger in cross section and, for that reason, better absorbs the external loads.

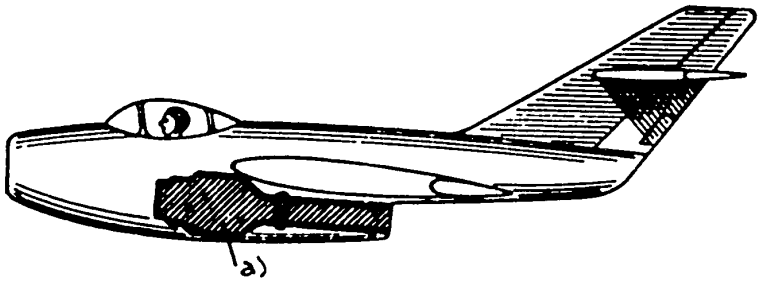

Fig.187 - Fuselage with Engine Outside the Power System

The structure is less extended and therefore less favorably absorbs the fuselage loading

a) Engine

The length of the tail section of the fuselage is determined by the necessarily great distance from the center of gravity of the airplane to the tail assembly for insurance of sufficient stability and control of the airplane. This length fluctuates within the limits of 2.5 to 3.2 lengths of the mean chord of the wing.

The presence of a landing gear with a nose wheel requires lengthening of the nose section of the fuselage.

Fuselages of high-speed airplanes are characterized by rounded cross sections.

Fuselages of jet aircraft have less free space. Consequently, because of the decreased size of the wings, the fuel usually is placed in the fuselage. The fuel capacity of jet aircraft is greater than that of piston-engine airplanes. In addition, on single-engine airplanes the engine is placed within the fuselage, taking up a considerable portion of the available space. The air scoops greatly influence the form and design of the fuselage. All this leads to the fact that on jet aircraft there is less free space within the fuselage.

Section 34. External Loads of the Fuselage

Stresses produced by parts riveted to the fuselage (wings, tail section, power plant) form the basic active loads of the fuselage. Besides this, the fuselage is loaded by stresses exerted by the cargo and various units placed within it and by the weight of its own structure.

The external loads of the fuselage, according to size, placement, and distribution, are determined by the basic existing norms of stability. The stability norms demand reliability of the fuselage in all types of flight and in all landing situations.

The computable cases of the fuselage are denoted as follows.

$$A_f,\ A'_f,\ B_f,\ C_f,\ D_f,\ E_f,\ H^z_f,\ H^n_f.$$

These cases can be subdivided into two groups: symmetric and asymmetric loads.

The first six instances are already familiar (see Section 7. "Norms of Stability") and belong to the group of symmetric loads, which are loads placed symmetrically with respect to the surfaces of symmetry of the fuselage. The group of asymmetric loads includes H^z_f and H^p_f (Fig.188).

The case H^n_f represents the transverse stress on the nose section of the fuselage, due to loads placed within it (Fig.188a).

The case H^z_f represents the transverse stress on the tail section of the fuselage, due to loads of the vertical tail surfaces (Fig.188b). STAT

In the general case of calculating the fuselage it is well to take into consideration all forces coming in contact with it, i.e., the entirety of its equilibrium, which is much too complicated. For simplification, it is possible, with a sufficient degree of accuracy, to calculate the fuselage in accordance with its parts, dividing it into tail, nose, and center section (Fig.189).

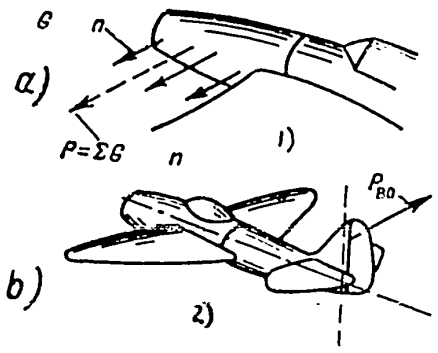

Fig.188 - Case of Asymmetric Load of the Fuselage

a- Case H_f^n corresponds to the situation when the nose section of the fuselage, under the effect of the force of inertia of the mass, turns sideways. b- Case H_f^z corresponds to the situation when the vertical tail surfaces are deflected sideways by the load $P_{v.t.}$

1) Case H_f^n; 2) Case H_f^z

Such a division of the fuselage is permissible since many computable cases can be calculated only for individual parts of the fuselage. For example, the case C_f - nose dive - is related only to the tail section. In the given instance, the internal load of the fuselage will be a load exerted only by the horizontal tail surfaces. Consequently, the tail section of the fuselage will work as a cantilever beam in bending.

The case H_f^z (see Fig.188a) also refers to the tail section of the fuselage which, in this instance, works in bending and torsion as a cantilever beam.

The case H_f^n is concerned only with the nose section of the fuselage, which in this instance works in bending as a cantilever beam.

The cases A_f, A_f', and E_f refer to the entire fuselage.

The fuselage as a whole must be considered as a double-support beam. The attachment bolts of the wing to the fuselage represent the supports.

Under symmetric load, the fuselage works in bending, and under asymmetric load in bending and torsion.

STAT

The given data for determining the normal σ and the tangent τ of stress are freehand curves of the lateral force Q, the bending moment M_b, and the torsion moment M_t. With the help of the curve, we may determine the stresses of a section of the fuselage and the magnitude of Q, M_b, and M_t of any section.

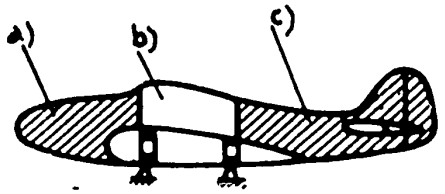

Fig.189 - Subdivisions of the Fuselage

For convenience in calculating the fuselage, it is subdivided into three parts: nose, center, and tail sections.

a) Nose section; b) Center section;

c) Tail section

In this way, for the calculation it is necessary not only to determine the external loads but also to establish a reference curve of the lateral forces as well as of the bending and torsion moments for all computable cases, in order to define these computable cases and to determine which sections may be most endangered. If we are interested in the stability of only one section of the fuselage, there is no need for a reference curve and it is sufficient to compute Q, M_b, and M_t only for that section.

As an example, we will discuss the character of the reference curve for several calculable cases.

Case C_f. In this case, it is necessary to calculate the fuselage according to the load of the horizontal tail surfaces (Fig.190) which begins with a dive of the aircraft [see eq.(83)]:

$$P_{h.t} = \frac{m_z S_t \frac{V^2_{dive}}{2}}{L_{h.t}} \qquad (91)$$

We may establish the reference curves Q and M_b as for the usual double-support cantilever beam.

Case H^z_f. Here the fuselage is calculated according to the load of the vertical tail surfaces $P_{B.O.}$ (Fig.191). The load is often ascertained by calculation.

STAT

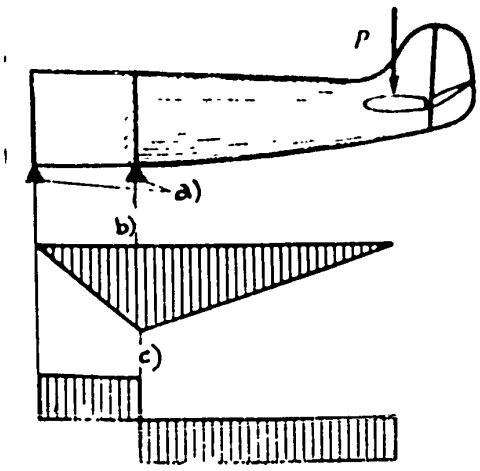

Fig.190 - Case C_f Airplane in a Dive

a) Attachment of center panel to fuselage; b) Reference curve M_b; c) Reference curve Q

In carrying out the dive, the airplane is calculated, in relation to the tail section of the fuselage, from the load of the horizontal tail surfaces $P_{h.t.}$ The tail section of the fuselage is a beam, working on the fixtures of the center panel to the fuselage.

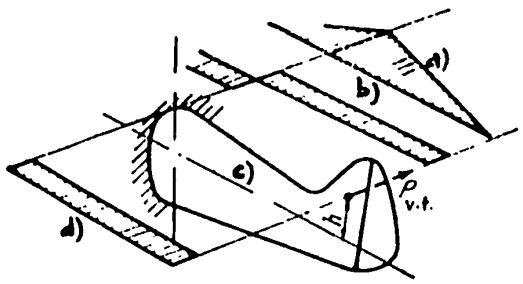

Fig.191 - Work of the Fuselage in the Case H_f^z

a) Reference curve M_b; b) Reference curve Q; c) Axis of fuselage; d) Reference curve M_t

In this case, the tail section of the fuselage will work in bending and torsion. The magnitude of the bending moment for the fuselage section is determined by generation of the force $P_{v.t.}$ over the observed section to the force $P_{v.t.}$ along the axis of the fuselage. The magnitude of the torsion moment is produced by the force along the longitudinal axis of the airplane.

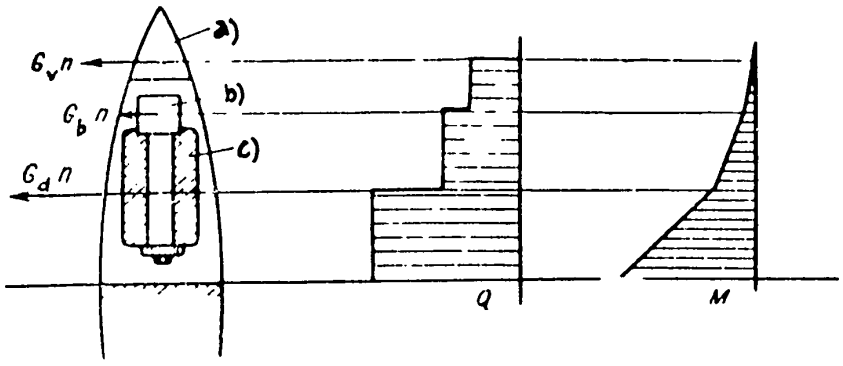

Fig.192 - Work of the Fuselage in the Case H_f^n

a) Propeller; b) Tank; c) Engine; d) Reference curve Q; e) Reference curve M_b

Here it is necessary to calculate only the nose section of the fuselage in bending, from the concentrated stress which are equally produced by the weight of each unit (engine, propeller, etc.) to the load factor n.

STAT

determined according to eq.(85):

$$P_{v.t} = 0.37 \frac{V_{max}^2}{2} S_{v.t} \qquad (92)$$

where V_{max} is the maximum speed of the airplane;

$S_{v.t.}$ is the area of the vertical tail surfaces.

In the case H_f^z, the fuselage works in bending and torsion. The torsion is produced by the activation of the upper axes of the fuselage.

Case H_f^n. As noted above, the case H_p^n is related to the nose section of the fuselage (Fig.192). Here, the nose section of the fuselage is calculated in bending as a cantilever beam from the line of the concentrated inertia force $G_{agr}n$.

Section 35. Fuselage Design

From a consideration of the action on the fuselage by loads we see that the fuselage works in bending and torsion. The design of the fuselage must be considered in relation to these deformations.

Depending on the type of power system, fuselages are of the truss type or girder type. As to the material used in construction, mostly metal and less often wood is used.

Truss-type fuselages, in turn, are divided into: rigid types, consisting of truss elements capable of either expansion or contraction; and braced types, in which the rigid diagonal rods are substituted by a pair of bracing struts capable of handling only expanding loads. Besides this, there are truss-type fuselages in which the nose and center sections consist of a rigid rod framework and the tail section of a braced framework.

Girder-type fuselages have longitudinal (longerons, stringers) and transverse framing (transverse trusses or bulkheads). The entire body is covered by a skin.

The Truss-Type Fuselage

The truss-type fuselage (Fig.193) consists of a system of rods differing

STAT

usually from the ideal spatial truss in that the connections at many angles are not hinged but fixed.

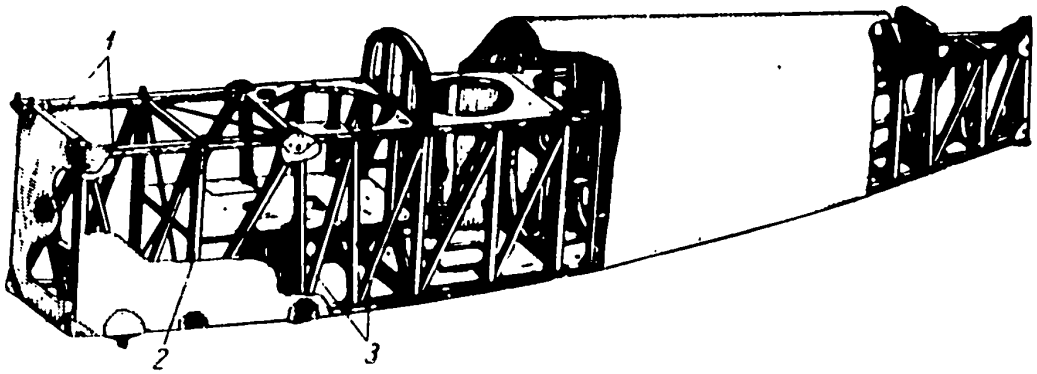

Fig.193 - Design of the Truss-Type Fuselage

The truss-type fuselage consists of a three-dimensional system made up of rigidly interconnected rods.

1- Longerons; 2- Strut; 3- Diagonal Brace

The spatial truss of the fuselage consists of four plane trusses, two horizontal and two vertical. Each two-dimensional truss consists of two booms joined to each other by struts and diagonal braces*.

In addition to the four flat trusses mentioned above, within the fuselage there are cross-wise connections. In Fig.193 there is shown a section of the fuselage whose elements consist mostly of fixed rods. The individual transverse connections may also be trusses or frames. In the case of truss connection, instead of one rigid diagonal, two boom braces or wires are used (Fig.194) which always are pre-stretched. At times of stress on the truss cell, one brace absorbs the strain while the other is relaxed; during maximum stress, this yields completely so that, according to calculation, it always takes only one of the two transverse booms, i.e., the one which works on the given load of expansion.

The strength of the brace construction depends greatly upon the degree of

---

*Ribbon types are the common type of the horizontal and vertical trusses.

STAT

preliminary stretching of the ribbon bracing. The method of calculation and practical recommendations for the brace construction were given by N.Ye.Zhukovskiy and his student, V.P.Vetchinkin.

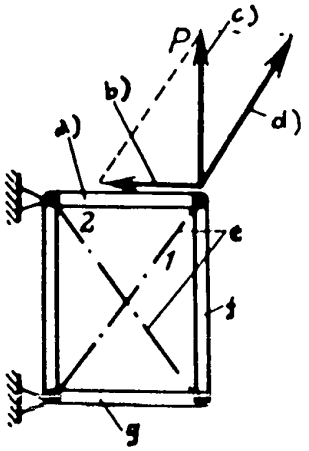

Fig.194 - Bracing Section of the Truss-Type Fuselage

In the installation of a ribbon truss instead of one diagonal two (more) trusses are installed. In this instance, the exterior force P stresses the truss (1) for expansion, truss (2) for buckling, and the upper boom for contraction.

a) Boom; b) Boom force; c) External force; d) Bracing-wire force; e) Bracing wire

The elements of the truss-type fuselage are usually tubes. Sometimes they have open profiles. The materials are steel and aluminum. Often the joining of the tubular elements is done by welding and the joining of the open profile elements by riveting.

The welded articulations are accomplished in the following manner. The tubes are welded to the ribbon and welded along the engaging flanges (Fig.195a). For greater strength, the abutting joints are often reinforced by open corner plates, with subsequent welding (Fig.195b). If the metal truss has braces, the welded corner plates can serve as mounting lugs (Fig.195c). In brace construction, the corner plates are sometimes replaced by welded tubes (Fig.195d).

Assemblies of riveted construction are made with the help of corner plates.

Very often it is impossible to install diagonals or braces in the separate cells, for example, in the cockpit. The lack of diagonals here may be compensated by rigid joints, i.e., by a framework (Fig.196).

In order to achieve a streamlined form of the truss-type fuselage, it is fitted with a special light-weight body which may be covered with fabric, laminated wood,

STAT

or aluminum. Part of this body or individual pieces, for convenience of utilization, may be of mixed construction.

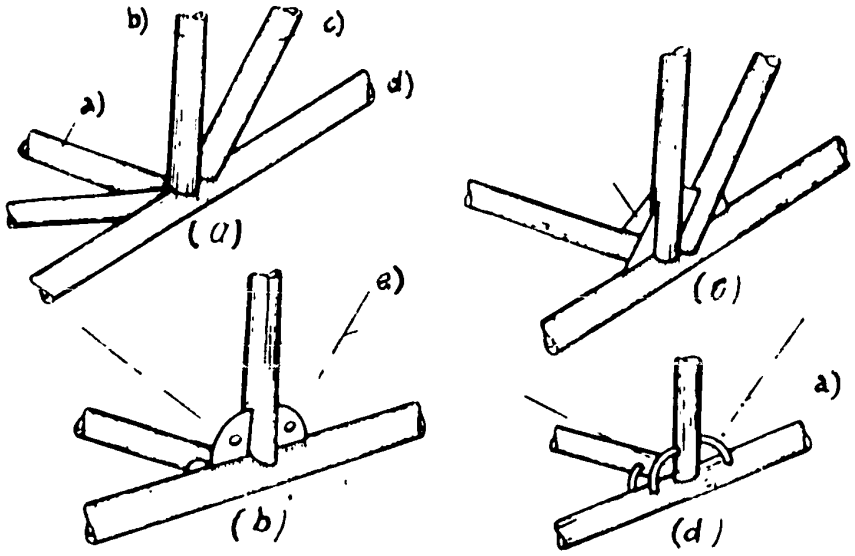

Fig.195 - Design of the Welded Nodes of the Fuselage

The joining of the elements (rods) is accomplished by welding. For increased strength, corner plates are often welded on.

a) Spacer; b) Vertical strut; c) Cross strut; d) Ribbon;

e) Corner plate; f) Bracing wire

Girder-Type Fuselages

Constructionwise, girder-type fuselages are more advantageous than truss types. Possessing a better aerodynamic form, they have smaller outside dimensions and permit a more ready displacement of the useful load. In a military sense, girder-type fuselages are preferable over truss-type fuselages. On receiving a hit in the longerons or diagonals, the truss-type fuselage may become unfit for combat. Conversely, in a girder-type fuselage (monocoque) even numerous hits are not very dangerous.

The girder-type fuselages (having the aspect of a beam) usually are of metal construction. They may be subdivided into three types:

Longeron girder fuselage;

STAT

Stringer girder fuselage;

Nacelle type fuselage.

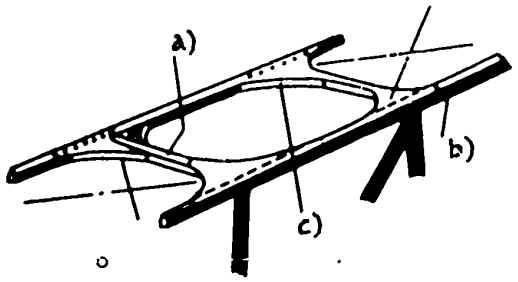

Fig.196 - Cut-Out in the Truss-Type Fuselage

In the production of cut-outs (cockpit, doors, portholes, etc.) no diagonals are installed in the cell. The lack of diagonals here is compensated by rigid joints, i.e., by a frame.

a) Spacer strut; b) Boom longeron;

c) Rigid framework

The longeron fuselage (Fig.197) has longitudinal frames, consisting of four strong longerons and a series of light stringers. The elements of the longitudinal frame are interconnected by the transverse frame or bulkheads. The power plant is covered by aluminum plates.

The stringer fuselage (Fig.198) has longitudinal elements consisting of a series of high-strength stringers, which are connected to each other by frames. There are no longerons. The covering, aluminum is often thicker than in the longeron fuselage.

The coque-type fuselage (Fig.199) consists of a relatively thick covering attached to the inside frames. There are no stringers or longerons. Fuselages of such type are found only in a few aircraft prototypes. In larger machines, because of the possibility of loss of stability (buckling), the skin must be thick, which exerts excessive stress on the structure.

At the present time, the basic type of fuselage is the stringer type, where all elements of the longitudinal frame and covering can absorb bending moments. But if the fuselage has many cut-outs (Fig.200), then to compensate the weakening of the structure, caused by these cut-outs, the longitudinal frame is fitted with longerons. In these instances, longeron construction of the fuselage is mandatory.

STAT

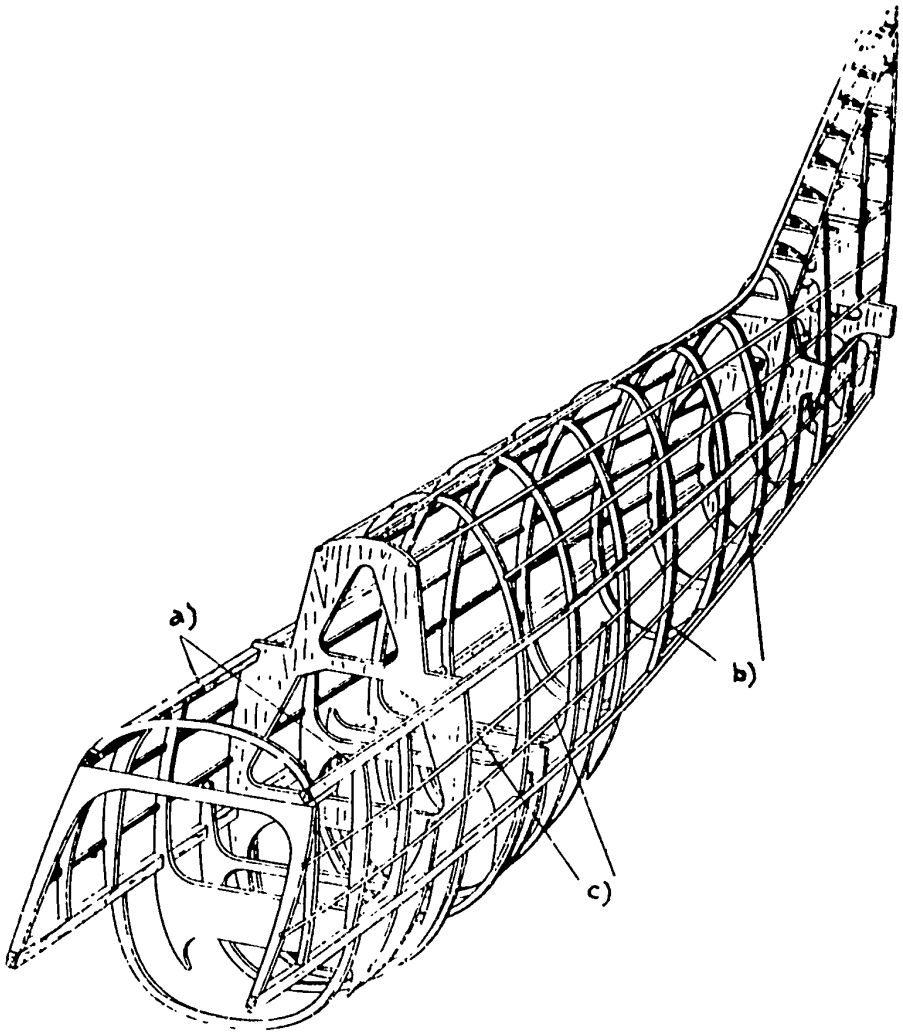

Fig.197 - Design of a Longeron Fuselage

The longeron fuselage has four strong longitudinal elements known as longerons.

a) Longerons; b) Transverse trusses; c) Stringers

Structural Elements of the Girder-Type Fuselage

The metal stringers (Fig.201) are pressed aluminum profiles in the form of angles (a), angles with bulb (b), Z-sections (c) or U-sections (d).

Longerons, in cross section, have the form of profiles (Fig.202) or tubes. Longerons may be riveted to the covering (Fig.203).

The bulkheads (Fig.204) are made either of an entire profile, more often a channel section, or from profiles and sheets riveted to each other. Reinforced

STAT

bulkheads, as a rule, are riveted into a box section.

The joining of the longitudinal frame to the transverse frame (Fig.205) is done

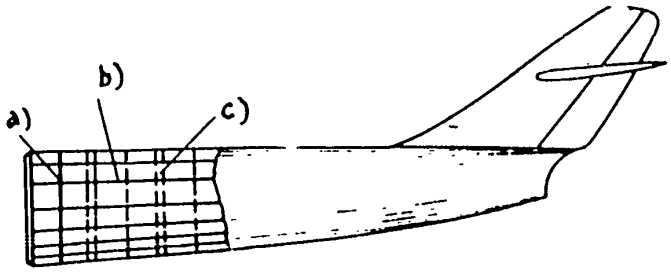

Fig.198 - Design of a Stringer Fuselage

In the stringer fuselage all the longitudinal elements (stringers) are roughly of one section.

a) Light transverse truss; b) Stringer;

c) Heavy transverse truss

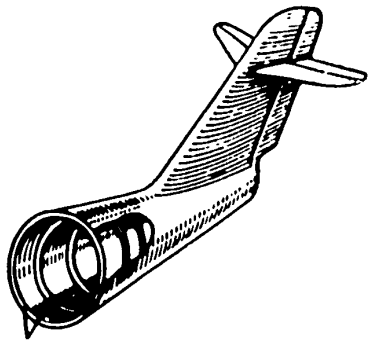

Fig.199 - Design of a Shell-Type or Coque Fuselage

The shell-type fuselage has no longitudinal frame; the body consists only of bulkheads.

a) Bulkhead

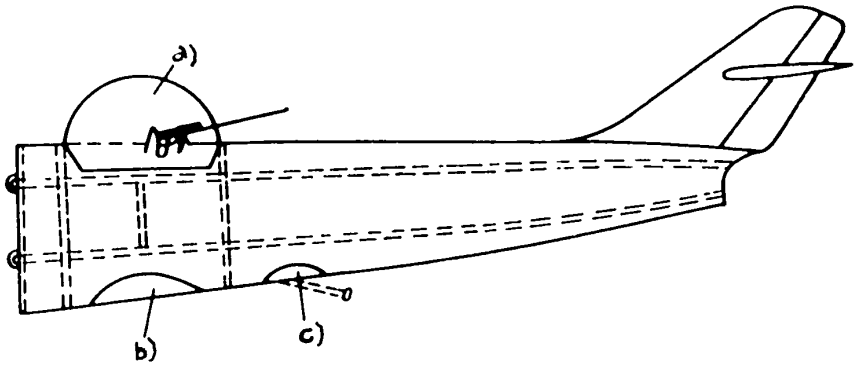

Fig.200 - Cut-Outs in the Fuselage

Cut-outs in the fuselage weaken its mechanical strength. This weakening is compensated by longerons.

a) Gunner station; b) Entrance hatch; c) Machine-gun mount

with rivets. Usually, the bulkheads are provided with inside holes for passing the stringers or longerons.

The joining of the stringers with the bulkheads is done through holes in STAT

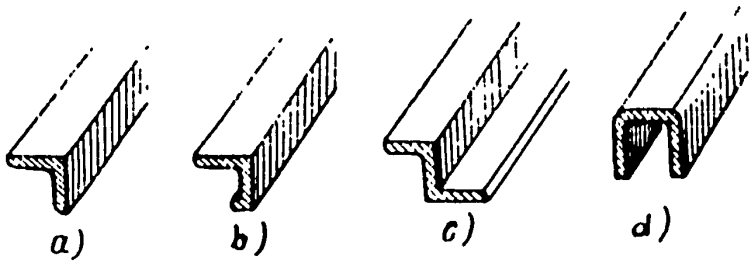

Fig.201 - Design of Stringers

Stringers consist of pressed aluminum profiles.

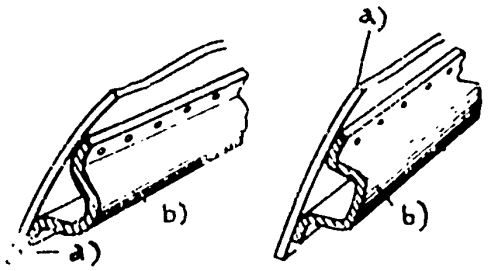

Fig.202 - Design of Longerons

Longerons are usually profiles which, together with the adjoining fuselage skin, form the sections of the completed contour.

a) Skin; b) Longeron

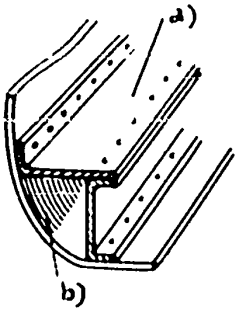

Fig.203 - Riveted Longeron

The longeron may be riveted from several profiles, forming the completed contour.

a) Longeron; b) Skin

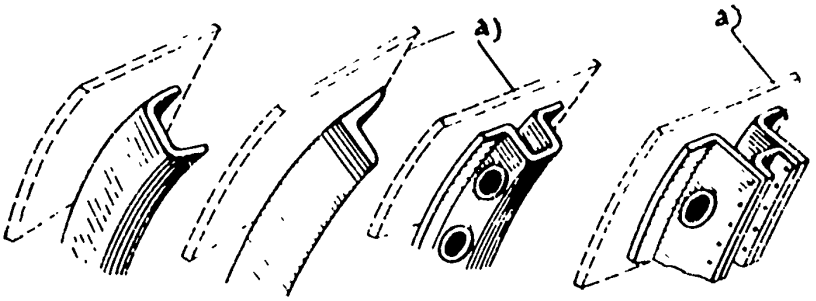

Fig.204 - Design of Bulkheads

The bulkheads are prepared from pressed profiles or riveted from several bent profiles.

a) Fuselage skin

STAT

bulkhead itself or through a special box or angle plate. In many designs, in general, the stringers are not joined to the bulkheads.

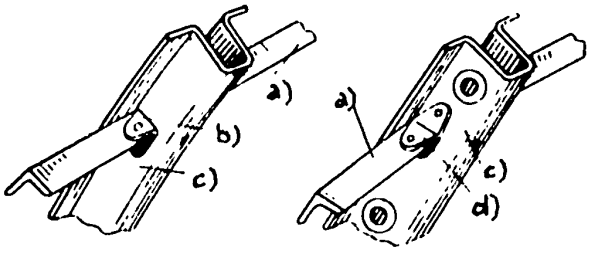

Fig.205 - Joining of Stringers and Bulkheads

The bulkheads, for joining with the stringers, are provided with holes. The stringers are riveted to the bulkheads with the help of reverse bulkheads or special angle plates.

a) Stringer; b) Fold; c) Bulkhead; d) Angle plate

The covering of the fuselage with a sheet metal is most often done with aluminum sheets. Every sheet is shaped in accordance with the form of the fuselage. The butt joint of the sheets is lashed to the stringers and bulkheads. The possibility of using wooden planking on a metal frame is not excluded.

The assembly of the individual fuselage parts is carried out in various ways: Longeron-type fuselages are assembled by means of joints, laid out on the butt ends of the longerons (Fig.206a); the parts of the stringer-type fuselage are assembled along the entire contour by screws or bolts, by means of tapes (Fig.206b) or fittings (Fig.206c).

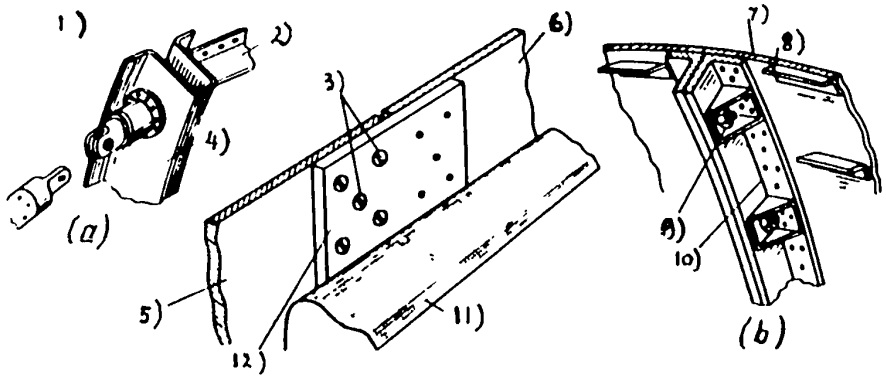

Fig.206 - Assembly Plan of Individual Parts of the Fuselage

In longeron design, the butt joints are prepared from four joints mounted to the longerons. In the stringer design, the butt joining is done along the entire contour of the fuselage.

1) Butt joint; 2) Longeron; 3) Screws; 4) Bulkhead; 5) Plate; 6) Stringer; 7) Fitting; 8) Fabric strip; 9) Connection under tape

STAT

Section 36. Design of a Semimonocoque Fuselage

In its strength characteristics a semimonocoque fuselage is very much like a monospar wing. Its energy diagram consists of longitudinal stiffeners, transverse frames, and a stressed skin. External loads deform the fuselage in the same manner as they deform the wing.

In a fuselage, concentrated forces are applied to the bulkheads. Concentrated loads are transmitted through the bulkheads to the skin in the form of distributed forces. These forces flow down the skin toward the wings and cause bending and twisting of the fuselage. Thus in separate cross sections of the fuselage lateral forces Q, bending moments M_b, and torsion moments M_t are present.

The bending moments M_b are absorbed by the longitudinal stiffeners and the skin. Lateral forces and torsional moments are absorbed by the skin. As in the energy diagram of a fuselage, i.e., the character of action of external forces, the flow of stresses through structural elements, and the work of the fuselage elements are similar in principle to the energy diagram of a wing, whereas the order of calculations - the order of determining the loads in the fuselage elements - is similar to that of the wing. Data necessary for these calculations consist of the diagrams of lateral forces, bending and torsional moments (see Section 34), and the size of fuselage elements.

Determination of Normal Loads

In a longeron-type fuselage (Fig.207) the bending moment M_b is absorbed by longerons in the form of compression and tension and to a lesser degree by stringers and the skin. This is explained by the thinness of the skin, only slightly reinforced by stringers, and by the presence of cut-outs.

In order to simplify these calculations let us assume that both skin and stringers do not participate in the work. In such a case, the total bending moment M_b of the fuselage will be absorbed by longerons (Fig.207b). Axial stresses will

STAT

also form in the booms

$$S = \frac{M_b}{2H_1}, \tag{93}$$

where H_1 is the distance between longerons.

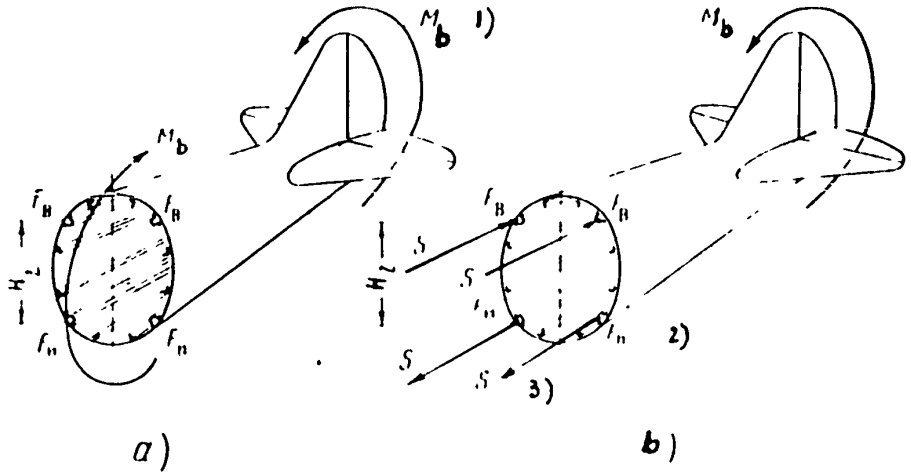

a) b)

Fig.207 - Action of the Bending Moment in a Longeron-Type Fuselage

The bending moment (a) is absorbed mainly by longerons in the form of contraction and expansion (b).

1) Bending moment; 2) Longeron area; 3) Tensile stress below longeron

When the magnitude of the axial stress S is known, it is possible to find the magnitude of the normal stress in longerons:

For the top boom

$$\sigma = \frac{S}{F_n},$$

where F_v is the cross-sectional area of an upper longeron;

For the bottom boom

$$\sigma = \frac{S}{F_n},$$

where F_n is the cross-sectional area of a lower longeron.

In a stringer-type fuselage (Fig.208a) the bending moment is absorbed by t

stringers and skin. The mechanical strength of such a fuselage is limited by the strength of the stringers.

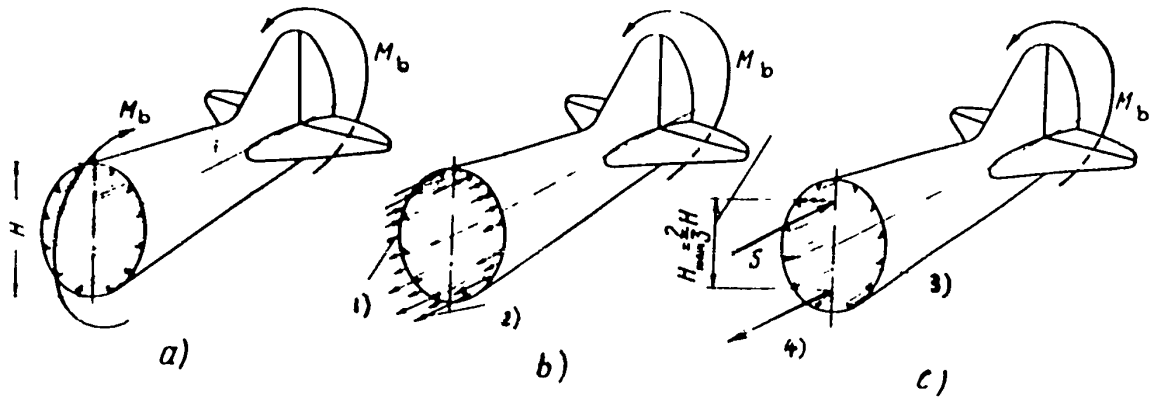

Fig.208 - Action of the Bending Moment in a Stringer-Type Fuselage

Here the bending moment acts on both stringers and skin, causing expansion and compressions in them.

1) S_{sk} = stress in the skin; 2) S_{str} = stress in the stringer; 3) Total compressive force; 4) S = total tensile force; 5) Arm pair

Forces which act separately on the skin and stringers in zones of tension and compression (Fig.208b), form two resultant forces S (Fig.208c) which, in turn, constitute a couple. Therefore the magnitude of S is determined by the formula

$$S=\frac{M_b}{H_{mean}}, \tag{94}$$

where H_{mean} is the lever arm of the couple.

In approximate calculations, it may be assumed that

$$H_{mean}=\frac{2}{3}H.$$

in such a case

$$S=\frac{M_b}{\frac{2}{3}H}. \tag{95}$$

In order to determine the stresses, we start with the well-known law of stress distribution through the depth of a beam (Fig.209), according to which the greatest stresses will be found near the fibers at the extremeties while in the neutral STAT

surface they diminish to zero. Thus, for our calculations we take the cross-sectional area of the elements located in the zone of greatest compression and tension, i.e., in the top and bottom arches.

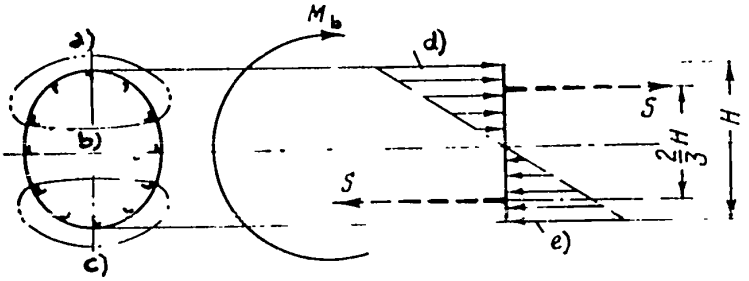

Fig.209 - Stress Distribution Through the Depth of the Fuselage

High stresses occur in the arches of the fuselage and lower stresses in the elements near to its neutral layer due to the action of the bending moment.

a) Upper arch; b) Neutral layer; c) Lower arch; d) σ_{co} = stress in the upper arch; e) σ_{exp} = stress in the lower arch

The common cross-sectional area of elements in one arch is equal to

$$F_{arch} = nf_{str} + F_{sk}\ \varphi, \tag{96}$$

where n is the number of stringers in one arch;

f_{str} is the cross-sectional area of one stringer;

F_{sk} is the area of skin of one arch;

φ is the so-called reduction coefficient which shows what section of the skin is working to its full capacity. In the zone of expansion, φ = I (i.e., the entire skin is working to its full capacity), while in the zone of compression

$$\varphi \approx \frac{30\delta}{b} < 1.$$

Here b is the distance between stringers; STAT

δ is the thickness of the skin.

Thus the normal stresses in stringers are equal to

$$\sigma_{str} = \frac{S}{F_{arch}} = \frac{M_b}{\frac{2}{3} \cdot H (n f_{str} + F_{sk} \varphi)} . \qquad (97)$$

In a true monocoque fuselage (without stringers), the bending moment M_b is absorbed by the skin alone. For full load performance it is necessary to secure an adequate stability of the skin (to prevent buckling). All considerations made in determining the strains and stresses in a stringer-type semimonocoque fuselage are

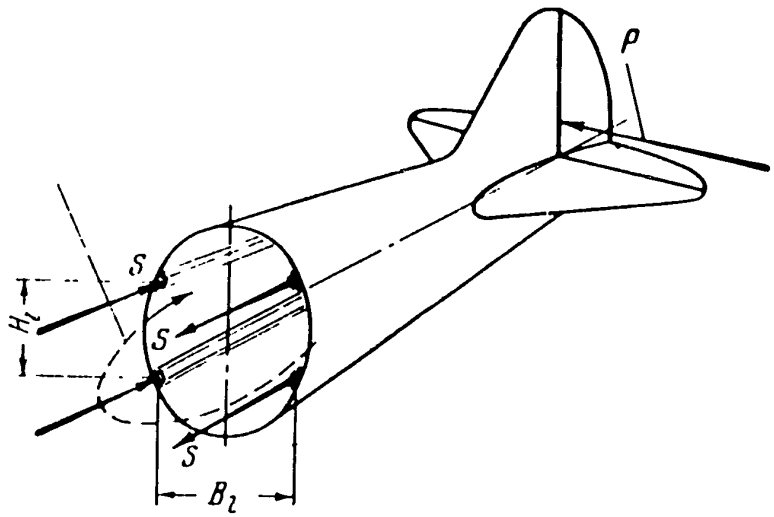

Fig.210 - Lateral Bending of the Fuselage

In case of lateral fuselage loading, strains and stresses are calculated in the same manner as in symmetrical bending.

a) M_b = bending moment of cross section; b) $P_{v.t.}$ = lateral load;

c) Axial stress on longeron (boom).

fully applicable to a true monocoque fuselage. Stresses in the skin caused by the action of M_b are determined by eq.(97) in the following manner:

$$\sigma_{str} = \frac{M_b}{\frac{2}{3} H F_{sk}} . \qquad (98)$$

As a result it can be stated that fuselages of all three types work in a

STAT

similar manner and differ only in the degree to which different elements participate in the absorption of M_b.

In a longeron-type semimonocoque fuselage moment M_b is absorbed by longerons and the loss of stability (buckling) of stringers and the skin does not affect the mechanical strength of the fuselage. The fuselage will fail only if longerons are destroyed.

In a stringer-type semimonocoque fuselage, most of the moment M_b is absorbed by stringers; therefore, their strength determines the strength of the fuselage and the loss of stability by the skin is not dangerous.

In case of a lateral asymmetric loading of the fuselage (Fig.210), the line of reasoning in determining strains and normal stresses is the same as before, with the exception that, in all formulas, the quantity B (cross section) must be used instead of H.

Determining Tangential Stresses

Tangential stresses τ in the skin of the fuselage occur under the action of the lateral forces Q and the torsional moments M_t.

Torque takes place in the case of asymmetrical loading of the fuselage. If the fuselage is loaded symmetrically, M_t is absent.

First let us examine the process of determining tangential stresses caused by symmetrical lateral forces Q (Fig.211). The force Q will be absorbed by the sidewalls of the fuselage, causing tangential bending stresses τ_b in them. Tangential stresses in the skin of the top and bottom arches of the cross section are negligible and can be disregarded.

In order to determine the tangential stresses produced by Q in the skin of the fuselage and assuming that these stresses are evenly distributed, let us find their magnitude by dividing the force by the sectional area of the skin portion on which Q is acting. In a longeron-type fuselage (Fig.211a), the force Q is mainly absorbed by the sidewalls, whose area is approximately equal to $2H_1\delta$.

STAT

Therefore,

$$\tau_b = \frac{Q}{2H_1\delta}, \qquad (99)$$

where δ is the skin thickness.

In a stringer-type and in a true monocoque fuselage (Fig.211b and c), the force Q is absorbed mainly by the walls $\frac{2}{3}$ H high. The area of these walls will be equal to $2\,\frac{2}{3}\,H\delta = \frac{4}{3}\,H\delta$.

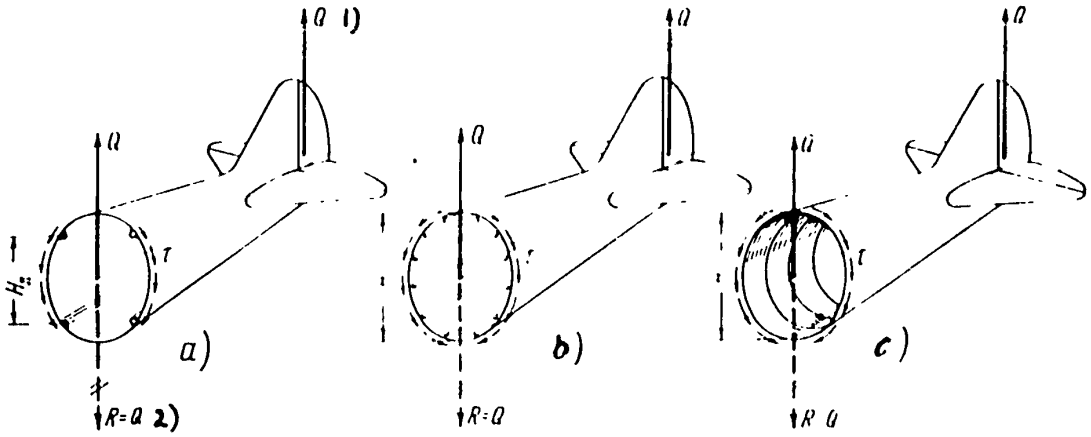

Fig.211 - Action of a Lateral Symmetric Force

The force Q acts on the sidewalls of the fuselage and produces tangential bending stresses τ_b. The force Q when applied to the tail unit, together with the resultant of the internal forces R forms a couple - the bending moment.

1) Q = resultant external force; 2) R = Q = resultant internal force τ_b

Therefore,

$$\tau_b = \frac{Q}{\frac{1}{3}\,H\delta}. \qquad (100)$$

Now let us define how the tangential stresses are determined when a fuselage is loaded asymmetrically. In this case, in addition to tangential bending stresses (due to the action of the force Q), other stresses will be produced by the torsional

STAT

moment M_t. For example, let us take the case of asymmetric fuselage loading with a load acting in the direction away from the vertical tail surfaces (Fig.212), the force $P_{v.t.}$ The action of the couple $P_{v.t.}$ and Q in the horizontal plane (action of M_b) has been examined above. Here we are going to examine the action of the force $P_{v.t.} = Q$ which, due to the lever arm a, produces a torque

$$M_t = Q \cdot a,$$

where the lever arm a is the vertical distance from the line of action of the force $P_{v.t.}$ to the middle of the cross section of the fuselage.

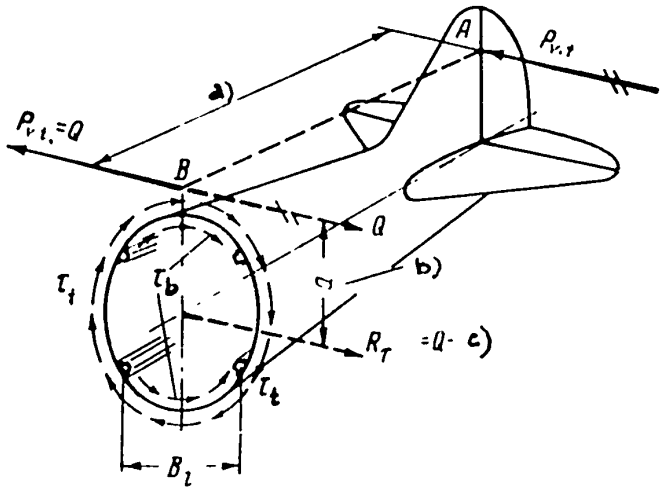

Fig.212 - Loading of a Fuselage, with the Load Acting Away From the Vertical Tail Surfaces, with a Force $P_{v.t.}$

The force $P_{v.t.}$ applied to a point A, together with the force Q applied to the point B, form a bending moment of the fuselage. The force $P_{v.t.}$ applied to B together with the resultant of the internal forces R_{τ_b} produce the torsional moment $M_b = P_{v.t.}a$. The force $P_{v.t.}$ is balanced by the stresses τ_b, while M_b is balanced by the stresses τ_t.

a) Arm of the bending moment; b) Arm of the torsional moment;

c) $R_{\tau_b} = Q$ = resultant force τ_b

The lateral force Q in any cross section of the fuselage is absorbed by the skin of the top and bottom arches and produces tangential stresses τ_b in it. The

STAT

magnitude of τ_b in a longeron-type semimonocoque fuselage is determined by eq.(99)

$$\tau_b = \frac{Q}{2B_1\delta}, \tag{101}$$

where B_1 is the distance between longerons.

The tangential stresses τ_b produce a resultant force $R_{\tau_b} = 0$ which, together with the force $P_{v.t.}$, forms a couple which produces twisting of the fuselage

$$M_t = Qa,$$

or

$$M_t = P_{v.t}\, a.$$

The determined torque will act on the entire contour of the cross section of the fuselage and produce torsional stresses there. The tangential torsional stresses are determined by the formula

$$t = \frac{M_t}{2F\delta}, \tag{102}$$

or

$$t = \frac{P_{v.t}\, a}{2F\delta}, \tag{103}$$

where F is the cross-sectional area limited by the contour of the fuselage.

All these formulas, with a single modification are also valid for the stringer-type and true monocoque fuselages; only B_1 must be replaced by $\frac{2}{3}B$, where B is the width of fuselage.

In order to determine the resultants of tangential stresses in the skin, an algebraic addition of tangential stresses of bending τ_b and of torsion τ_t must be performed.

STAT

$$\tau = \tau_b + \tau_t.$$

Section 37. Design of a Truss-Type Fuselage

In its strength characteristics, a truss-type fuselage is similar to a semimonocoque fuselage, except that in this case the main strength element is not the skin but the girders and diagonal braces. Therefore, the determination of external forces and the process of plotting the loading diagram of Q, M_b, and M_t as the initial data in our calculations, remains the same as a semimonocoque fuselage.

When the loading diagram and the dimensions of the fuselage are determined, it is possible to find the stress and strain in its elements.

The bending moment of the fuselage (Fig.213) will be fully absorbed by compression and tension of its longerons. The magnitude of the axial stresses in the longerons (booms) is determined from the formula

$$S_{boom} = \frac{M_b}{2H}. \qquad (104)$$

The lateral forces Q (Fig.214) produce axial stresses in the girders and diagonal braces of the lateral plane trusses. The lateral force Q is evenly distributed between the two plane trusses: $\frac{Q}{2}$.

If the angle α between the vertical girders and diagonal braces is known, we can determine the axial stresses in the latter from the following formula:

$$S_{brace} = \frac{Q}{2 \cos \alpha}. \qquad (105)$$

The stress in a vertical girder according to the conditions of equilibrium of the assembly is equal to the shearing force of a plane truss. In this case,

$$S_{girder} = \frac{Q}{2}. \qquad (106)$$

STAT

A vertical loading of the tail unit will cause bending of the fuselage in the horizontal plane and twisting.

Since the stresses produced by Q and M_t in the upper truss are cumulative, this truss is usually reinforced by double tie-rods or stronger diagonals.

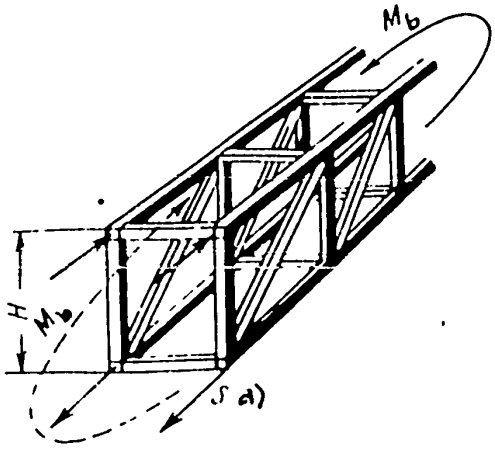

Fig.213 - Action of the Bending Moment

The bending moment of the fuselage will be fully absorbed by compression and tension of the longerons.

a) S_{boom} = tension in the lower boom

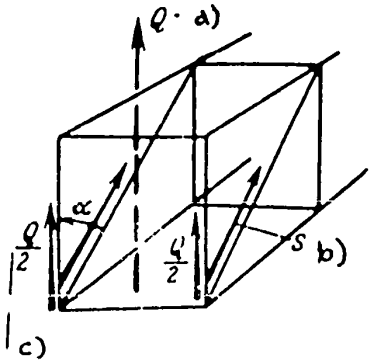

Fig.214 - Action of the Lateral Force

The stress in the vertical girder is equal to the lateral force of the plane truss $\frac{Q}{2}$. The stress in the diagonal braces is equal to the lateral force of the plane truss divided by cos x, i.e., $S_{brace} = \frac{Q}{2 \cos \alpha}$.

a) Q = transverse force on fuselage;

b) S_{brace} = stress in brace; c) Transverse force in plane truss

In order to increase the rigidity of the fuselage and to include all four plane trusses in the resistance work to M_t, use is made of internal cross braces, diagonal braces, or frames are employed inside the fuselage. These lateral elements perform the functions of wing ribs, i.e., they distribute local loads over the entire longitudinal assembly of the fuselage. More elaborate calculations demonstrate that the load on these lateral elements is negligible.

Section 38. Pressurized Cabins

Designation of Pressurized Cabins

With the advent of jet aircraft, not only did the speed of flight but also the

STAT

altitude increase considerably. Thus, the problem of creating the necessary vital conditions for the crew and maintaining its combat efficiency at high altitudes acquires now more significance than ever before.

Atmospheric pressure decreases with altitude and so does the partial oxygen pressure (the percentage of which, as that of other gases in the air, remains practically constant up to an altitude of approximately 2000 m). This leads to a shortage of oxygen or anoxia; for flights at altitudes above 4500 m man needs an additional supply of oxygen. A harmful effect on the human body is also produced by the low pressure of the surrounding atmosphere: pains in the joints, stomach, teeth, etc., and attacks of altitude sickness (aeroembolism). These symptoms appear during long flights at altitudes above 8000 m.

Vital conditions for the crew and passengers at high altitudes are created by oxygen equipment, pressurized suits, and pressurized cabins.

Oxygen equipment is ordinarily used at altitudes above 4500 m. It adds some oxygen to the inhaled air and just prevents symptoms of anoxia, but only below a certain altitude. Prolonged flights at altitudes above 10,000 m, even with oxygen equipment, are very difficult both because of the low atmospheric pressure and because of an inadequate partial oxygen pressure produced by the oxygen equipment.

Therefore, even though individual flights in open cockpits with oxygen equipment at altitudes of the order of 15,000 m are known, it must be considered that the highest altitude for mass flights in open cockpits is 12,000 m and that, as a rule, above 9000 - 10,000 m pressurized suits or cabins must be used which make it possible to increase the pressure on the body and create a higher partial oxygen pressure.

Pressurized suits are complicated and hinder the movements of the pilot and therefore did not come into wide use (they are used only for record flights).

Due to the fact that a pressurized cabin is completely or partially insulated from the surrounding atmosphere, it is possible to raise its oxygen content and

STAT

increase the pressure (with respect to the surrounding atmosphere), thus creating the necessary conditions for sustaining life and efficiency of the crew and passengers.

The problem of temperature control may be solved by insulating pressurized cabins and by installing heating equipment. This problem acquires special importance in connection with high-altitude flights in regions of low temperature and in connection with airplane heating at high speeds.

Flying in pressurized cabins at high altitudes is less tiring than high-altitude flights with oxygen equipment.

Pressurized cabins are the surest means toward securing the efficiency of the crew of a modern airplane at high altitudes under combat conditions.

The idea of building pressurized cabins was first forwarded and proved in 1875 by the great Russian scientist D.I.Mendeleyev.

Types of Pressurized Cabins and How They Operate

In accordance with the means by which vital conditions are produced in pressurized cabins, these are divided into two main types: 1) pressurized cabins, 2) sealed cabins.

In pressurized cabins which are now the most widely used type, a blower constantly blows air under pressure into the cabin, thus producing a certain supercharging; at the same time, through certain valves which keep up the necessary pressure in the cabin, the air is discharged into the atmosphere. As a result, a continuous ventilation of the atmospheric air throughout the cabin is achieved. Thus, supercharging and ventilation are the characteristics of a pressurized cabin. Pressurized cabins are sometimes called supercharged cabins. The percentage of oxygen in the air blown into the cabin is the same as that in the outside atmosphere, but the partial oxygen pressure is proportional to the absolute pressure in the cabin.

STAT

Let us now examine how a cabin is supercharged. It may seem that, in order to create the most favorable conditions, it is necessary to keep up a normal atmospheric pressure in the cabin at all altitudes. However, in case of a blowout at high altitudes, due to puncturing of the cabin or to some other damage, the pressure drop will be extremely sharp. At an altitude of 16,000 m in such a case the pressure would diminish 10 times within a fraction of a second, which would lead to serious physiological consequences for the crew members. Also, in order to sustain a higher positive pressure in a cabin, it is necessary to reinforce its structure considerably which, in turn, leads to a substantial gain in weight.

Therefore, the pressure produced in the cabin is such that it secures comfortable living conditions and that, at the same time, even a sharp pressure drop in case of a blowout will be endured by the crew without injury.

Up to 2000 - 3000 m, the pressure of the surrounding atmosphere is ordinarily maintained in a pressurized cabin (segment 1 of the curve in Fig.215). In a pressurized cabin, this is accomplished by a suitable valve. The absolute pressure thus attained is maintained in the cabin up to a certain altitude where the pressure is raised so that it will be higher than that of the surrounding atmosphere (segment 2 of the curve). This positive pressure is usually equal to 0.25 - 0.30 atm and is kept constant during the rest of the climb (segment 3 of the curve). Thus the cabin altitude is lower than the airplane altitude. According to Fig.215, at an altitude of let us say 15,000 m, conditions in the cabin will represent those at an altitude of 7000 m.

However, even though the absolute pressure in the cabin will be adequate for the crew, there will be a shortage of oxygen. Therefore, it is necessary to use oxygen equipment in pressurized cabins above a certain altitude. Such oxygen equipment has to be switched on in open cockpits at an altitude of 4000 m while, in pressurized cabins, oxygen equipment must be put into use only at much greater altitudes (in our example, at 9000 m).

STAT

Ventilation of a pressurized cabin consists of constant circulation of fresh air through the cabin and is measured by the volume of air flowing through the cabin in unit time. Ventilation is used in order to maintain a certain concentration of a given substance in the cabin air (oxygen, water vapor, carbon dioxide, etc.).

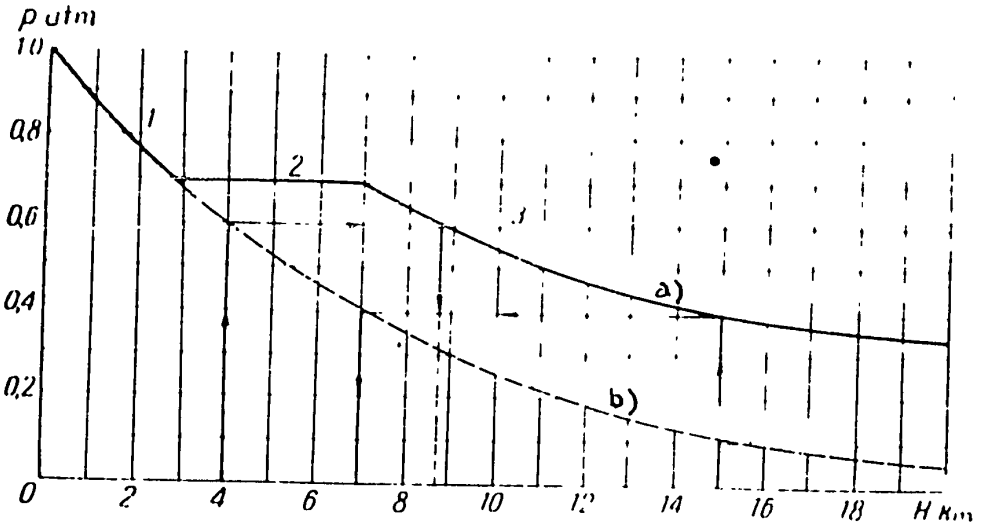

Fig.215 - Character of Change in Atmospheric Pressure With Respect to Altitude and Corresponding Change in Pressure in a Pressurized Cabin

The cabin altitude is generally lower than the airplane altitude.

a) Pressure in cabin; b) Standard atmosphere

The general diagram of a pressurized cabin (Fig.216) includes 1) feed system; 2) air release and pressure control equipment.

The feed system consists of a blower (engine compressor or a special cabin supercharger) from which the air is blown through a check valve (4) into a manual supply cock (2), with which the pilot can manually control the delivery of air from the blower or stop it completely and connect the cabin directly with the outside atmosphere by opening a special scoop (depressurize the cabin and switch on ventilation with atmospheric air). From the cock (2), the air flows into the collector (3) from where, through a number of small openings, it enters the cabin, blowing

over the canopy and the windshield. Air is heated by compression in the supercharger and thus heats the cabin (completely or partially) and prevents fogging of the pilot's enclosure. An automatic air-intake volume control (1) may be added to the feed system, in order to control irregular supercharging of the compressor during fluctuation in engine operation. A filter (5), containing active charcoal, silica gel, cotton, and the like, may be used to clean the air of oil and decomposition products (which are present when the cabin is supercharged by the engine compressor).

The air release and pressure control equipment consists of pressure regulators designed for maintaining the given pressure in the cabin and of safety devices protecting the cabin from extreme internal and external pressures. The regulator or the valve of permanent absolute pressure (6) remains open until a certain altitude is reached, and the cabin freely communicates with the surrounding atmosphere (see segment 1 of the curve in Fig.215). The valve (6), according to its adjustment, maintains a permanent absolute pressure (see segment 2 of the curve in Fig.215); when the required positive pressure in the cabin is reached, the regulator for permanent positive pressure (9), which functions on the principle of pressure variation, comes into operation and secures the segment 3 of the curve (see Fig.215).

Sometimes the valves (6) and (9) are combined into a single aggregate, a pressure regulator (PR). To protect the cabin from excessive internal pressures in case of failure of the pressure regulator, a connecting safety valve (10) is inserted. This valve is adjusted to a somewhat greater pressure drop than that of the valve (9). The pressure-variation check valve (8) allows atmospheric air to enter the cabin when a vacuum starts forming there (during rapid descents) and thus protects the cabin from collapse due to external pressure. The pressure-variation check valve (8) is often used as a manual control valve for the cabin pressure. Manual control is accomplished by changing the design of the valve accordingly and providing it with a hand wheel (7). In case of necessity, it is possible to blee

the cabin air into the atmosphere.

Pressurized cabins may also be supplied with heating equipment (if the temperature of the supercharged air is not sufficiently high), air-cooling equipment, air filters, humidity control equipment, and general control equipment (control of air intake, air pressure, temperature, humidity, purity, etc.).

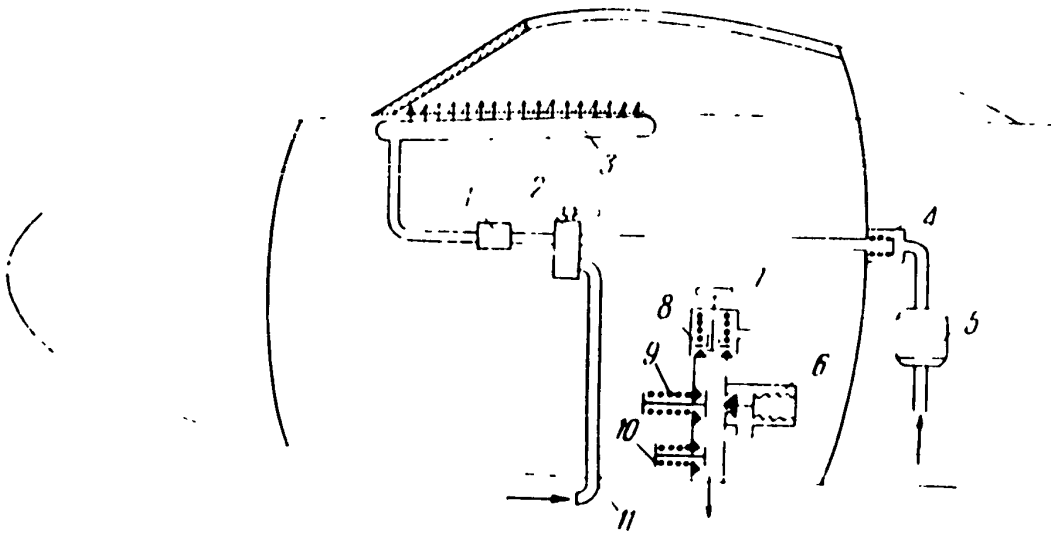

Fig.216 - Principal Diagram of Cabin Ventilation

The switching diagram includes the air-feed system itself (intake, supercharging) and the air-discharge system and pressure control.

While using pressurized cabins, the technician must carefully check the good working condition of all altitude equipment and of the devices that keep the cabin sealed, since their failure at high altitudes may lead to crashes or even catastrophe.

In a sealed cabin, air is pumped through an air purification plant where the respiration products (water vapor, carbon dioxide) are absorbed. Simultaneously, oxygen from tanks and air are continuously added to the cabin atmosphere (as a compensation for the oxygen used in breathing). Thus a certain positive pressure is created in the cabin and is maintained by valves which regulate the discharge of air from the cabin.

STAT

Thus, in this type of cabin not only a positive pressure (supercharging) but also a constant ventilation of the cabin, regulating the concentration of the various air components, is achieved.

The high percentage of oxygen in sealed cabins makes it possible to produce the necessary partial oxygen pressure at lower cabin pressures (in comparison with a pressurized cabin) but at the same time fire hazards are increased. One of the advantages of sealed cabins is that their functioning does not depend on the conditions of the outside atmosphere. This fact makes it possible to use sealed cabins at such altitudes where pressurized cabins can no longer be used. The duration of flight in a sealed cabin is limited by the amount of oxygen in the tanks. Cabins of this type are also more complex than pressurized cabins.

Energy Diagrams and Loads Acting on Pressurized Cabins

The loading of a pressurized cabin and its functions as a unit of power largely depends on the degree to which it is included in the energy diagram of the fuselage.

A pressurized cabin may be built as a separate unit of power, which is installed (suspended) inside the fuselage without being included into its energy diagram (Fig.217a). Such a cabin is sometimes called a suspensed cabin. It is loaded with the difference of internal and external pressures, and also with loads (forces of inertia and the mass) of men and cargo distributed inside the cabin. Since the loads of the fuselage are not transmitted to the cabin, its deformations due to such loads is less which, in turn, makes the sealing of the cabin more reliable.

The shape of a suspended cabin when the fuselage is large does not depend on its contours so that the cabin can be given a shape that is more advantageous in relation to strength. It can then be of minimum size, which will be determined only by the accommodation of the crew and the requirements of its work. This permits a decrease in the cabin weight, but its structural material, not included in the energy diagram of the fuselage, is not adequately exploited.

Cabins forming airtight sections of the fuselage (Fig.217b) are also widely

STAT

used. These are completely included into the energy diagram of the fuselage. Such cabins represent sections of the fuselage and accordingly, in addition to the loads mentioned above, they also absorb aerodynamic loads distributed over the entire surface of the cabin and the loads of other parts of the aircraft connected with the pressurized cabin (such as wings, tail assembly, fuselage, etc.).

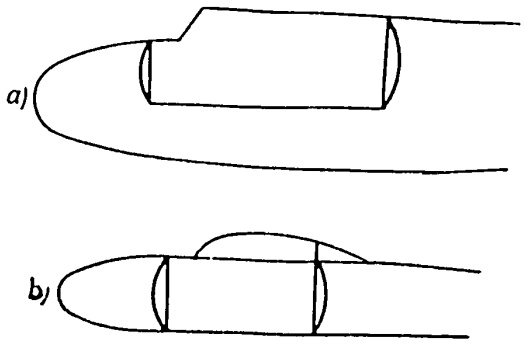

Fig.217 - Diagram Showing Inclusion of Pressurized Cabins into the Structure of the Fuselage

Suspensed cabin (a) increases the reliability of its sealing, since it does not participate in the work of the energy diagram of the fuselage; pressurized section of a fuselage (b) constitutes a part of the fuselage.

Therefore loading of a pressurized cabin with a pressure difference is included in the energy diagram of both cabins. Under normal conditions, the cabin is loaded with internal positive pressures. However, if the aircraft would descend rapidly, the cabin would be subject to an external pressure. Since a pressurized cabin, due to its form and structure, is more capable of withstanding internal pressures, loading the cabin with excessive external pressures is more dangerous. Such a condition may arise if, during a rapid descent, the valve (9) (see Fig.216) fails to equalize the pressure inside the cabin with the pressure of the surrounding atmosphere.

Canopies, due to the curvature of their surface and due to considerable speeds, are loaded with large aerodynamic forces. These loads are usually directed toward the outer side of the enclosure.

Design of Pressurized Cabins

The design of a pressurized cabin must meet the requirements of strength, rigidity, pressurization, heat insulation, survival, and must be free from fire

STAT

hazards, etc.

A pressurized cabin, when loaded, acts first of all as a thin-walled vessel under the action of internal or external pressures and secondly (not always) as a thin-walled vessel subjected to bending and twisting in the energy diagram of the fuselage.

The strength of a pressurized cabin is secured by making its construction similar to that of the fuselage and by selecting a suitable assortment of profiles for the power units.

The work of a pressurized cabin as a vessel has its own peculiarities, which influence the choice of a rational form, its structure, and strength. As it is well known, the most advantageous form for a closed vessel loaded with internal pressures, in relation to its strength, is a sphere. But a spherical cabin cannot be used in aircraft since it would be difficult to accommodate the crew in a cabin of such a form, and since it does not correspond to the outline of the fuselage. Consequently, there is a general trend to design pressurized cabins in the form of cylinders with circular cross sections, closed on the ends with spherical or conical end pieces. The transition from the walls of the cylinder to the end pieces must be smooth, without sharp edges. If any sharp edges are present, the end pieces will compress the walls of the cylinder in radial directions and it will then be necessary to place reinforced frames at the point of junction. Even when the transition from the end pieces to the cylinder is smooth, additional local stresses occur, and the destruction of the cabin during strength tests by the use of internal pressure, usually begins at the joint of the end pieces with the cylindrical part of the cabin.

In the walls of a cabin of a cylindrical form with a circular cross section, under the action of internal forces, only normal tensile stresses occur in the longitudinal and transverse cross sections. But if the cabin has another form (and this is often necessary, due to the design of the airplane) the cabin walls will

subjected to bending and therefore must be made thicker and more heavily reinforced. All this tends to increase the cabin weight. Strength and weight requirements are the most important factors that limit the use of positive pressures exceeding 0.25 - 0.30 atm in noncylindrical cabins.

The walls of pressurized cabins are usually riveted from duraluminum sheets of a rather small thickness (1.5 - 3 mm), reinforced by longitudinal and transverse frames. Since canopies are loaded with large aerodynamic forces, careful attention must be given during manufacturing and operating to their strength and to mechanisms securing them to the cabin.

Adequate sealing of the cabins is one of the most important conditions that make it possible to sustain the necessary positive pressure. This is achieved by 1) an airtight structure of the cabin and the canopy (sealing of riveted seams and canopy connections); 2) making hatches and enclosures airtight; 3) sealing the outlets of rods, fillets, cables, electric wiring, etc. Failure of the airtight structure of the cabin or its partial inadequacy may lead to such air losses that the work of the supercharger is unable to compensate them. Therefore, when operating pressurized cabins, special attention must be given to the condition of the cabin seal and to elimination of any defects.

The rigidity of the structure of a pressurized cabin is especially important at the outlets of movable leads, controlling various units, since this makes the sealing of these outlets more reliable.

A wider margin of safety for the crew working in a pressurized cabin is achieved by preventing explosive decompression. With an increase in altitude, greater positive pressures in the cabin become necessary and a sudden blowout will be accompanied by an even more dangerous pressure drop. If the cabin is shot through, an explosive decompression may be prevented by a rapid increase in the amount of air blown into the cabin by the supercharger or by impeding depressurization by covering the walls of the cabin and the enclosure with special protectors hinder

the flow of air through the hole. This protector may simultaneously serve as a heat insulator.

To prevent fogging and freezing of the canopy, it is heated with a stream of hot air. The sections of the enclosure not heated by this air flow, for the same reasons (and also in order to decrease heat losses), may be designed with double windows, with desiccator cartridges inserted in the air gap between them.

Section 39. Ejection Seats for the Crew

Design of Ejection Seats and the Principle of Their Operation

With the increase in flying speed, the problem of leaving the cabin of the airplane in case of emergency becomes more difficult. These difficulties increase for the following reasons.

1) As the speed increases, the aerodynamic forces acting on the body of the pilot as he bails out from the cabin, increase greatly in magnitude. For instance, at a speed of 600 km/hr the body of the pilot, showing only halfway above the cockpit, is subject to an aerodynamic force of about 450 kg from the oncoming air stream; the head alone is subject to an impact of about 60 kg. Therefore, bailing out at high speeds requires considerable time and strength, which may prove to be above the physical possibilities of the pilot.

2) With the increase in speed, the danger increases of colliding with the tail assembly or some other part of the aircraft after the pilot has left the cockpit. Therefore even if the pilot left the cabin successfully and on time, for instance by climbing over the side of the cabin, there still remains the danger of colliding with the tail assembly.

3) A high-speed air stream has a marked effect on the unprotected face and on the lungs of the pilot.

For these reasons (the first two being the most apparent), bailing out from the aircraft in the usual manner (bailing out directly from the cabin) is restricted to flying speeds of 500 - 600 km/hr. One of the means for getting clear of the air-

STAT

craft is a bail-out (ejection) from the cabin of the pilot's seat together with the pilot himself.

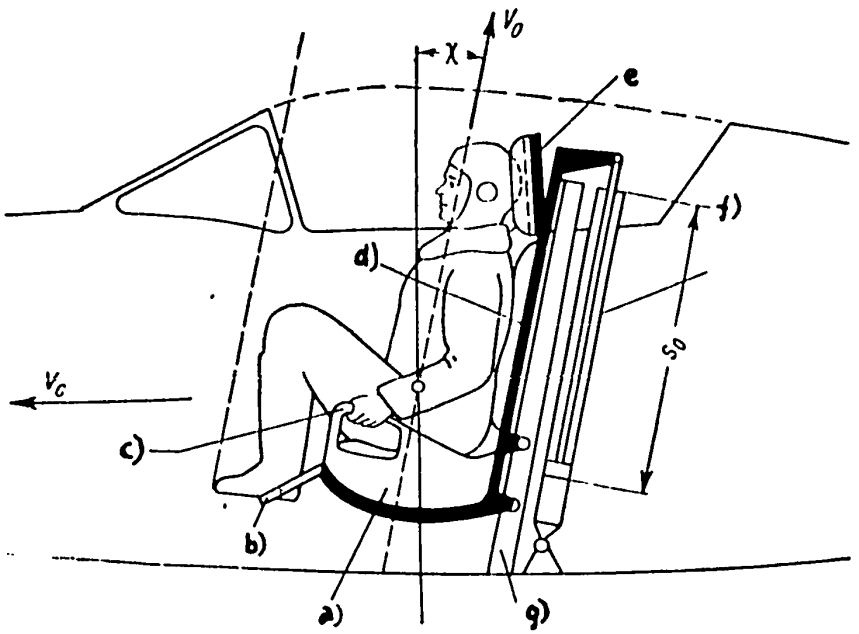

Fig.218 - Principal Diagram of an Ejection Seat

During ejection, the canopy is automatically jettisoned after which the ejection mechanism is actuated.

a) Seat; b) Footrest; c) Hand rail; d) Backrest; e) Headrest; f) Ejection mechanism; g) Guide rail

Ejection may be performed upward through the open cabin enclosure or downward through a special porthole in the fuselage. Ejection of the pilot's seat upward by means of compressed air or firing of a cartridge is structurally more simple.

Figure 218 shows the principal diagram of an ejection seat. Two pairs of rollers are fastened to the backrest of the seat. These slide over two guide rails. The guide rails are placed on both sides of the backrest and are fixed to the bulkheads of the fuselage. The ejector consists of a cylinder hinged to the fuselage with its lower end, and a piston with a rod. The latter is placed inside the cylinder, and the upper end of the rod is hinged to the backrest of the seat. During a normal flight, the piston is locked inside the cylinder by a special retainer in STAT der to prevent movement of the seat in the guide rails during negative acceleration.

During ejection, the canopy is jettisoned automatically, followed by actuation of the ejector mechanism. The cylinder is filled either with gases under high pressure from firing of a cartridge or with compressed air from a special tank under a pressure of 100 - 150 atm. Under the action of this high pressure, the retainer of the piston inside the cylinder unlocks and the piston, pushed by the gases, entrains the seat, together with the pilot, secured to it by his harness. The seat moves along the guide rails for only a very short period of time (0.15 - 0.20 sec), but the acceleration is great so that, by the time the piston leaves its cylinder, the seat has acquired a very high velocity. With this velocity V_o, known as the initial velocity, the seat begins its free flight relative to the airplane.

When the seat enters the air stream and experiences its braking effect, it starts lagging behind the aircraft which continues its flight. In the air, a second or two after the ejection, the pilot harness is unlocked, the seat starts moving away from the pilot so that even a few seconds after ejection it is already possible to open the parachute without running any risk.

To permit use of ejection at any altitude, the chute is provided with oxygen equipment, which supplies the pilot with oxygen after he leaves the cabin. The use of automatic devices for unlocking the pilot harness, opening the chute, etc. greatly increases the reliability of functioning of the entire ejection system.

Ensuring the Necessary Trajectory of the Seat

In order to ensure safety, the path of the seat should follow a trajectory somewhat above the tail assembly. The actual magnitude of this height depends on the flying speed. With an increase in flying speed, the braking effect of the air stream on the seat increases greatly (in proportion to the dynamic head) so that it will lag behind the airplane to an even greater extent. Therefore, with an increase in the speed of the aircraft V_c the path of the seat drops (if at the same time the initial velocity of the seat V_o remains constant). This can be observed in Fig.219, where examples of seat trajectories at different aircraft velocities V_c

STAT

are plotted (the positions of the seat correspond to a time approximately 0.3 sec after ejection).

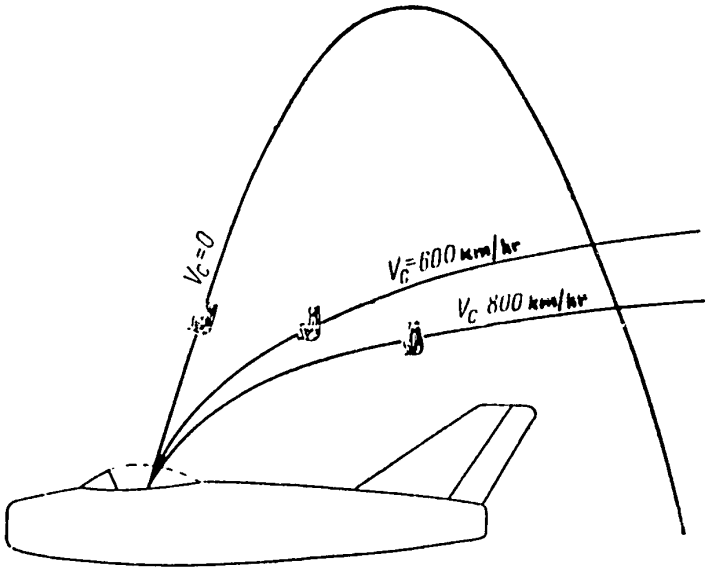

Fig.219 - Relation Between Trajectory of the Seat and Airplane Speed

The greater the speed of the aircraft V_c, the closer will the trajectory of the seat approach the tail assembly.

In addition to being influenced by the speed of the airplane, the trajectory of the seat is also greatly affected by the initial velocity V_o. The higher V_o, the higher will be the trajectory above the tail assembly (Fig.220). The necessary initial velocity of ejection V_o is usually so selected that it secures the needed elevation of the trajectory over the tail assembly. Thus, an increase in the aircraft speed V_c requires an increase in the initial velocity V_o. The initial velocity V_o for fighters with an indicated speed of 800 km/hr is 10 - 15 m/sec; if the speed of the airplane is increased to 900 - 1000 km/hr, the required velocity V_o may reach 20 m/sec.

At a constant aircraft speed V_c and initial velocity V_o, the path of the seat may be elevated by increasing the weight G of the seat and by decreasing the drag

STAT

of the seat (which is proportional to $C_D F$) and its lift usually directed downward (and proportional to $C_L F$). Therefore, streamlined seats with a higher value of the ratios $\frac{G}{C_D F}$ and $\frac{G}{C_L F}$ are most favorable. This is particularly apparent at high speeds.

The angle of inclination χ of the seat (see Fig.218) has very little effect on the height of the trajectory. The most effective magnitude for ξ is 5 - 20°.

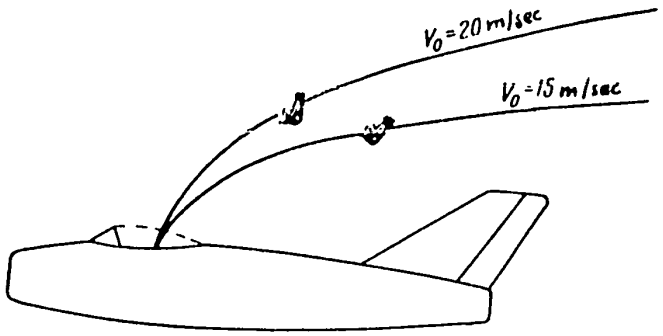

Fig.220 - Relation Between the Seat Trajectory and Initial Velocity of the Seat

The greater the initial velocity of the seat V_o, the greater will be the elevation of the seat path above the tail assembly.

In relation to the aspects of a given flight, it must be noted that, as far as the height of the trajectory is concerned, a curvilinear flight is usually not more dangerous than a horizontal flight. This is due to the lower speed in a curvilinear flight. In a dive, the distance by which the seat is separated from the tail assembly is 15 - 20% greater than in a horizontal flight and, thus, is more favorable.

Acceleration During Ejection

The required initial velocity V_o is acquired by the ejected seat during a comparatively short time which is equal to the power stroke of the ejector mechanism s_o (see Fig.218). Therefore the seat moves in the guide rails at high acceleration. This produces brief but large G-forces which act on the seat and the pilot. At a given power stroke s_o, the overloads will be proportional to the required magnitu

of the velocity V_o. G-forces produced during ejection, tend to exert excessive loads on the spine.

Figure 221 shows the maximum overloads n_g (the weight of the pilot is not taken into consideration), which can be endured by man, depending on the duration and the direction of their action. During ejection, the pilot can withstand brief overloads

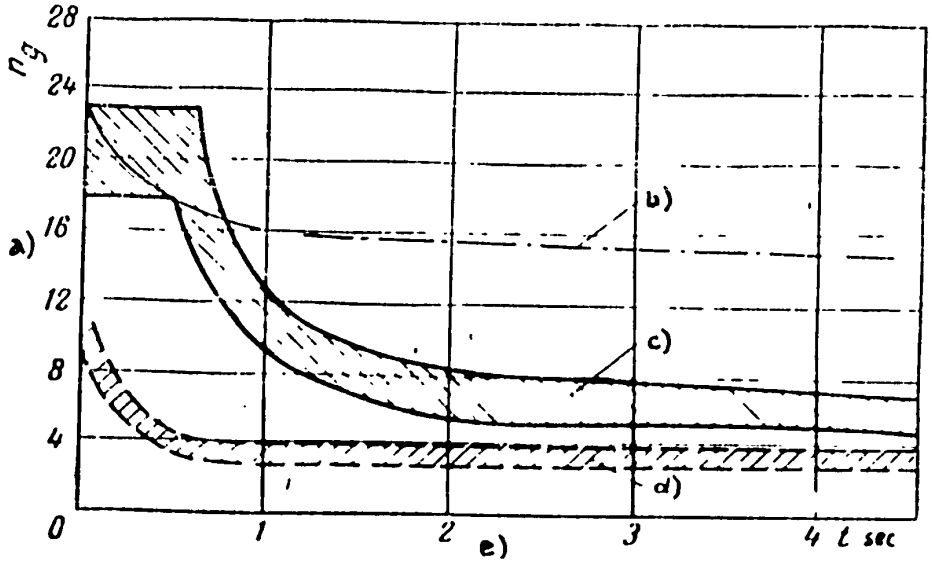

Fig.221 - Maximum G-Forces n_g Withstood by Man

The magnitude of n_g depends on the duration and direction of their action.

a) Tolerated overload n_g; b) Spine-to-chest; c) Head-to-pelvis; d) Pelvis-to-head; e) Duration of action

acting in the direction of head → pelvis as high as 18 - 20 G and, in case of a special construction of the seat (see later), even up to 28 G. Ejection seats are designed for the average pilot, and therefore overloads during ejection must not exceed 18 - 20 G. Such G-forces, due to their brevity (0.1 - 0.2 sec), can be withstood by the average flight crew without harmful effect.

It could have been possible to decrease the overloads produced by ejection by extending the power stroke s_o, during which the seat gains speed, but the stroke is limited by the height of the cabin and is ordinarily equal to 0.7 - 1.0 m. With

such a power stroke and the overloads mentioned above, the initial velocity V_0, necessary at high-speed flights, is reached.

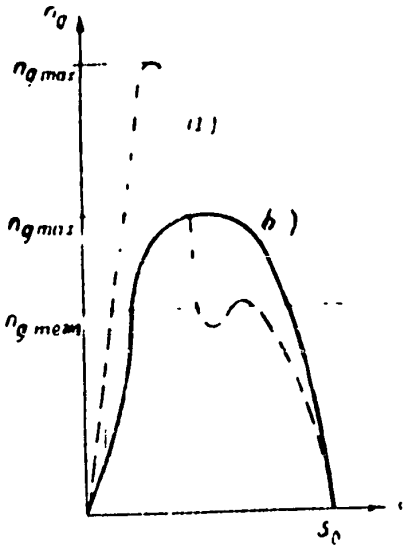

Fig.222 - Diagram Showing the Overloads n_g on the Seat During the Piston Stroke s_0.

In case of an unfavorable diagram (a) the pilot will experience greater accelerations n_{gmax}.

Since the magnitude of the initial velocity V_0 depends on the average acceleration in the process of ejection, it is a prerequisite to avoid any fluctuations in the acceleration and, therefore, avoid overloads (Fig.222a), striving for a smooth increase and decrease of overloading throughout the entire stroke of the piston (Fig.222b), i.e., an attempt should be made at increasing the magnitude of η (the coefficient of acceleration) during a full stroke. This would tend to decrease the maximum overload n_{gmax} during ejection.

The magnitude of the maximum overload n_{gmax} is connected with the initial velocity V_0, the power stroke s_0, and the coefficient η by the following relation

$$n_{g\,max} = \frac{V_0^2}{2g\eta s_0}, \qquad (107)$$

from where

$$V_0 = \sqrt{2g\eta n_{g\,max} s_0}. \qquad (108)$$

Therefore, at a given velocity V_0 it is possible to decrease the overload n_{gmax} by increasing the power stroke s_0 and the coefficient η. But if it is necesSTAT to

increase the initial velocity V_o without, at the same time, increasing the overload n_{gmax} (for instance, in connection with an increase of the flying speed), this can be accomplished by enlarging the power stroke s_o and the pressure coefficient η.

The product $n_{g\ mean}\ s_o$ (where $n_{g\ mean} = \eta\, n_{g\ max}$) is an important characteristic of the ejector performance, and its magnitude is equal to the distance of the free fall of an object during which the velocity V_o is attained. The influence of the overload $n_{g\ mean}$ and of the power stroke s_o on the magnitude of the initial velocity V_o is exactly identical.

The Influence of the Air Stream During and After Ejection

Even while the seat is moving along the guide rails, the face and body of the pilot, as they emerge from the cabin, are subjected to the impact of the air stream, moving at the speed of flight. In an air stream of such velocity the pilot remains for only about 0.1 sec, until the seat disengages itself from the guide rails. After that, the movement of the seat is greatly retarded and the speed of the air jet diminishes. At indicated speeds lower than 800 km/hr, a direct impact of the air stream on the face produces heavy loads which, however, are tolerated without harmful consequences or ill effects. At flying speeds over 800 - 850 km/hr, the pilot's face must be protected during ejection.

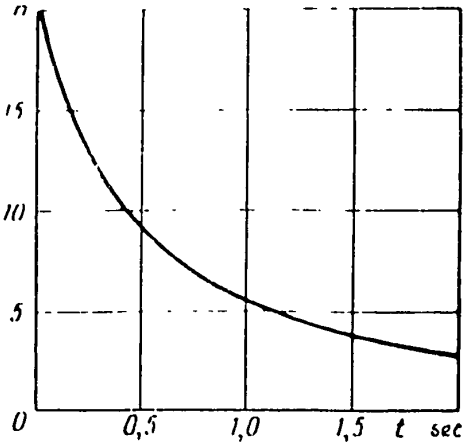

Fig.223 - Overloads Caused by Abrupt Deceleration of the Velocity of the Seat in the Air Stream

The G-forces reach their maximum at the instant the seat leaves the guide rails and then diminishes sharply.

Due to the abrupt deceleration of the seat in the air stream, considerable accelerations are produced in the direction of flight and in the corresponding

STAT

forces of inertia. Forces of inertia, equal in magnitude to the aerodynamic forces acting on the seat, produce heavy acceleration in the back-to-chest direction. This overload reaches its greatest magnitude at the instant the seat clears the guide rails and then diminishes abruptly (Fig.223). Near the ground, at a velocity of 900 km/hr, the magnitude of the overload due to the braking effect may be about 20G. This magnitude of G-forces despite their brevity, is near the maximum (see Fig.221). With an increase in altitude, the rarefaction of the air causes a reduction in the forces that produce the braking effect on the seat and, accordingly, a decrease in the overloading. Overloading due to the braking effect may be reduced by increasing the weight G of the seat and by streamlining its form (decreasing the braking effect), i.e., by increasing the relation

$$\frac{G}{c_x F}.$$

After the seat leaves the cabin, besides the phenomena just discussed, a sharp deceleration of the upward movement takes place, produced by the gravity of the seat and by the negative lift (directed downward). As a result, the overload which, during the ejection, acted in the head-to-pelvis direction changes its sign to the negative and, after the seat is ejected, acts in the pelvis-to-head direction. These overloads usually are not great (about 4G), and are brief (less than one second), but they act in the most unfavorable direction (see Fig.221).

After the seat leaves the cabin, it may start rotating about its lateral axis. This is produced by the moment of the aerodynamic forces acting on the seat and, also, by the initial moment of the eccentrically applied ejection forces, and by the action of aerodynamic forces on the upper part of the seat during ejection. The magnitude of the angular moment depends greatly on the height of the headrest. If the height of this headrest is chosen correctly, the rotation is not great and does not lead to unfavorable consequences.

STAT

Ejector Seat Mounts

An ejection seat (Fig.218), as previously stated, consists of a seat, guide rails, and the ejector mechanism.

An ejection seat is designed to assist in counteracting the heavy overloads during ejection. For this reason, the seat is supplied with a footrest, hand rails, and an inclined backrest with a headrest. Before ejection, the pilot raises his feet, places them on the footrest, grasps the hand rails, and leans on the backrest thus considerably relieving the spine of overloads. In order to decrease overloads and to soften the impact, the seat, backrest, and headrest are covered with elastic cushions. With the use of such devices the maximum overload, tolerated by man, is increased to 28G with the duration of its action being equal to ~ 0.015 sec.

Placing the feet on the footrest relieves the pelvis of large loads, prevents catching the legs on some part of the cabin during ejection, and decreases the drag of the seat and of the pilot on reaching the air stream. An inclination of the seat, best for relieving the spine, is chosen. The pilot must strap himself to the seat securely with the shoulder harness to prevent his body from leaning forward during ejection under the action of inertia forces. At the same time, the shoulder harness must not be too tight since this would cause an additional compression of the spine.

To decrease overload during deceleration and to elevate the trajectory of the seat, it is desirable to streamline its form.

Ejectors may be pyrotechnical (operated by explosion of a cartridge) or pneumatic (operated by a tank with compressed air). The advantage of a pyrotechnical mechanism over the pneumatic type lies in its small weight and simplicity of design. But pyrotechnical mechanisms have less stable operating characteristics: at low temperatures the time of explosion is increased and, therefore, the initial velocity V_0 decreases. Since the temperature changes in the cabin during flight are not great, this drawback of cartridges has no practical significance. STAT

Careful testing of all the elements of ejection seats and a control of the high quality of their manufacture guarantee reliability of their functioning.

The ejection seats described above can be effectively used at velocities of about 900 km/hr, at low altitudes. At greater altitudes, this maximum speed also increases.

Possibilities of Ejection at Higher Flying Speeds

The method of ejection described above is restricted to flying speeds of the order of 900 km/hr for the reasons discussed below. If these causes could be eliminated, this limiting speed could be increased.

1) On increase in the flying speed, the elevation of the seat trajectory above the tail assembly becomes smaller. Elevation of the trajectory by increasing the initial velocity V_o, without at the same time enlarging the overloads, demands an elongation of the power stroke of the ejector s_o. Since the height of the cabin is limited, the use of telescoping ejector mechanisms, together with an increase in the coefficient η by using a cartridge train may be the solution to this problem.

An elevation of the trajectory may be achieved by increasing the weight of the seat (at a simultaneous increase of the power of the cartridge) and by improving the streamlining of the seat, i.e., by increasing the ratio $\frac{G}{C_D F}$.

In aircraft with vertical tail surfaces, the elevation of the trajectory can be decreased so that, with this type of tail assembly, the flying speed can be increased, which would allow ejection without increasing the initial velocity V_o and the overloads.

Ejection downward requires smaller initial velocities and, therefore, permits a considerable reduction in the overloads; for this reason, ejection downward can be used at much greater velocities than ejection upward.

2) At high flying speeds, the impact of the air stream on the face is painful. This can be eliminated by the use of a special blind, pulled down in front of the pilot's face during ejection and protecting him from the impact of the relative

stream.

3) With the increase in flying speeds, the overloads from the braking effect of the air stream increases. The fight against such overloads is very difficult. Some results may be obtained if the weight of the seat is increased and its streamlining made more perfect (an increase in $\frac{G}{C_D F}$).

4) As the velocities increase, the rotation of the seat becomes more intensified. This may produce large additional overloads due to the centrifugal force. In this respect, a forward rotation is the most unfavorable. Rotation of the seat can be prevented by means of a small auxiliary parachute, attached to the upper part of the seat and opening automatically as soon as the seat leaves the cabin.

In this manner, although increasing flying speeds make ejection of the crew more difficult, these difficulties can be overcome. By making use of the measures discussed above, which tend to decrease the difficulties of ejection at high speeds, it is possible to employ ejection seats up to speeds near the velocity of sound.

Flying at supersonic speeds would require closed, detachable cabins, and also discovery of an effective means for decreasing the speed of the aircraft.

STAT

CHAPTER XI

LANDING GEAR

Landing gears serve for taxiing, for take-off runs, and for landing runs. Also, the landing gear must absorb the kinetic energy of the aircraft during touch-down.

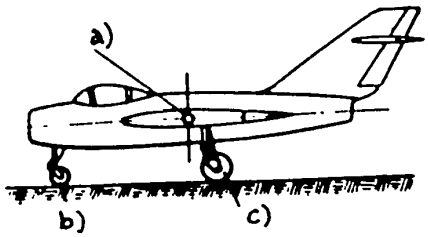

Fig.232 - Landing Gear Diagram of a Modern Aircraft

The main wheels are placed slightly behind the center of gravity of the aircraft, and the nose wheel is carried far ahead.

a) Center of gravity of aircraft;

b) Nose wheel; c) Main wheel

The predominating landing-gear type in modern high-speed aircraft is a retractable tricycle landing gear with a nose wheel (Fig.232). In this type, main wheels are placed slightly behind the center of gravity of the aircraft, and the front wheel is carried far toward the nose.

Retractable landing gears make it possible to decrease the drag of the aircraft in high-speed flights. At the same time, they somewhat complicate the structure and increase the weight. Landing gears with a nose wheel were used even in the early years of aeronautical development (Ufimtsev's spheroplane, 1909), with the nose wheel having the function of an anti-nose-over device. Landing was performed on the two landing gear wheels and the tail skid. After some time this anti-nose-over device went out of use. This can be attributed to the fact that

nose of the fuselage was built quite short and, therefore, the nose wheel was placed very near the main wheels. This caused frequent failures of the front landing gear strut due to heavy loads. Moreover, this short distance led to rocking of the aircraft and created the danger of wing-over (ground loop).

A diagram of a landing gear with nose wheel was revived in the Thirties, since it had some advantages over a landing gear layout with a tail wheel or a tail skid. The presence of a nose wheel permits applying the brakes more fully in order to shorten the landing run. Here there is no danger of nose-over. The existing landing gear types do not require a very exact landing performance. In fact, no matter what the landing speed may be, reactions of the main wheels will always rotate the aircraft so as to diminish the angle of attack of the wing. This will

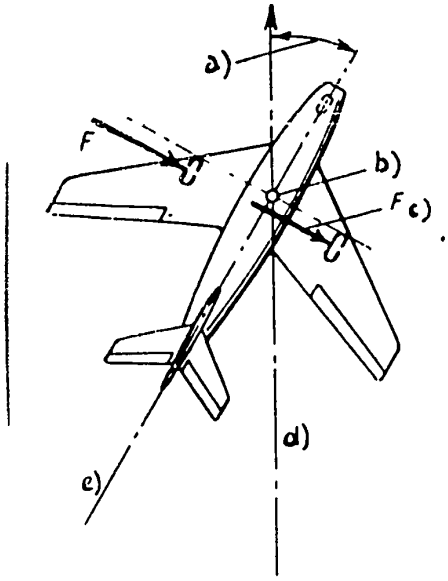

Fig.233 - Landing of an Aircraft with Drift.

Since the direction of motion of the aircraft does not coincide with the plane of symmetry, the wheels of the landing gear will be loaded with lateral forces F.

a) Angle of crab; b) Center of gravity of aircraft; c) F = force of ground reaction; d) Direction of motion of aircraft; e) Axis of aircraft

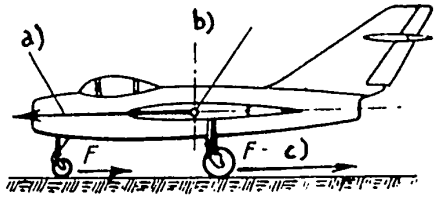

Fig.234 - Motion of the Aircraft

The forces of friction F and the force of inertia N_1 of the aircraft form a couple which forces the aircraft to nose over.

a) N = force of inertia; b) Center of gravity of aircraft; c) Force of friction

lead to a decrease in lift, forcing the aircraft closer to the ground. A lower value of lift during the run insures greater normal loads on the wheels, and, STAT

therefore, greater friction forces. It is true, however, that the length of the run is negatively affected by the fact that the head resistance of the aircraft is small in this case because of negligible angles of attack.

Finally, statements are required on the presence of directional stability during runs over an airfield. If, for some reason, the aircraft moves with a crab (Fig.233), either in case of landing with a cross wind or if the landing gear strikes an obstacle asymmetrically, the lateral forces of the main wheels will decrease the angle of crab. No lateral forces are created in the nose wheel since the front strut is designed as the swiveling type, i.e., it can rotate freely. A tricycle layout of the landing gear has two disadvantages.

1. When an airplane moves over a rough runway, the nose wheel surmounts ditches and hillocks with greater difficulty than the tail wheel. This is due to the fact that the friction force F and the inertia N (Fig.234) of the aircraft form a couple which forces the nose down and causes the nose wheel to be pressed hard to the ground.

2. When an aircraft runs along the runway at a high speed, self-oscillations of the front strut may occur (shimmy phenomenon), whose physical aspect is described below.

Self-Oscillations of the Front Strut of a Landing Gear

The front strut of the aircraft may always perform two independent types of motion, i.e., it has two degrees of freedom (Fig.235). First, the wheel (since it is able to swivel) can turn through some angle γ about its vertical axis. Secondly, the wheel (or, more correctly, the point of its contact with the ground) can deviate from the direction of motion to a certain magnitude y. This motion is caused mainly by the elasticity of the tire, and partially by the elasticity of the strut, and as a result of crabbing of the aircraft nose. From here on, in order to simplify our reasonings, we will consider only the elasticity of the strut.

The two indicated degrees of freedom create the possibility of transverse STAT

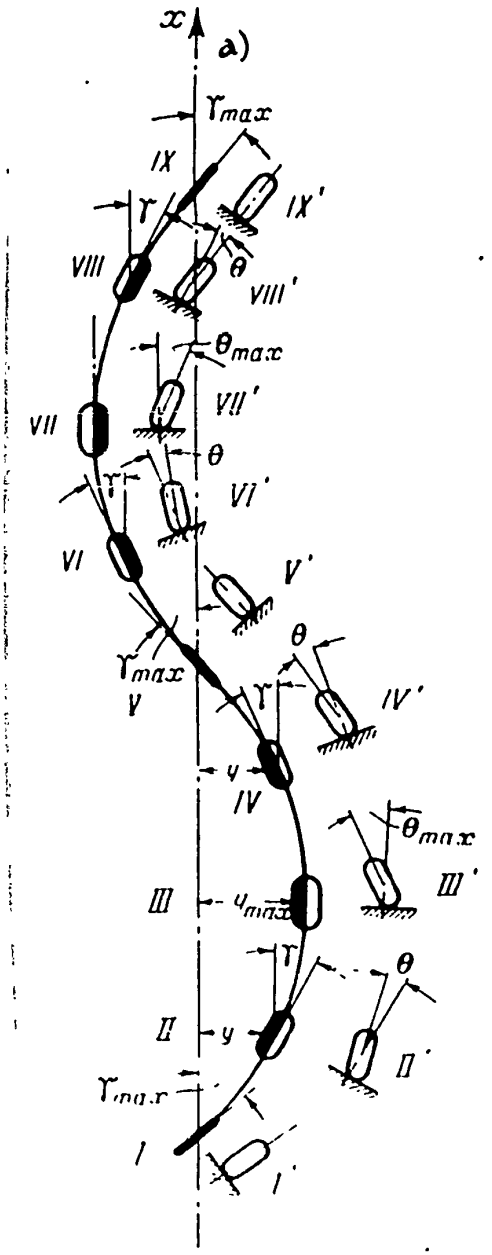

Fig.235 - Diagram of Self-Oscillations of the Front Strut of the Landing Gear

Due to the presence of the initial angle of drift, the wheel vibrates with respect to the direction of motion of the aircraft.

a) Direction of motion of aircraft

oscillations.

Figure 235 shows a diagram of kinematic transverse oscillations, i.e., oscillations due to the lack of possibility of the wheel to turn in a plane parallel to the ground (i.e., relative to the vertical axis), without advancing motion. Moreover, it is assumed that the wheel cannot have any advancing motion in a direction perpendicular to its plane.

Let us assume that while the airplane moves along the x-x axis, the wheel, under the action of external forces, turns to make a certain angle γ_{max} with it (position I). In such a case, the wheel will tend to move at an angle of γ_{max} with respect to the motion of the aircraft. If, during the first moment of motion of the turning wheel (at y = 0), the plane of the latter is normal to the ground (I'), in the consecutive moments (y greater than 0) the wheel will tilt so as to form a certain angle Θ (II').

In Fig.235, the positions of the wheel, placed on the right side (I', II' etc.), demonstrate its inclination with respect to the vertical (angle Θ). STAT

Due to the presence of the angle θ (position II'), the point of intersection of the wheel axis with the plane of the ground, with respect to which the wheel is turning, will not be located at infinity, and the wheel while deviating from the path x-x (enlarging of y) will turn so as to decrease the angle γ. At a certain moment, the wheel will occupy the point of greatest deviation III ($y = y_{max}$ $\theta = \theta_{max}$), and the angle γ will be equal to zero.

Starting with position III, as a result of the presence of the same angle θ, the wheel will begin to approach the axis x-x, i.e., y and θ will become smaller and the angle γ will increase in magnitude but only with a negative sign. At the moment of intersection of the axis x-x by the wheel (position V) the angle θ will be equal to zero, and the angle γ will have its maximum negative value. All further positions of the wheel (VI - IX) represent a mirror image, on the left side, of the first five positions.

It can be concluded from the above diagram that, during self-oscillations, the front strut will execute harmonic oscillations.

Under real conditions, the angular distances γ and the lateral shifts y will be performed with variable speeds, and, therefore, with acceleration. Due to these accelerations, the strut will be loaded with forces of inertia.

Moreover under real conditions, sideslip also occurs. Because of the presence of inertia forces, elasticity of the tire, and possible sideslip, the self oscillations at high speed may proceed with an increasing amplitude (up to y_{max}), which might lead to detachment of the tire, breaking of the front strut, and to other troubles.

In order to damp the oscillations of the front strut, a vibration damper is mounted to it in which, with every turn of the wheel, a fluid flows through a small aperture from one container into another. The energy of oscillation of the front strut is thus transformed into heat, and as a result the vibrations are damped.

The most complete and thorough research data on self-oscillations of the fro

strut can be found in the book of Academician M.V.Keldish "Shimmy of the Nose Wheel", which was honored with a Stalin prize.

Section 43. Basic Requirements of a Landing Gear

The basic requirements made on a landing gear are as follows:

1) Ensure free movement and maneuvering of the airplane on the ground. In order to improve the maneuverability of the aircraft, the wheels are supplied with brakes, and the nose wheel is made to swivel (braked wheels tend to shorten the length of the runs).

2) Sufficient strength of the landing gear to satisfy all design cases which are foreseen by the normal strength requirements.

3) Possibility of absorbing the kinetic energy of the tires and shock struts, with relatively small overloading.

4) Minimum drag in flight, which is obtained by using a mechanism for retracting the landing gear.

5) Absence of nose-over tendency, sufficient stability, and controllability of the aircraft during its motion on the ground. All these requirements are satisfied by a rational layout of the landing gear on the aircraft.

The layout of the landing gear is defined by the basic geometric parameters, which are described in Fig.236: the stagger of the main wheels e, the wheel base b, the track gage B, and the height of the landing gear h.

The stagger of the main wheels must be very small so as to decrease the loads acting on the front strut. But at the same time the stagger must allow the plane to take its parking position at any landing. This is insured by making

$$\beta_{\text{з}} \cdot \varphi.$$

For real aircraft, the following relationship exists:

$$\frac{e}{b} = 0{,}1 - 0{,}15.$$

STAT

Since $e = h\,tg\beta$, the ratio $\frac{e}{b}$ can be diminished by increasing the wheel base b, lowering the center of gravity h of the aircraft, and decreasing the angle β.

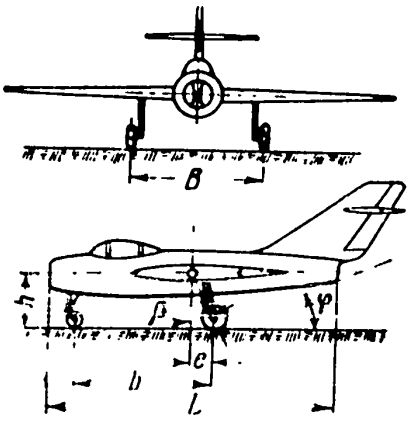

Fig.236 - Layout of the Landing Gear

Basic geometric parameters: e - Stagger of the main wheels; b - Wheel base; B - Track gage; h - Height of landing gear.

Increasing of the wheel base b is usually attained by elongating the nose section of the fuselage and, partially, by carrying the front strut forward. Generally,

$$\frac{b}{L} \approx 0{,}25 \div 0{,}35,$$

where L is the length of the fuselage.

Lateral directional stability and controllability of the aircraft when taxiing on the ground depend on the track gage of the landing gear B. For greater lateral stability and increased maneuverability of the aircraft on the ground, greater track gage is desirable; this will reduce swaying of the airplane, permitting the use of softer shock absorbers. But the directional stability of an aircraft with a wide track gage is impaired. This is explained by the presence of the arm formed by the wheels with respect to the center of gravity of the aircraft which, in case of a rough runway, will create large torsional moments. A wide track gage is not advantageous from the point of view of the strength of the wing, as this will cause excessive bending. In modern airplanes, the track gage fluctuates between 20 and 32% of the wing span. In multiengine aircraft the track gage is usually determined by the position of the engine nacelles.

The distance of the center of gravity from the ground is determined by the height of the landing gear. The height chosen for the landing gear is such that, during a three-point landing of the aircraft, the wing has a landing angle of attack. Sometimes the height of the landing gear is determined by the minimum

STAT

allowable distance of the lower tip of the propeller blade from the ground.

In the general case, any landing gear forms a three-dimensional energy diagram with an axis to which the wheel is mounted. The shock absorber will be within this energy diagram.

Section 44. Bicycle Type Landing Gear Diagram

High-speed jet aircraft have a relatively thin airfoil. This very often creates unsurmountable difficulties if the main wheels of the landing gear have to

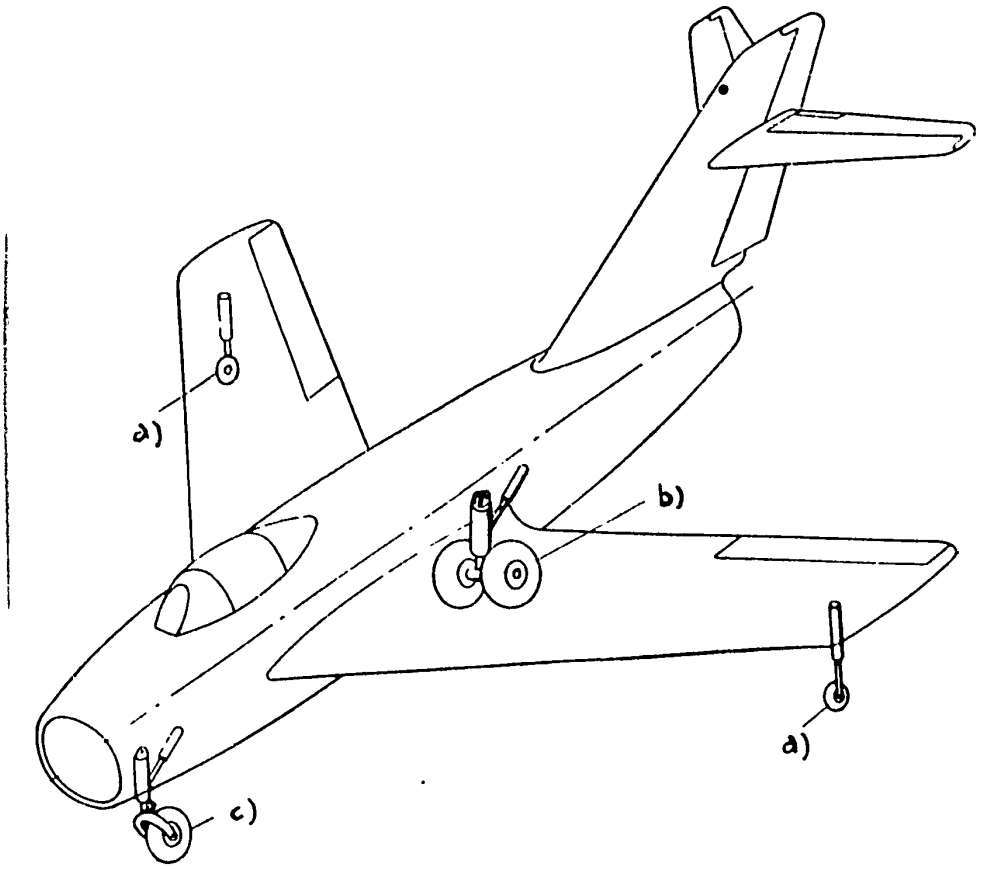

Fig.237 - Bicycle Type Landing Gear

The main wheels are placed under the fuselage.

a) Wing-tip wheel; b) Main wheel; c) Nose wheel

be retracted into the wings. The mounting of special bays or wells for the retraction of the landing gear impairs the aerodynamics of the aircraft.

STAT

The disadvantages and difficulties of main-wheel retraction pointed out above are eliminated in some aircraft by the use of bicycle landing gears. In this layout, the main wheels are not placed (Fig.237) under the wings but under the fuselage, into which they are retracted. Therefore, the basic difference of this layout from the usual one is the almost zero track gage of the landing gear. This last fact deprives the aircraft of lateral stability during taxiing on the ground and does not permit maneuvering of the aircraft with the help of the main-wheel brakes of the landing gear.

Lateral stability of an aircraft with a bicycle landing gear is attained by mounting relatively light-weight shock struts under the wings (wing-tip wheels, Fig.237). Maneuvering of the aircraft on the airfield, especially at low speeds, when the tail unit is not effective, is achieved with a controllable nose wheel (controllable nose wheels are also encountered in ordinary landing gears).

It must be noted that lateral stability of an aircraft at high taxiing speeds is present even without the wing-tip wheels, as a result of the action of the aerodynamic forces of the wing. Also, the bend of the wing makes the air-gap between the ground and the wing-tip wheels large enough so that they will not strike a rough runway. Wing-tip orienting struts make contact with the runway when the aircraft is parked and when it moves at low speeds.

The presence of a bomb bay in the fuselage makes it necessary to mount the main wheels of the landing gear in bombers far behind the center of gravity of the aircraft. This increases the loading of the nose wheel considerably and does not permit the aircraft to move on its main wheels alone. Consequently, both take-off and landing of an aircraft must be performed with the help of the nose wheel, in conjunction with the main wheels.

In order to be able to use the $c_{y\ max}$ of the wing during landing and to perform the take-off at the most advantageous angle of attack, turning wings and extension landing gears are used. With a turn of the wing or extension of the landing

STAT

gear the aircraft can move over the runway under different angles of attack.

Section 45. Landing-Gear Wheels

Landing-gear wheels ensure the roadability of the aircraft and absorb the shock energy with their tires. The main elements of the wheels are the wheel rim and the tire. The rim (Fig.238) is usually cast from an aluminum or magnesium alloy. It is cast together with the hub.

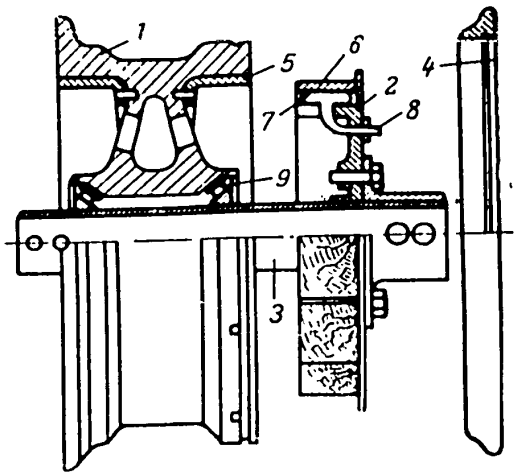

Fig.238 - Landing Gear Wheel

1 - Wheel rim with hub; 2 - Brake disk; 3 - Wheel axis; 4 - Removable rim; 5 - Brake jacket; 6 - Brake blocks; 7 - Brake chamber; 8 - Air intake pipe; 9 - Ball bearings

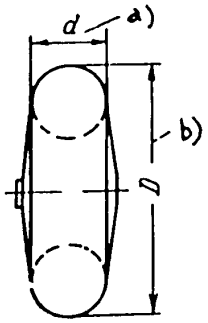

Fig.239 - Wheel and Tire

A wheel has two characteristic dimensions: the outside overall diameter D of the wheel and the diameter of the cross section of the tire d.

a) Diameter of tire; b) Diameter of wheel

For convenience in mounting and stripping the tire, one of the rims is removable. Roller bearings are mounted inside the hub. All modern wheels are supplied with brakes, whose disks are fixed on the axis; the steel brake-drum jacket is pressed into the rim. Brakes may be of the following three types: tire brakes, block brakes, and disk brakes. Brakes are mostly either pneumatically or hydraulically controlled.

STAT

Wheels have two characteristic dimensions (Fig.239): overall outer diameter D of the wheel and diameter of the cross section of the tire d.

Types of Wheels

Wheels in use at the present time may be subdivided into three types:

a) high-pressure wheels;

b) low-pressure wheels (Balloon type);

c) medium-pressure wheels (semiballoon type).

High-pressure wheels have a tire with a small diameter (d) and a high pressure of the preliminary charge (about 8 atm). They can be used on airfields with hard soil. Under these conditions, the wheel will have a small area of contact with the ground. One of the defects of such wheels is that, due to the small volume of the tubes, they do not absorb shocks very well; moreover, they sink too much into swampy ground, which in turn hinders take-off and may cause nose-over during landing. Tires with superhigh pressure can be also grouped with this type. Their preliminary air charge may be 10 or more atmospheres. High-pressure wheels because their overall dimensions are small, can be retracted more easily into an aircraft.

Low-pressure wheels have a larger tire diameter (d) and, therefore, a larger volume of air, which helps them to absorb more kinetic energy. The roadability of such wheels is greater than that of wheels with high pressure, because of low unit pressure (less than 3 atm). Such tires are rarely used because of their large overall size, which makes their retraction into the aircraft during flight, quite difficult.

Medium-pressure wheels have all the good points and all the defects of the first two types. They are used predominantly in our country. The pressure in the tires of these wheels ~ 3–4 atm.

On wheels with small diameters, chamber brakes are generally used. Block brakes are mounted on large wheels. Friction-disk brakes are used on some wheels.

The basic requirements of brakes are as follows: STAT

dependability of performance;

speed of braking and brake release;

simplicity and comfort of operation.

Tire Performance

A complete tire performance characteristic is given in the diagram showing the load P_w, acting on the wheel, as a function of elongation of the tire δ at different values of the preliminary charge. Figure 240 shows a simplified diagram of this dependence.

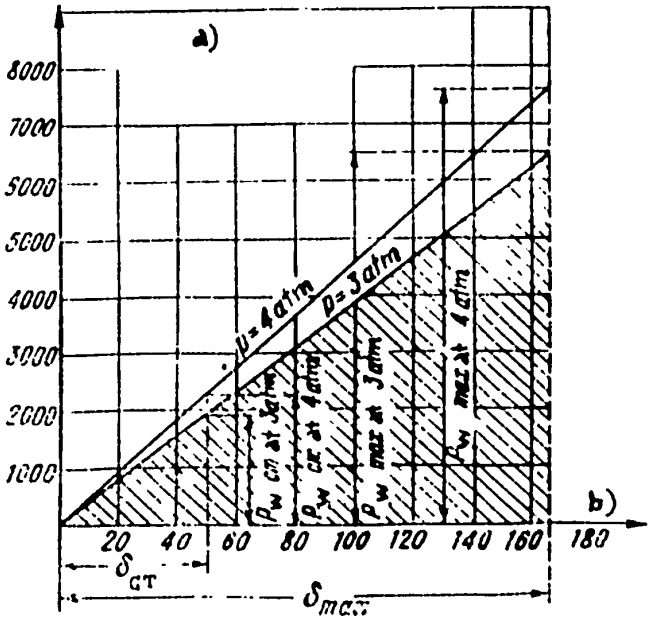

Fig.240 - Wheel Characteristic D/d = 750/250

With the growth in the load acting on the wheel, deflation of the tire δ increases (lowering of the wheel axis). The shaded area of the triangle represents the work A_{ti}, absorbed by the tire during its deflation. When the tire has a preliminary charge of p = 3 and is fully deflated $\delta_{max} \approx$ 170 mm; $A_{ti\ max}$ = 552 kg-m.
In the diagram δ_{ct} is the deflation of the tire, which is desirable during parking.

a) $P_{w\ kg}$ - load on the wheel 750/250; b) δ mm - deflation of the tire

It can be seen from this diagram that the load P_w acting on the wheel, in relation to the deflation of the tire δ, changes according to a rectilinear law

STAT

(from the pressure p). The hatched area of the triangle shows the work A_{ti}, absorbed by the tire during deflation. The work done is the product of force times distance. In our case, the force is the loading P_w of the wheel and the distance is the deflation of the tire δ. Therefore, the work must be approximately equal to the product

$$P_w \cdot \delta.$$

This would have been true only if the force P_w would have been permanent in value throughout the whole of the path δ. Since the loading of the wheel P_w throughout the path δ (deflation) differs from zero, the work done can be calculated only by using the product of the mean value of P_w times δ. The mean value of the load acting on the wheel will be equal to one half the greatest value of P_w. For this reason A_{ti} is expressed in the following manner:

$$A_{ti} = \frac{P_w \delta}{2}. \qquad (115)$$

It may be seen from this diagram that, at a lower preliminary charge and at the same deflation the tire will do less work. But if two wheels are loaded with an equal load P_w the greater work A_{ti} will be done by the wheel, which will have a lower pressure. The greatest amount of work will be absorbed by the tire at its full

$$A_{ti\ max} = \frac{P_{w\ max} \delta_{max}}{2} \qquad (116)$$

In this way, the work absorbed by the tire depends completely on the magnitude of its deflation δ and the load acting on the wheel P_w.

The main wheels of an aircraft are selected according to a standard, depending on the deflation on parking δ_{ct} and the parking load $P_{w.ct}$. The deflation on parking δ_{ct} is determined by the conditions of the life of the tires and prevention of their detachment by lateral forces.

STAT

According to the standard

$$\delta_{ct} \approx 0.2 - 0.25 \text{ for d}, \tag{117}$$

$$\delta_{max} \approx 0.7\ d. \tag{118}$$

The pressure in the tires is so selected that, at a given deflation on parking, the wheel load according to the standard would equal the real parking load.

The relation between wheel loading at maximum deflation of the tire to the parking loading $(\frac{P_{w\ max}}{P_{w\ ct}})$ is called the coefficient of load carrying capacity of the wheel.

In order to make utmost use of the wheels on landing, it is necessary to use an acceleration coefficient of operation n_E^e close to the load carrying capacity of the wheel. Then, in case of a rough landing, the greatest loading of the wheels will equal $P_{w\ max}$, and the tire will be deflated to such an extent, that any further increase in this force will not diminish the volume of air in the tire.

STAT

CHAPTER XII

SHOCK STRUTS

Section 46. Designation of Shock Struts

During the landing of an aircraft, at the instant its wheels touch the ground, the path of motion of the center of gravity is somewhat inclined; in addition to the horizontal speed component there is also a vertical component. The horizontal velocity component is damped during the landing run L_{run} due to the drag of the aircraft and the forces of friction caused by the movement of wheels over the ground. The vertical velocity component is damped during the path s, connected with the deflation of the tire and contraction of the shock struts.

It can be demonstrated by simple calculations that the mass of the aircraft, after touching the ground, undergoes vertical accelerations which are greater than the horizontal ones. Therefore, the mass of the aircraft will experience large forces of inertia, acting in a vertical direction.

Let us assume that the horizontal velocity component V_{hor} is equal in magnitude to V_{land}

$$V_{hor} \approx V_{land} = 50 \text{ m/sec.}$$

The vertical rate of descent V_y may practically become ~2 m/sec.

But V_{hor} is damped during the path $L_{run} \approx 1000$ m, when V_y is damped during the path $s \approx 1$ m.

Therefore, the velocity ratio is

STAT

$$V_{hor} : V_y = 50 : 2 = 25.$$

And the ratio of the path

$$L_{run} : s = 1000 : 1 = 1000.$$

As a result, we find that the ratio of the paths is a magnitude many times greater than the velocity ratio. This confirms the above statement as to the magnitude of the accelerations and the forces of inertia.

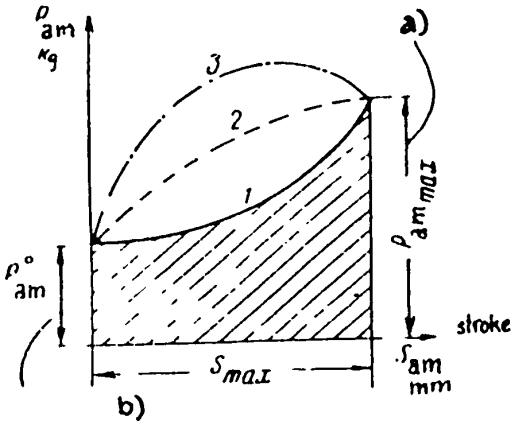

Fig.241 - Diagram of Shock Strut

The diagram shows the stresses occurring in the strut during its contraction. The hatched area represents the work done by the strut when fully contracted. Curves 1, 2, and 3 correspond to different struts.

a) Maximum stress in strut; b) Stress produced by contraction

The shock absorbers of the landing gear are designed to absorb the kinetic energy of the aircraft during landing and moving over the airfield.

The landing gear shock struts must meet the following basic requirements:

1) A shock absorber, during its power stroke, must absorb its share of kinetic energy of the shock.

2) A shock absorber must perform its work with small stresses. Moreover, the stresses in the shock absorber must increase gradually, the greatest stress coming at the end of a complete stroke.

3) In order for the shock absorber to make the succeeding stroke, it is necessary to limit the duration of the forward and reverse strokes. This time interval must not exceed 0.8 sec (maximum time for one stroke).

4) A shock absorber must have as large a lag as possible, i.e., the greater part of the absorbed work must be converted into heat, and must not return in the

STAT

form of a reaction that would cause the aircraft to swerve.

A full performance diagram of a shock absorber is given in Fig.241 which shows changes in the load P_{am} acting on the shock absorber as related to its deflation s.

This diagram contains the following characteristic values: stress of preliminary contraction $P_{am}{}^{o}$ and the maximum stress $P_{am\ max}$, which corresponds to the maximum stroke of the strut s_{max}.

The area of the shaded portion of the diagram gives the magnitude of the absorbed work (kinetic energy), since it represents the product of the mean stress of the strut (force) by the stroke (path).

The curves of Fig.241, which belong to different shock absorbers, clearly demonstrate the different character of change of loading of the strut as a function of the deflation. The smoothest growth of loading of the shock absorber is shown by curve 1, and the most abrupt by curve 3. But curve 3 is the one which absorbs most work at the same stroke of the strut.

A shock strut must never work in the manner shown by curve 3, since the greatest stresses there do not occur at the end of the stroke. As a result, large overloads will occur during landings that are not too rough, and this would lead to a premature wear of the structure.

On modern aircraft, landing gear shock absorbers consist of separate force struts of the landing gear, which are so designed that they can greatly contract under the action of external forces. Absorption of the shock takes place because of contraction of the strut's length. Such struts may be constructed with rubber, springs, or air as the shock-absorbing elements. At present, shock absorbers that are a combination of pneumatic and hydraulic chambers are used. The fluid is highly compressed in the air chamber and thus serves as an additional means of absorbing the shock. Such shock absorbers are called oleo-pneumatic.

The skeleton diagram of this type shock absorption was first developed and proposed by Prof. V.P.Betchinkin in 1921.

STAT

Section 47. Function of An Oleo-Pneumatic Shock Strut

Pneumatic Leg

In order to better comprehend the function of an oleo-pneumatic shock absorber let us first examine the working principle of a strut of the old design (Fig.242).

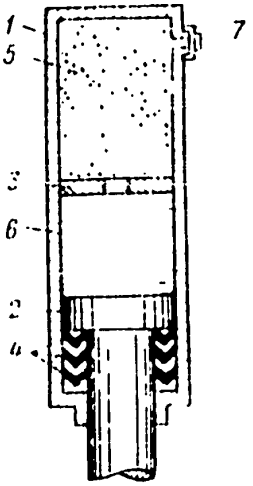

Fig.242 - Diagram of a Shock Absorber

1 - Cylinder; 2 - Piston; 3 - Diaphragm;

4 - Packing; 5 - Air; 6 - Liquid;

7 - Filler plug

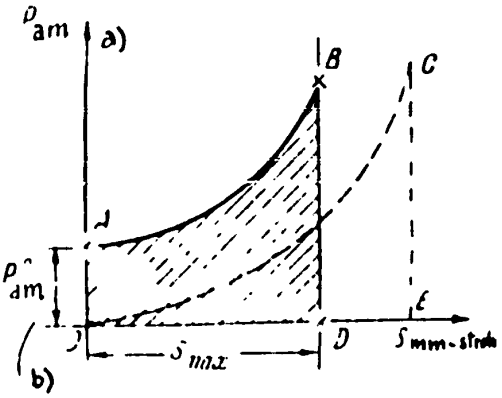

Fig.243 - Diagram of a Pneumatic Strut

If there is no diaphragm, the shock strut will work like a wheel tire with the only difference that the curve AB will not pass through the origin of the coordinates, due to the preliminary contraction.

a) Stress in the strut; b) Stress produced by compression

Let us imagine a strut charged with a fluid (6) and air (5), but without a diaphragm (3) in the cylinder. Under such a condition, the strut will work like a pneumatic tire. The work, in this case, is absorbed by the compression of air. The magnitude of the load P_{am} acting on the strut, with respect to the power stroke of the piston s will change according to the curve AB (Fig.243), which is called a polytropic curve.

In order to absorb more energy during a shorter power stroke of the leg, it is necessary to create in it a preliminary initial pressure P_o (segment OA). In reality, during the power stroke of the leg, which corresponds to the given diagram AB, the work will be expressed by the area OABD (shaded area). If the

STAT

preliminary pressure in the strut is equal to zero, the pressure diagram will have the form of the curve OC; however, then in order to absorb the same amount of energy as in the case AB, i.e., in order to absorb the area OABD, it is necessary to increase the base by the magnitude of DE, i.e., to increase the power stroke of the strut s. In other words, in case of soft shock absorption, the stroke of the strut OE must be greater than in case of rigid shock absorption.

In case no diaphragm is used, the shock strut will work like a wheel tire. Such a strut will have a small hysteresis, which does not satisfy one of the requirements made on shock absorbers. In this design, the air first stores the work and then gives it off again. The nature of the change of the working diagram depends very little on the rate of contraction of the strut.

Hydraulic Leg

Let us examine the function of a strut filled with a fluid and having a diaphragm in the cylinder, but with an open filler plug (7) (see Fig.242). It is clear that when the strut contracts, the pressure of the air (5), which communicates with the outside atmosphere, will not change; therefore, the strut will operate like a hydraulic leg. The whole of the shock energy will be expended on overcoming the hydraulic resistance during the flow of this fluid through the opening of the diaphragm. All the energy will be converted into heat and the strut will not return to its initial, straight position. Therefore suc

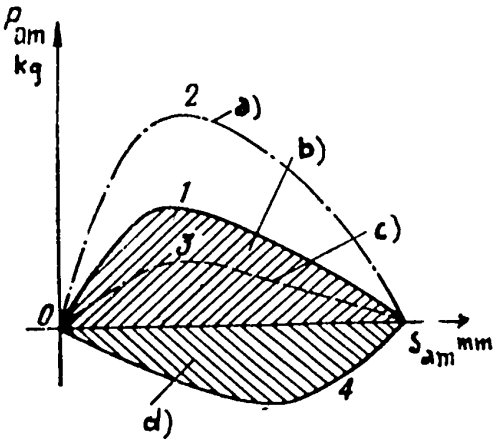

Fig.244 - Diagram of a Hydraulic Strut

The shaded area is the work done by friction, which is absorbed by the strut because of the flow of the liquid through the opening in the diaphragm.

a) Small orifice; b) Work during power stroke of strut; c) Large orifice; d) Work during idling stroke of strut

a strut has a larger hysteresis than a purely pneumatic one.

Let us see what factors are influencing the diagram that shows the dependence of the force P_{am} on the stroke of the strut s (Fig.244), for the case of a purely hydraulic shock absorber.

The force that forces the fluid through the opening in the diaphragm depends on the hydraulic resistance of the liquid. This resistance is proportional to the square of the rate of flow of the liquid and inversely proportional to the area of the cross section of the opening through which it flows. The initial and end velocity of the strut contraction are equal to zero; therefore, the force P_{am}, which is necessary for strut contraction, is also equal to zero at the beginning and the end of the stroke. As demonstrated by research, the rate of the strut contraction and also the force P_{am} increase rapidly in the beginning in magnitude and then start to decrease gradually. For this reason, the diagrams showing the dependence of P_{am} on s have the form of the curves shown in Fig.244.

With respect to the dependence of the hydraulic resistance of the fluid on the cross-sectional area of the orifice, it is expressed in the following manner: If the cross-sectional area of the orifice is small, the curve of P_{am} as a function of s is much steeper (curve 2). Therefore, here the stresses in the strut will be much greater in magnitude and they will increase very rapidly. As the cross-sectional area of the orifice in the diaphragm increases, the diagram will correspondingly lower (curve 3). In modern aircraft, the area of the orifice is equal to about 2% of the area of the piston. The form of the orifice also has an influence on the magnitude of the stresses in the strut P_{am}. The viscosity of the liquid has an effect of the same kind.

If there are forces which return the piston of the strut to its initial position, some additional work will be spent on this. In such a case, P_{am} has a negative value (curve 4).

The character of the curve P_{am} as a function of s will change in accordance

STAT

with the roughness of landing, on which the rate of the strut contraction depends.

In designing a shock strut, measures can be taken to influence the slope of the curve P_{am}. This is achieved by changing the cross-sectional area of the orifice with the help of a metering pin (Fig.245), which moves together with the piston through the orifice in the diaphragm.

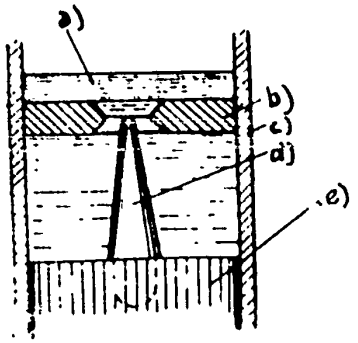

Fig.245 - Metering Pin in a Shock Strut

A metering pin changes the cross-sectional area of the orifice through which the liquid flows and, thus, affects the shape of the curve 1 (Fig.244).

a) Stress of liquid; b) Diaphragm;

c) Cylinder; d) Pin; e) Piston

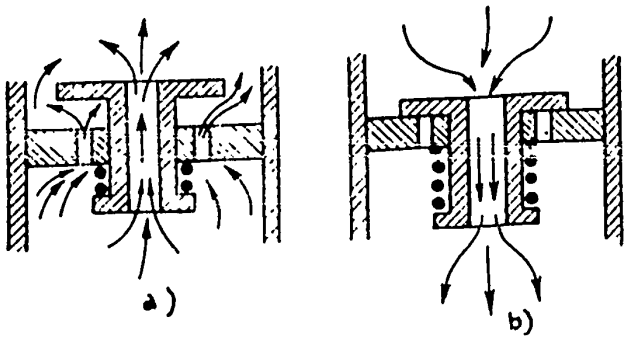

Fig.246 - Return Valve

During the forward stroke the valve opens a larger orifice for the flow of fluid than during the return stroke. Therefore during the return stroke the path of the liquid will be more inhibited than during the forward stroke.

a) Forward stroke; b) Return stroke

The pin is chosen of such a shape that, at the beginning of the stroke when the velocity of the piston is great, the area of the orifice would be larger, while later, as the strut contracts and the velocity of the piston diminishes, the area of the orifice would diminish too. In case of a rough landing, the stresses P_{am} will increase more smoothly.

In order to achieve a smoother shock absorption, it is desirable to have a larger hysteresis during the return stroke. For this purpose, the strut must be supplemented by an additional device, which would partially close the cross section of the orifice during the return stroke. Such a device is a diaphragm with a return valve (Fig.246).

STAT

If such a return valve is employed, the curve (4) (see Fig.244) will follow a lower path, as there will be a greater resistance to the flow of the liquid.

Combined Strut

Let us now imagine an ordinary strut, filled with a liquid and air at an initial pressure p_o. The function of this strut will represent a combination of the

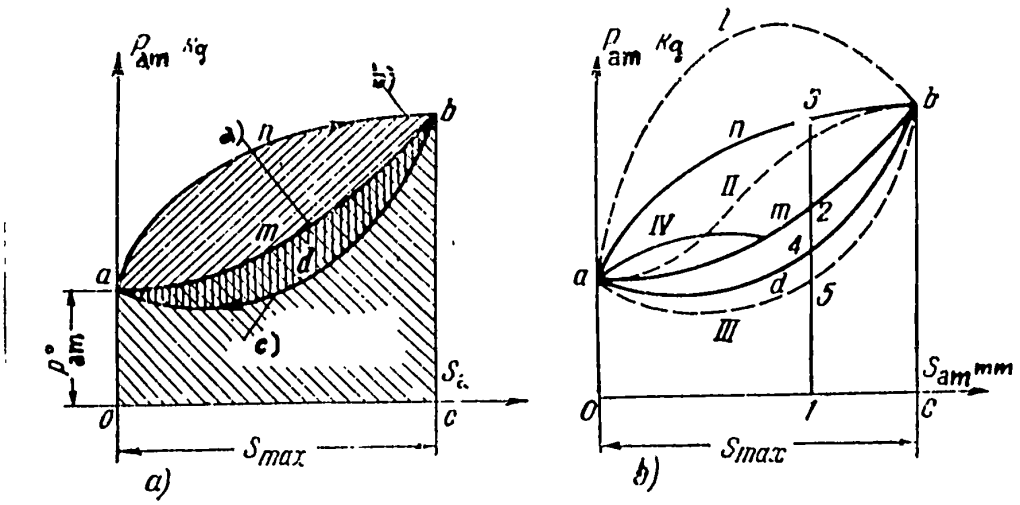

Fig.247 - Stress-Strain Diagram for an Oleo-Pneumatic Strut

a - Variation in stress in the strut during the stroke, both during forward and return stroke; b - Curve 1 represents the forward stroke of the liquid when the cross section of the orifice is small; curve II is produced by the metering pin; curve III represents the return stroke of the liquid when a return valve is used; and curve IV corresponds to the forward stroke of the liquid in case of a soft landing.

a) Air pressure; b) Forward stroke; c) Return stroke

functioning of the two struts examined above, i.e., air (pneumatic) and oil (hydraulic) struts. This operation may be expressed by the diagram shown in Fig.247a.

The first force (the air pressure) will vary both during the forward and the return stroke according to the curve amb, with which we are acquainted from Fig.243

STAT

(curve AB). The energy absorbed by the air during the forward stroke and liberated during the return stroke is represented by the area OambcO.

The second force (additional load) on the strut due to the flow of fluid through the orifice in the diaphragm is known from Fig.244.

In order to obtain the curve representing the sum of pressures of the liquid and air, it is necessary to add the pressures (ordinates) of the curve 1, 2, or 3 (see Fig.244) to the pressures (ordinates) of the curve amb. Then we will obtain the cumulative curve anb, and the energy absorbed by the strut during the forward stroke will be expressed by the area OanbcO.

For the return stroke, the air pressure must follow the curve bma, and the magnitude of the pressure exerted by the liquid (see Fig.244, curve 4) is traced below the curve bma. This will give the curve bda, which will give us the cumulative curve representing the pressures of both air and liquid during the return stroke. The area anbda represents the energy converted into heat during the forward and the return strokes. The energy not converted into heat will be expressed in the diagram by the area OadbcO.

In order to have the liquid flow through the orifice in the diaphragm and thus perform work of friction, the pressures in the liquid and in the air chambers must differ. The total force of the liquid pressure (ordinate 1 - 3, Fig.247b) is composed from the force of air pressure (1 - 2) and the force of friction of the liquid through the diaphragm (2 - 3).

We already know that it is possible to change the slope of the curve representing the loading of the hydraulic strut (see Fig.244), by changing the area of the orifice in the diaphragm by mounting a metering pin or by using return valves. If we make the cross-sectional area of the orifice smaller, the loading will increase sharply in magnitude (curve I, Fig.247b). Such a strut (a more rigid one) makes it possible to have more work done during a shorter stroke s_{max}.

We can obtain a curve of the shape II by mounting a metering pin. Struts with

STAT

such characteristics have smooth shock absorption during taxiing. But in order to absorb the required amount of energy, the stroke of the piston must be greater.

If we introduce a device to impede the flow of the liquid during the return stroke (see Fig.246), the energy absorbed by the liquid during the return stroke increases (curve 4 in Fig.244 will become lower), and instead of the ordinates 2 - 4 (Fig.247b) we will obtain the ordinates 2 - 5, i.e., the characteristic of the return stroke will be in the form of the curve III. The amount of energy converted into heat increases in such a case (area anbIIIa).

Therefore, in order to decrease the stroke of the piston it is necessary to have a strut with a greater braking during the forward stroke (a higher diagram); however, shock absorption in this case will be more rigid and will give greater overloads during taxiing. At present, such struts are not used.

To ensure a smooth growth of the stresses during the forward stroke and a decrease of stresses in the shock absorber during short strokes, it is necessary to have a strut that brakes during the return stroke but not during the forward stroke. The greatest amount of shock energy is converted into heat during the return stroke.

In case of a medium rough landing, the stroke of the strut and the work of the fluid will be smaller (see curve IV in Fig.247b).

Section 48. Influence of the Forces of Friction Produced by the Packing Collar on the Work of the Strut

Until now we have been examining the load acting on the strut P_{am} only as a function of the force exerted by the air pressure in the air chamber and as a function of the force of the hydraulic resistance of the fluid in the orifice of the diaphragm. But in reality, P_{am} depends also on the forces of friction produced by packing collars and bearing axles. This can be found by a static test of the strut (a slow contraction and extension of the strut), since then the rate of the strut contraction is small; therefore, the fluid does not produce a braking effect and

STAT

cannot influence the curve P_{am} above s. Thus we would have to obtain a curve of the type shown in Fig.243, i.e., the same curve AB for the forward and the return stroke.

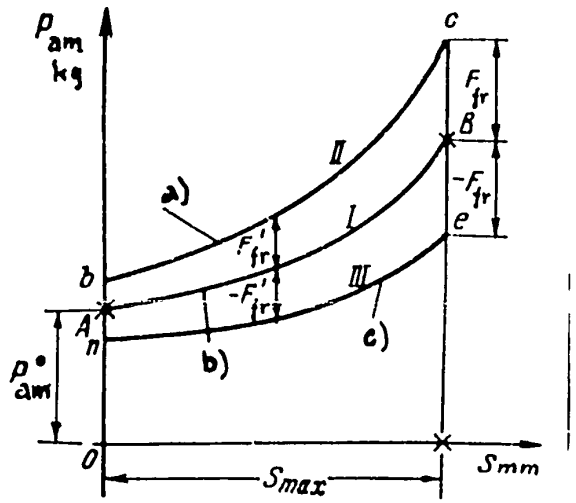

Fig.248 - Diagram of Stresses in a Pneumatic Strut when the Friction of the Packing Collar is Taken into Account

Under the action of friction of the packing collars and bearing axles, the air-pressure curve is shifted upward during the forward stroke and downward during the return stroke.

a) Forward stroke; b) Return stroke; c) Curve of air pressure

However, experiments give curve II (Fig.248) during the forward stroke and curve III during the return stroke, but not curve I which corresponds to curve AB in Fig.243.

We see that the curve of an actual strut will be shifted upward with respect to the air-pressure curve I during the forward stroke, and downward during the return stroke. This shift exactly corresponds to the force of friction F_{fr}. But the force of friction does not remain constant through the entire length of the stroke; it will increase during the forward stroke and decrease during the return stroke. This is explained by the fact that the force of friction depends on the air pressure; the greater this pressure the more will the collar rings be pressed to the surface of the cylinder.

Therefore, until now we were examining the performance of ideal struts which do not have any friction forces produced by collar rings and bearing axles. In reality, however, the characteristics of shock struts include the magnitude of friction forces corresponding to the given position of the piston. At every instant of the piston stroke, it must overcome air pressure and the force of friction. STAT

Friction will produce work during both forward and return stroke; this work is irreversible, i.e., it constitutes an additional hysteresis. In Fig.248, work produced by the forces of friction during the forward stroke is expressed by the area AbcB, and during the return stroke by the area ABen.

Here the force of friction produced by packing rings is added directly to the air pressure, while the friction produced by the liquid is absent because of the slow movement of the strut. In order to obtain the characteristics of a strut under actual working conditions, i.e., during a rapid contraction and expansion of the strut, we must take curves anb and bda (see Fig.247a) representing air pressure and liquid pressure and add to them the forces of friction both up and down, i.e., corresponding to the forward and reverse strokes. Then we will obtain the characteristics of the strut (Fig.249).

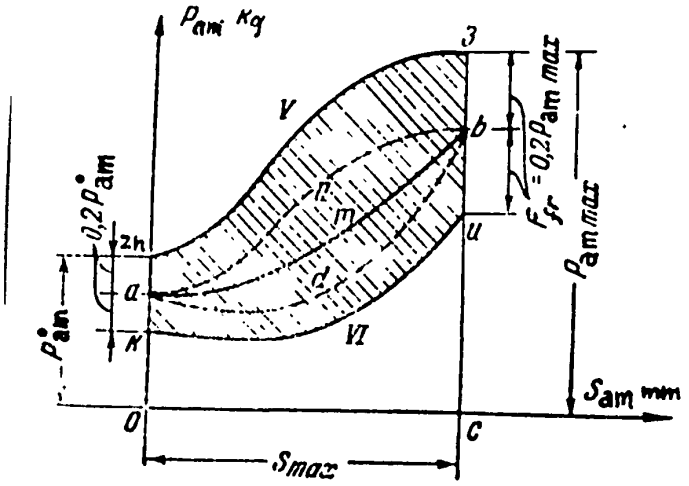

Fig.249 - Diagram Showing the Stresses in an Oleo-Pneumatic Strut, Taking the Friction Forces Produced by Packing Rings into Consideration

Under the action of friction, produced by the packing collars and bearing axles, the curve representing the stresses in the struts will be shifted upward during the forward stroke and downward during the return stroke.

Here:

STAT

Curve amb denotes the performance of the air during the forward and return strokes;

Curve II is the performance of the liquid during the forward stroke;

Curve bda is the performance of the liquid during the return stroke;

Curve V is the performance of the liquid, including the friction forces produced by the collar rings during the forward stroke;

Curve VI is the performance of the liquid, including the forces of friction produced by the collar rings during the return stroke.

At any instant of the piston stroke, it must overcome air pressure, hydraulic resistance of the liquid passing through the diaphragm, and friction produced by the packing rings and bearing axles.

The area zhzik (shaded) represents the hysteresis of the strut work during the forward and return strokes. We see that the force of friction produced by packing rings and bearing axles increases the hysteresis of work.

It has been established through tests that the friction produced by packing rings and bearing axles comprises about 20% of the total force P_{am} of the strut.

For decreasing the length of the strut, an initial air pressure is created in the strut, which according to the type of landing gear, varies from 25 to 100 atm. The initial stress in the strut, friction forces not considered, will be equal to

$$P_{am} = F_p p_0, \tag{119}$$

and the total initial stress in the strut, friction forces taken into consideration, will equal

$$P_{a\ m} = 1.2\ F_p p_o, \tag{120}$$

where F_p is the piston area in cm^2;

p_o is the initial air pressure in kg/cm^2.

P_{am} is the maximum dynamic load on the strut.

STAT

Therefore, in order to contract the strut, the external force, acting on the strut, must be greater than $1.2\ F_p \cdot p_o$.

Ordinarily the magnitude chosen for p_o is such that the product $1.2\ F_p \cdot p_o$ would be less than the parking stresses. Then during parking of the aircraft, the strut will be already somewhat compressed.

The relation of the initial loading to the parking compression is called the coefficient of preliminary compression and is designated by the letter n_o.

Therefore,

$$n_o = \frac{1.2\ F_p p_o}{P_{am.park.}} \qquad (121)$$

In modern aircraft, $n_o \approx 0.6 - 0.8$, and sometimes even smaller. The smaller is the magnitude of n_o, the softer will be the absorption of shocks. Given n_o and using eq.(121), it is possible to calculate the necessary air pressure

$$p_o = \frac{n_o P_{am.\ park.}}{1.2\ F_p} \qquad (122)$$

The principle of calculations involved in oleo-pneumatic shock absorbers was first given by Prof. M.M.Shishmarev in 1930.

Section 49. Incorrect Filling of Shock Absorbers

The shock absorbers of an aircraft will work properly and will perform their functions only if they are correctly filled. To charge the strut correctly, is to fill it with the necessary quantity of fluid, so that the volume of air V_o will be in accordance with the calculations, and the initial air pressure p_o will correspond to the coefficient of preliminary compression n_o used in the calculations.

Let us analyze the functioning of shock absorbers when they are charged incorrectly, i.e., in cases when there is less or more fluid in the strut than necessary, and the initial air pressure does not correspond to the design pressure. The entire analysis will be performed only qualitatively, taking note of the positive

STAT

and negative sides of shock absorption during incorrect charging. Moreover we will specify that the struts perform the work required by strength standards. Also, the maximum stroke of the shock absorber s_{max} and the maximum stress in the shock strut $P_{am\ max}$ must not exceed the magnitudes acceptable in a normally filled shock absorber.

In order to simplify our reasonings, we will disregard the friction of collar rings and bearing axles; this will not alter the qualitative result.

First Case

The amount of liquid in the strut is less than that required, and the initial air pressure p_o corresponds to the design pressure:

Obviously the volume of air V_o will be greater than required for normal work of the strut.

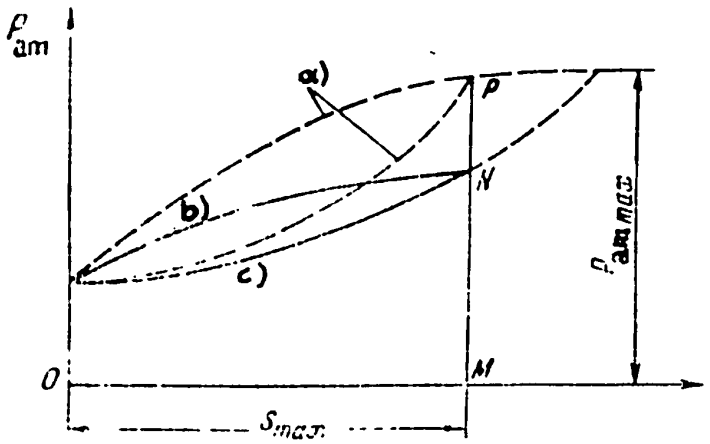

Fig.250 - Stress Diagram for the Strut When Filled With Less Fluid (by Volume) Than Required

In this case, the curves have a steeper slope. Shock absorption becomes softer but, at the given s_{max} and $P_{am\ max}$, is not able to absorb the required work.

a) Air pressure and forward stroke of the fluid at normal filling;

b) Forward stroke of fluid; c) Air-pressure curve

Due to the increase in air volume, the curve representing its pressure

STAT

(Fig.250 - solid curve) will be more sloping than in the case of normal charging. Therefore, the stresses in the strut will increase more smoothly and the shock absorption will be softer. As a result of the limited stroke of s_{max} (abscissa OM) the maximum stress in the strut MN will be smaller than the stress MP, which is equal to $P_{am\ max}$, and at the same time the strut will absorb less work (in magnitude). It is necessary to add to this that, due to the incorrect charging of the strut, the wheel is less deflated and, therefore, also absorbs less work. This smaller deflation of the wheel is explained by the fact that it is impossible to apply forces to it that would be near $P_{w\ max}$ in magnitude, since these forces will cause stresses in the strut, which will be close to $P_{am\ max}$, which is not permissible due to the limitedness of the stroke s_{max}.

As a result, when the volume of air is increased, a shock absorber at a given stroke s_{max} will not be able to perform the work required of it by the strength specifications. The necessary work may be performed during the stroke s, which is greater than s_{max}, which in turn may cause the breakdown of a shock absorber as the strut would strike the stop.

Moreover, at certain instants of the piston stroke, the valve may happen to be above the liquid level, which also creates abnormal working conditions of the strut.

Second (Opposite) Case

Shock absorber is filled with a greater amount of fluid than required, and the initial air pressure p_o is equal to the design pressure:

In this case, the initial volume of air V_o is smaller than required, which causes the air-pressure curve to rise more steeply (Fig.251). This condition will make the shock absorption more rigid since the stresses in the strut will grow faster than when the strut is normally charged. Since the strength of the strut is limited (by the permissible magnitude of $P_{am\ max}$), we will not be able to utilize all of the permissible stroke s_{max}. And, finally, the shock strut will absorb less work. For this reason, we again will not satisfy strength specifications. STAT

The total work will be absorbed when the values of P_{am} are greater than $P_{am\ max}$ which may lead to a breakdown of different parts of the aircraft.

Third Case

The volumes of both liquid and air correspond to the normal filling of the strut, but the initial pressure of the air p_o is less than the design pressure:

A decreased value of p_o lowers the magnitude of the stress on the strut, which corresponds to the preliminary compression. Therefore, the shock strut, during landing, will start contracting sooner - at smaller stresses (Fig.252), and the curve representing the air pressure will slope more.

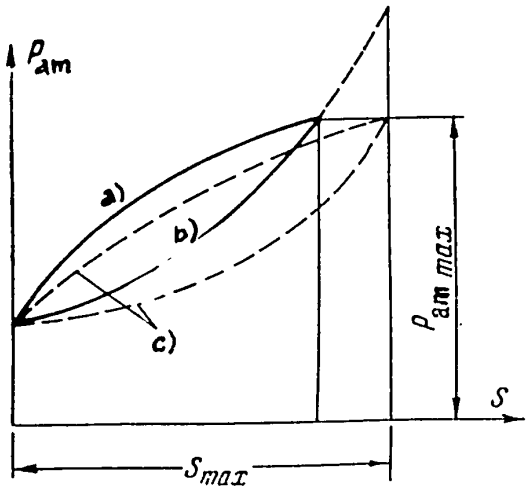

Fig.251 - Stress Diagram for a Strut Filled with More Liquid Than Required

In this case, the curves are steeper. Shock absorption becomes more rigid and, at the given s_{max} and $P_{am\ max}$, is not able to absorb the required work.

a) Forward stroke of fluid; b) Air pressure curve; c) Air pressure and forward stroke of the fluid at normal filling

When the slope of the curve is steeper, the stresses in the strut increase more smoothly, which results in softer shock absorption. In addition to this positive factor, the limited stroke s_{max} will result in the fact that the greatest stress in the strut will be smaller than $P_{am\ max}$, as in the first case (see Fig.250), and will absorb less work.

Here, just as in the first case, it is not permissible to allow the tire to deflate completely; for this reason, the wheel will also absorb less work. As a result shock absorbers (tire and shock strut) are unable to absorb the work required by the strength specifications. In a rough landing, a shock

occur at the end of the stroke of the strut, accompanied by a sharp increase in the stress P_{am}.

Fourth Case

Volumes of liquid and air correspond to the required values, but the initial air pressure p_o is greater than that corresponding to normal filling:

Due to the greater value of p_o, an increase in the preliminary compression of the strut will occur. This will result in the fact that, during landing of the aircraft, the shock strut will begin to contract at greater stresses (Fig.253), and the air-pressure curve will be steeper.

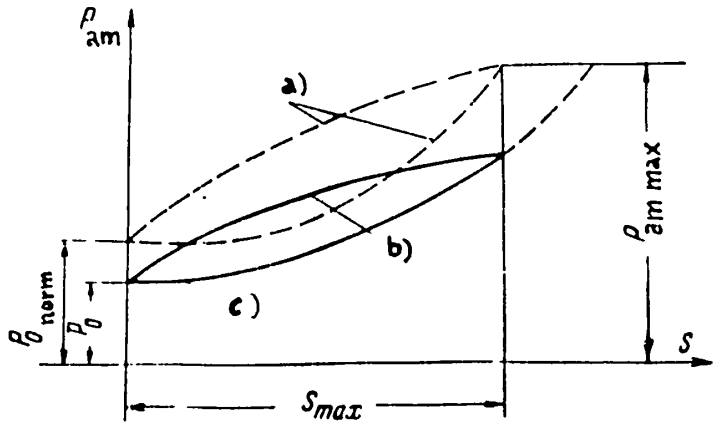

Fig.252 - Diagram of Strut Performance When Charged with Initial Air Pressure p_o Smaller Than Required

In this case, the curve has a steeper slope. Shock absorption becomes softer but, at the given s_{max} and $P_{am\ max}$, is not able to absorb the required work.

a) Curves for air and forward stroke of fluid at normal filling;

b) Forward stroke of fluid; c) Air-pressure curve

As a result, the shock absorption will be more rigid since the stresses in the strut will grow much more intensely during the stroke. Moreover, due to the limited strength of the landing gear (limited by the permissible magnitude of $P_{am\ max}$), it

STAT

is impossible to utilize the permissible stroke s_{max}. This latter fact will cause the strut to absorb a diminished amount of work. As a result, the shock absorption will not only be much more rigid but will also not satisfy the strength specifications with respect to the possibility of absorbing work.

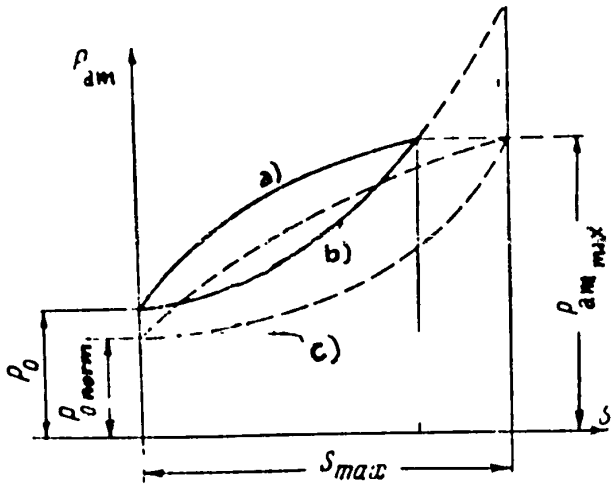

Fig.253 - Diagram of Strut Performance When Charged with an Initial Air Pressure p_0 Greater Than Required.

In this case, the curves lie higher. Shock absorption becomes more rigid and, at the given s_{max} and $P_{am\ max}$, is not able to absorb the required amount of work.

a) Forward stroke of fluid; b) Air-pressure curve; c) Curves for air pressure and forward stroke of fluid at normal filling

On the basis of the four cases we have just examined, we can conclude that shock absorbers must be filled in accordance with the design data, since only in such a case they will ensure the design value of maximum overload, when they are absorbing the greates work possible at a given stroke s_{max}.

Section 50. Shock Strut Design

Shock absorbers of the old design (see Fig.242) made a long piston stroke impossible, so that the shock absorption was rigid (coefficient n_E^e was large). The reason for this was that, in order to make the stroke of the piston longer, the length of the strut had to be increased; however, this length was quite great since the fluid occupied a considerable portion of the cylinder (vertically), and the diaphragm was placed inside the cylinder.

Modern struts have no special volume for the fluid inside the cylinder. The fluid is placed in the inner pocket of the piston rod. This change in structure makes it possible to increase the stroke of the piston without changing the len...

STAT

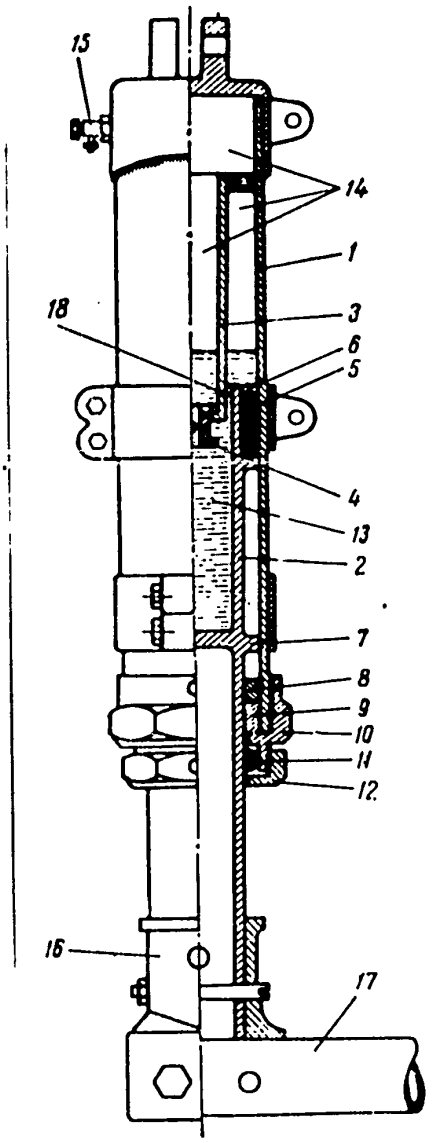

Fig.254 - Shock Strut of the First Type

The characteristic feature of this strut is that the packing is mounted on the piston rod and the return valve is placed on the bottom part of the piston.

of the strut itself, to decrease the initial pressure in the strut, and to make shock absorption more elastic. In such struts, a diaphragm is placed inside the piston rod.

Shock Strut of the First Type

The strut consists (Fig.254) of a steel cylinder (1), in which a piston rod (2) is mounted so that it can move freely inside the cylinder. Sealing between the piston and cylinder is achieved by leather packing collars (5). These are mounted in the upper part of the piston rod and are tightened by a bearing axle nut (6). The packing gland (11) is mounted in the control nut (10) of the cylinder and is tied with a stuffing gland nut (12). The return stroke of the piston rod is limited by the shoulder of the rod (7) and the control nut (10), together with a bronze journal box (9) and a shock absorption ring (8). Inside the cylinder a steel tube (3) (plunger) is mounted, which forms the body of the diaphragm. The lower end of this

STAT

tube is lowered and positioned at the beginning of the piston pocket. On this same end of the pipe, a slide valve (4) is mounted. This valve has one 8mm orifice running through its axis and four slanting side orifices of 5 mm each, as in the valve shown in Fig.246. In the upper portion of the cylinder there is a filler pipe (15). A steel ring (16) for fastening the wheel axle (17) is fixed on the lower end of the rod.

The shock strut is filled with fluid and air through a filler pipe (15). The liquid usually is an antifreeze mixture of glycerol and ethyl alcohol. The liquid is placed in the upper portion of the pocket (13) of the piston rod (2). The level of the mixture must be above the valve (4). Air occupies the volume (14).

The strut functions in the following manner: During the forward stroke, liquid flows from the pocket (13) of the piston into the pocket (14) of the cylinder. Liquid flows through the central and the four slanting orifices of the valve (the valve will be lifted) and through the clearance in the collar (18), between the body of the plunger (3) and the piston (2). During the return stroke, the valve lowers into its position and the four slanting orifices are closed (see Fig.246). In this case, the mixture will flow only through the central orifice of the valve and the play of the collar. This results in braking of the liquid.

The strut has a limited possibility of controlling the velocity of the piston return during the return stroke. The speed of the return stroke can be lowered by making the orifices for the liquid flow smaller. But in reality, even at zero opening of the valve, the strut will still be extended since the boost pressure of the air in the cylinder will always create a force, which will be greater than the suction of the vacuum under the plunger.

Shock Strut of the Second Type

In a shock absorber of this type (Fig.255) the flow of liquid is also braked mainly during the return stroke. The strut consists of a steel cylinder (1), inside of which, in the lower portion, a piston rod (2) is moving. Between the

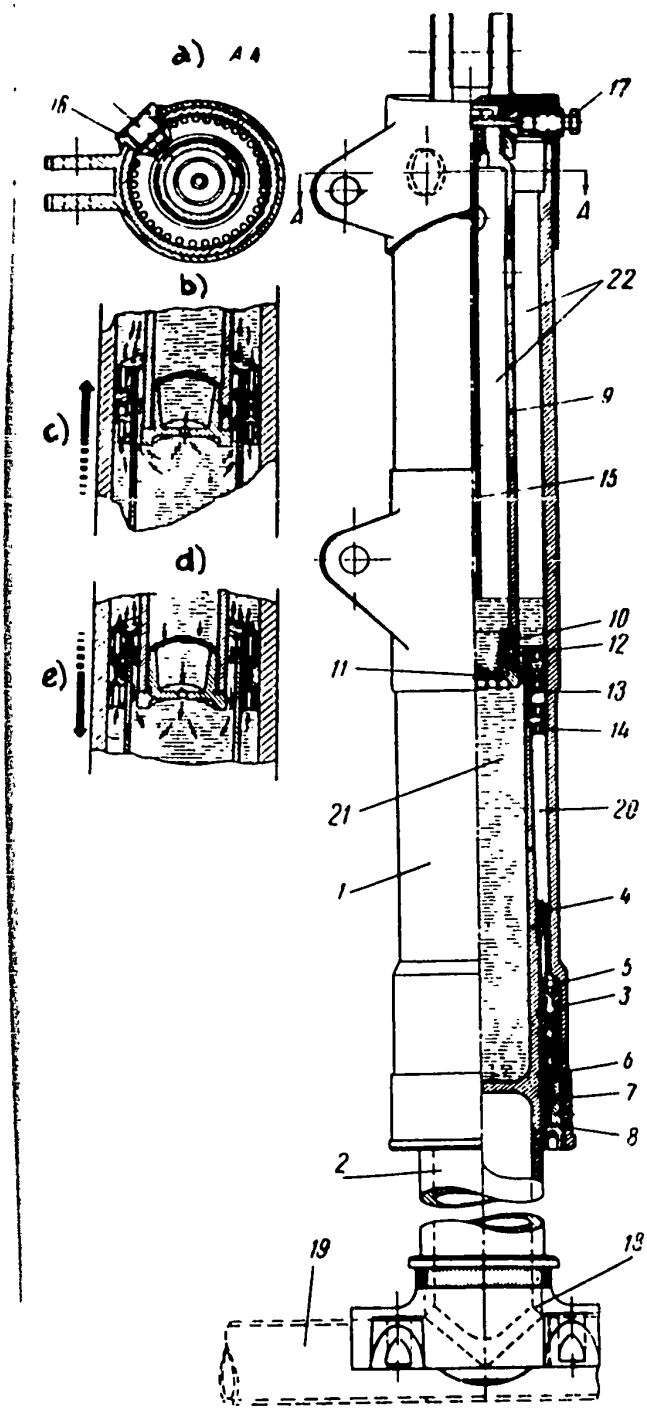

Fig.255 - Shock Absorber of the Second Type

It is characterized by the fact that the packing is mounted on the cylinder and the reverse valve is placed inside the piston.

a) Direction of piston stroke; b) Forward stroke (compression); c) Return stroke (expansion); d) Cross section through A-A

cylinder and the piston, a permanent packing is mounted at the lower portion of the cylinder. It consists of leather packing rings (3) and an oil felt pad (8), tied with a nut (7). The return stroke of the piston is limited by a stop bushing (4), fixed on the rod, and a thrust ring (5). Inside the cylinder, in its upper portion, a plunger (9) is mounted, whose lower end is lowered into the pocket of the piston.

A nut (10) is fixed on the lower end of the plunger. It has a central hole (11). Inside the plunger a liquid-level control (15), is fixed which is connected with a plug (17). The technician can remove the extra liquid from the strut with the help of this pipe. On the upper end of the piston rod, two permanent bronze rings (12) and (14) are mounted. These rings have a large number of vertical holes around their circumferences. In between these rings, a movable ring valve (13) is mounted, which has two holes and a ring groove. Between the rod

STAT

and the cylinder there is a pocket (20). This pocket is filled with the fluid. During the forward stroke, an additional amount of the fluid enters this pocket through the holes of the bronze rings (12) and (14) and through the radial gap between the valve (13) and the cylinder. The function of bearing axle of the piston rod is taken over by the bronze rings (12) and (14) and by the bronze spacer (6). The inner pocket of the rod (21), in its upper portion, into which the plunger enters, is fashioned in the form of a cone. This changes the size of the orifice through which the liquid flows. A ring (18) for fixing the wheel axle (19) is welded to the lower end of the rod.

The shock absorber is charged with a liquid consisting of a mixture of glycerol and ethyl alcohol through the filler plug (16). Charging of the strut with air is performed from the general inflation valve through the filler plug (16).

The strut operates in the following manner: During the forward stroke, liquid flows from the piston pocket (21) into the pockets (20) and (22) through the orifice (11) of the plunger, holes (12) and (14) in the bronze rings of the piston, and through the annular clearance between plunger and rod, and between the floating ring valve (13) and the cylinder. During the return stroke, the floating ring valve (13) is pressed to the ring (12) and closes all its holes, except two. Then the mixture flows slowly from the pocket (20) through these two holes in the rings (13) and (12) into the pocket (22), from there through the orifice in the plunger (11) and through the play in the ring between the plunger and the piston, into the piston pocket (21).

The peculiar feature of this strut is that the piston area, on which the magnitude of the air pressure depends and which balances the external force of the strut, is defined by the outside diameter of the rod. This makes it possible to increase the piston stroke. In this case, there is a greater possibility to regulate the speed of the piston return during the return stroke by decreasing the cross section of the holes in the valve (13). The level of the liquid during the entire period of

STAT

the strut performance must be such that the ring (12) is always submerged in the liquid. This prevents air from reaching the pocket (20) and avoids hydraulic shocks during the return stroke of the strut.

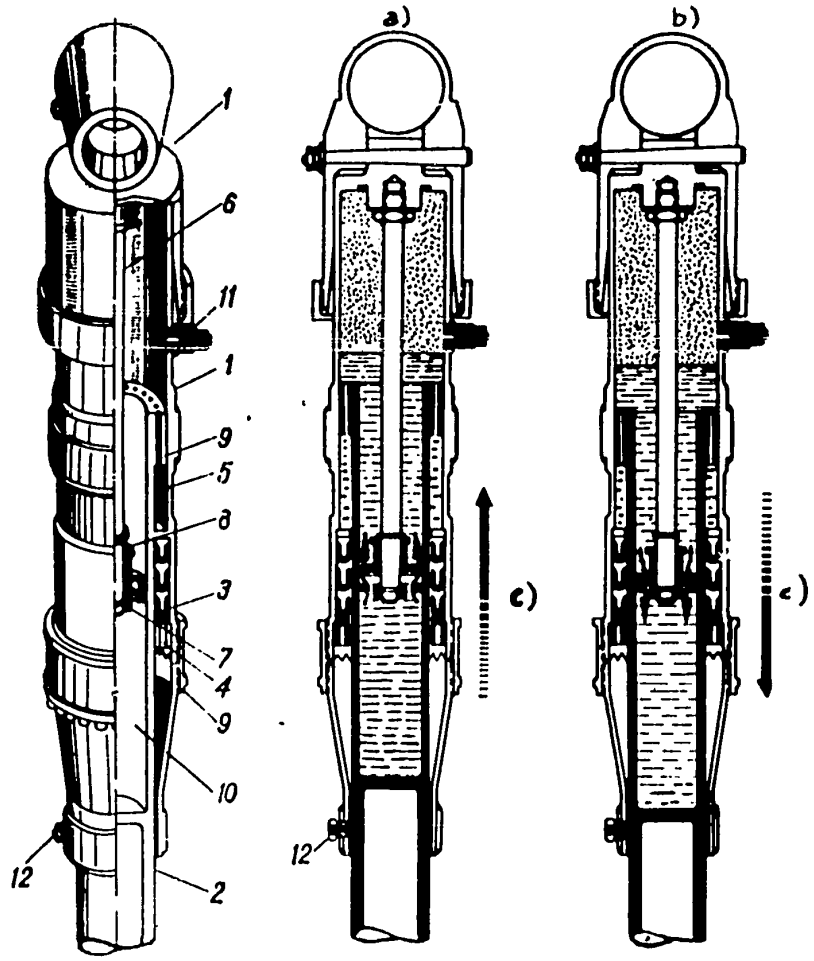

Fig.256 - Shock Strut of the Third Type

It is characterized by the fact that the packing is mounted on the cylinder and the reverse valve is placed on the lower portion of the pin (plunger).

a) Forward stroke; b) Return stroke; c) Direction of piston stroke

Shock Strut of the Third Type

This strut (Fig.256) is a combination of the first two types and consists of a steel cylinder (1) and a piston rod (2). The packing of both cylinder and rod is permanent and consists of leather packing collars (3) and a tie nut (4), mounted to

STAT

the lower portion of the cylinder.

The piston (9) is mounted to the upper end of the rod (2). It has an orifice for free passage of the mixture. The upper pocket of the piston (10) forms a reservoir for the mixture. Inside the cylinder, a stationary pin (6) is mounted, whose lower end carries a diaphragm with an orifice (7), together with a slide valve (8) with two orifices. The cylinder has a filler plug (11).

A welded clevis with an axle for attachment of the wheel is mounted to the lower end of the rod.

The strut operates in the following manner: During the forward stroke, the mixture flows from the pocket (10) through the diaphragm orifice (7) and annular gap between the valve (8) and the rod (2) into the pocket, which is filled by compressed air. Moreover, the mixture from the cylinder will reach the circular pocket (5) between the cylinder and the rod through the hole in the piston (9). During the return stroke, the valve (8) lowers and closes all openings in the diaphragm, except two. This achieves the braking effect.

The peculiar feature of this strut is that it possesses an additional possibility to increase the piston stroke by lowering the level of the liquid, since here it is not necessary that the piston (9) be covered by liquid all the time. There may be air in the space behind the piston (5), without causing any hydraulic shocks. The same cannot be said on struts of the second type. But this strut, just as the strut of the first type, does not permit complete control of the return speed of the piston.

Conclusions. Experimental tests have shown that the best strut of the three types examined above is the second one. A fluid of sufficiently high viscosity must be used. It must also withstand cold weather during winter and low temperatures at high altitudes (must be an antifreeze). A mixture of glycerol and alcohol is most frequently employed. The amount of the liquid is controlled by the liquid-level control pipe, by the filler pipe, or by a calibrating vessel. Air-pressure contr-

STAT

is achieved either with the help of a pressure gage or by the position of the piston rod while the aircraft is parked.

STAT

Declassified in Part - Sanitized Copy Approved for Release @ 50-Yr 2013/09/11 : CIA-RDP81-01043R002300220004-4

CHAPTER XIII

PERFORMANCE OF A LANDING GEAR ENERGY DIAGRAM

The landing gear performs the coupling between the wheel and the aircraft. The external loads acting on it are determined on the basis of applicable strength specifications.

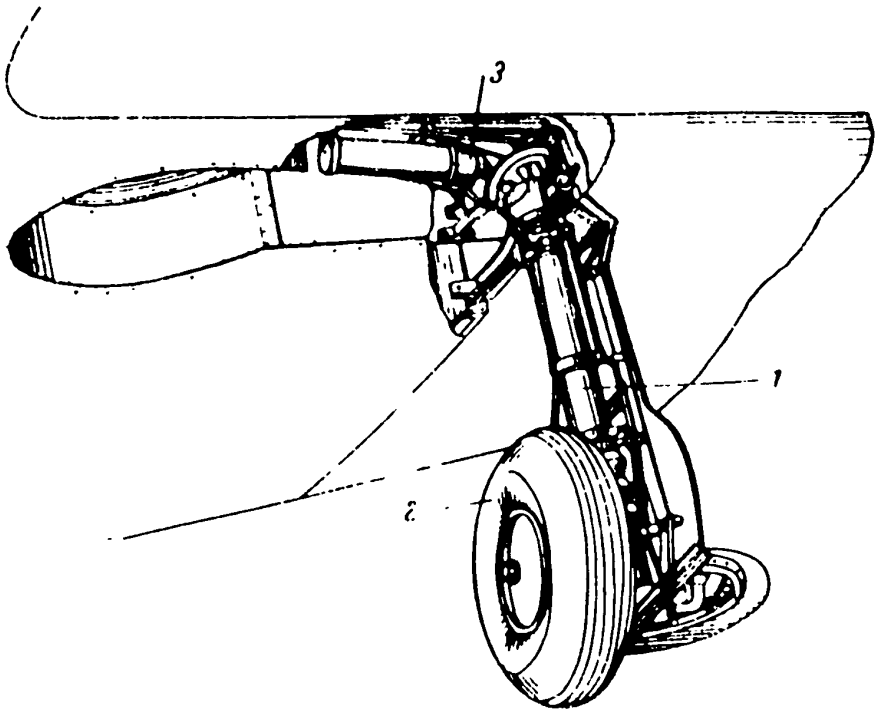

Fig.257 - Cantilever Landing Gear

1 - Shock strut; 2 - Wheel; 3 - Mechanism for retraction of the landing gear

On modern aircraft, three basic types of landing gears are used: STAT

a) Cantilever (Fig.257);

b) Semicantilever, with one or two inclined struts (Fig.258);

c) Lever suspension of wheels (Fig.259).

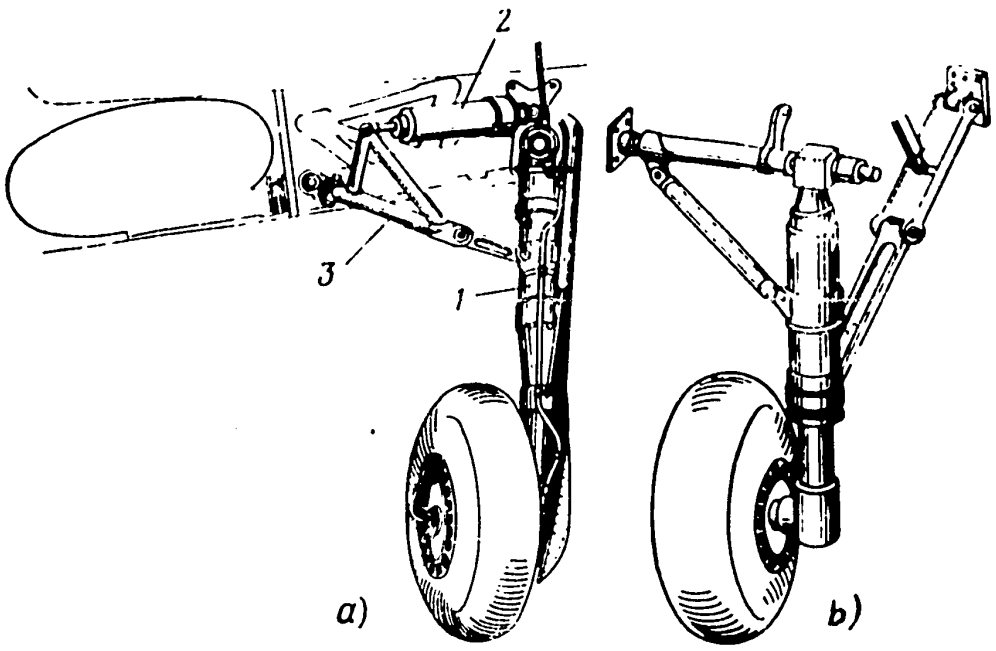

Fig.258 - Semicantilever Landing Gear

a - With one inclined strut: 1 - shock strut; 2 - landing gear retraction mechanism; 3 - articulated cantilever.

b - With two cantilevers.

Section 51. External Loads Acting on a Landing Gear

The basic external loads exerted on the landing gear are the reaction forces of the ground, generated during landing and taxiing of the aircraft. The ground effect (Fig.260) completely balances the weight and inertia force of the aircraft mass

$$2P_{mw} + P_{nw} = G + N - Y, \qquad (123)$$

where $P_{m\,w}$ is the load on the main wheel;

$P_{n\,w}$ is the load on the nose wheel;

G is the aircraft weight;

STAT

N is the inertia force of the aircraft mass.

Y ≈ 0.75 G which is the lift of the aircraft during touchdown is equal to about 0.75 of its flying weight.

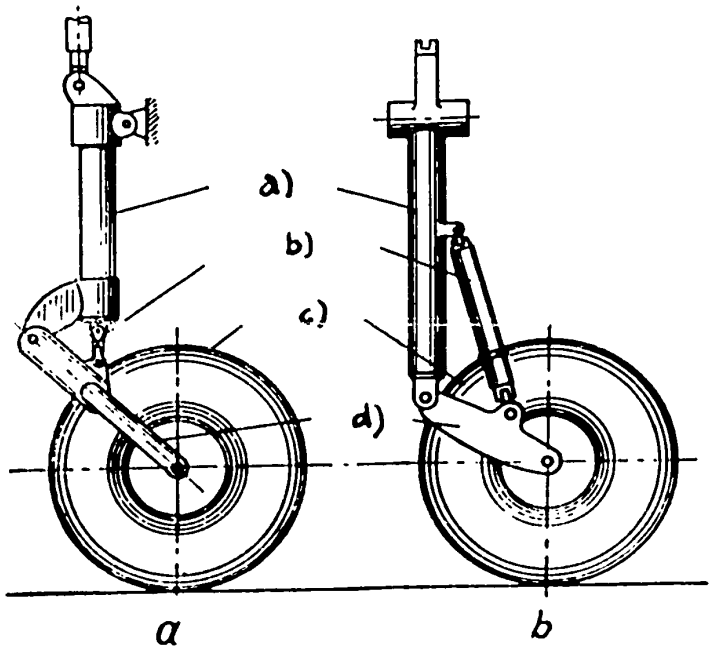

Fig.259 - Landing Gear With Lever Suspension of the Wheels

a - Shock absorber inside the strut; b - Shock absorber carried outside of the strut

a) Strut; b) Shock absorber; c) Wheel; d) Fork arm

Equation (123) may be rewritten in another form:

$$2P_{m\,w} + P_{n\,w} = Gn, \qquad (124)$$

where n is the overload coefficient.

The magnitude of the ground effect and the line of its action may differ depending on the quality of the landing, the character of the ground run, the roughness of the runway, and the rigidity of its shock absorption. Ground-reaction forces may be distributed throughout the elements of the landing gear in different ways: on three points, i.e., on the main wheels and the nose wheel; on two poi

and even on one point, which also depends on the character of the touchdown and the movement of the aircraft on the ground.

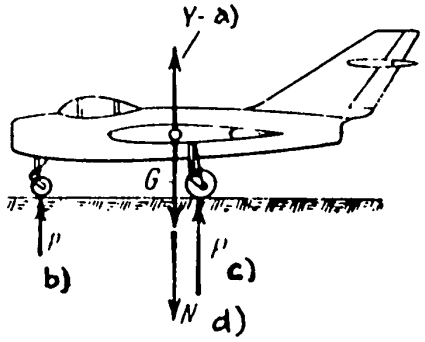

Fig.260 - Loading of the Landing Gear at Touchdown

The forces of ground reaction (external loading of the landing gear) balance the weight and inertia forces of the aircraft mass.

a) Lift; b) Load on nose wheel, $P_{n\,w}$; c) Load on main wheel $P_{m\,w}$; d) Inertia

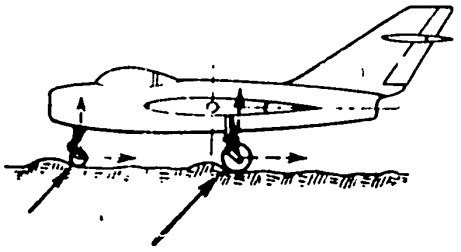

Fig.261 - Loading of the Landing Gear on a Rough Airfield

The forces of the ground effect will act at an angle to the horizontal, i.e., vertical and horizontal components of forces will act on the landing gear.

In case of an aircraft landing on a smooth runway without the use of brakes, the forces of the ground reaction will in the main act in a vertical direction.

During touchdown or taxiing on a rough runway, the ground effect will act at an angle to the horizontal, i.e., the landing gear will be acted upon by the vertical and horizontal components of forces (Fig.261).

Horizontal components of the reaction forces of the ground will also act during the movement of the aircraft over a smooth runway and in cases of brake application to the wheels (Fig.262).

When an aircraft makes ground contact with its wheels not locked, horizontal forces are generated which include forces of friction of the wheels on the ground, which tend to rotate the wheels. It must be noted that, at high touchdown velocities, these considerable friction forces cause rapid wear of the tires and greatly

STAT

load the landing gear. For this reason, in some cases a special device is installed for preliminary untwisting of the wheels before touchdown of the aircraft.

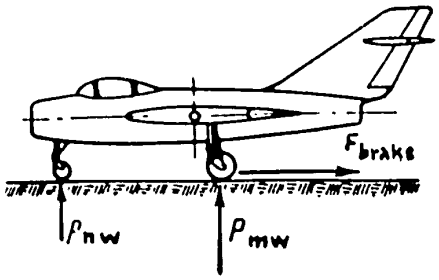

Fig.262 - Loading of the Landing Gear When Brakes Are Applied

The horizontal components of the ground reaction will act during the movement of the aircraft over a smooth runway if the brakes are applied.

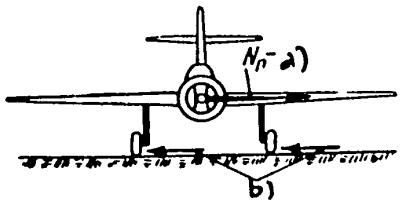

Fig.263 - Loading of the Landing Gear During a Touchdown With Drift

In this case, the landing gear will be acted upon by forces of friction directed perpendicularly to the plane of symmetry of the aircraft.

a) N_n = Force of inertia; b) Force of friction

During touchdown with a drift or in case of a sharp turn during the ground run, the aircraft will be subject to the action of horizontal components of the ground reaction acting in a lateral direction (Fig.263). The outside wheel will always be loaded more than the inner one, since its normal force is greater, and since the horizontal components are the product of the normal force times the coefficient of friction.

Normal forces are greater at the outside wheel since, under the action of lateral forces, the aircraft will crab.

The landing gear must be strong enough to withstand all possible cases of loading during its operation. The existing aircraft strength specification list a number of typical situations. The landing gear have sufficient mechanical strength to resist these forces. The external forces are determined according to the existing strength specifications.

Rough Touchdown

As a typical example, let us examine a case of a rough touchdown ($E_{l.g.}$). STAT

At the instant of touchdown (Fig.264), as previously mentioned, an aircraft possesses two velocity components:

V_{hor} is the horizontal component;

V_y is the vertical component;

while V_{hor} is a little greater than V_y.

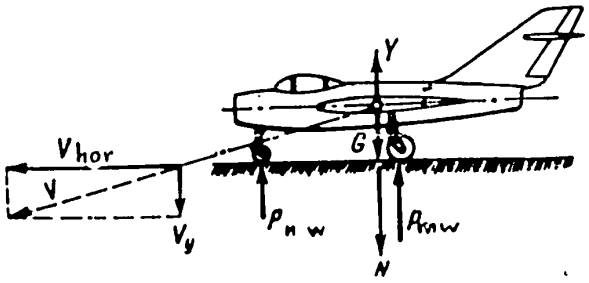

Fig.264 - Design Case $E_{l.g.}$ for Rough Landing

During a rough landing of an aircraft, its vertical velocity component V_y must be canceled during contraction of the strut and deflation of the tire. Therefore, because of the short path, large accelerations must be in operation, large forces of inertia, which means large landing-gear reactions.

After touchdown, the aircraft continues to run on the ground, slowing down gradually and with slight negative acceleration. Horizontal inertia forces, also of a small magnitude, correspond to these.

But the vertical velocity component V_y is damped within a very short period of time (fraction of a second). Therefore, here we have large acceleration and inertia forces of high magnitude, which corresponds to greater landing-gear reactions ($P_{m\,w}$ and $P_{n\,w}$) and to greater overloads.

The overload coefficient will equal to

$$n_l^e = \frac{P_{mw}}{P_{mw}^o}, \qquad (125)$$

Where P_{mw} is the load on the main wheel during touchdown;

$P_{m\,w}^o \approx 0.42G$ is the load on the main wheel during parking of the aircraft.

For modern aircraft, n_E^e may reach 2.6 - 3.5 and may even be larger.

At touchdown, the magnitude of $P_{m\,w}$ depends on the magnitude of the acceleration. Acceleration, in turn, depends on the stiffness of shock absorption.

Strength specifications do not give the magnitude of n_E^e, but the degree of roughness of touchdown, i.e., they determine the vertical velocity components (V_y) of the aircraft generated during a rough touchdown. In this manner, the kinetic energy A is given, which is determined by the well-known formula

$$A = \frac{GV_y^2}{2g}, \tag{126}$$

where g = 9.81 m/sec^2 is the acceleration of gravity.

The magnitude of the vertical velocity of the aircraft V_y for a rough touchdown is assigned according to the weight of the aircraft and the magnitude of the landing speed (V_y is equal to about 2 - 4 m/sec).

In modern aircrafts, in order to obtain V_y = 3 m/sec, it is necessary to approach the ground at a small angle, equal to about 5°. This will be a rough landing.

S.N.Shishkin has published the results of experimental work on actual loading of the landing gear in 1936. This work later served as a basis for planning the strength.

Section 52. Cantilever Landing Gear

The landing gear shown in Fig.257, strictly speaking, is not a beam fixed at one end, since its strut (Fig.265) has two supports. However, since the distance between the two supports is very small, and in order to simplify the stress analysis, we assume that the strut is of the cantilever type whose end is fixed while an external force P is applied to the other.

Let us take a concrete case, for instance, a case of rough landing $E_{1.g.}$ Here the external load (design), which acts on the main wheel, is equal to

$$P_{l.} = \alpha G n_{l.}^e f, \tag{127}$$

where d ≈ 0.42 is the coefficient showing which portion of the aircraft weight G

STAT

acts on one main wheel in parking; this coefficient is obtained as a result of the resolution of gravitational forces of the aircraft according to the lever law between main wheels and nose wheel;

$f = 1.65$ is the safety coefficient;

$N_E^e = 2.6 - 3.5$ is the overload coefficient; the exact value of n_E^e depends on the rigidity of shock absorption.

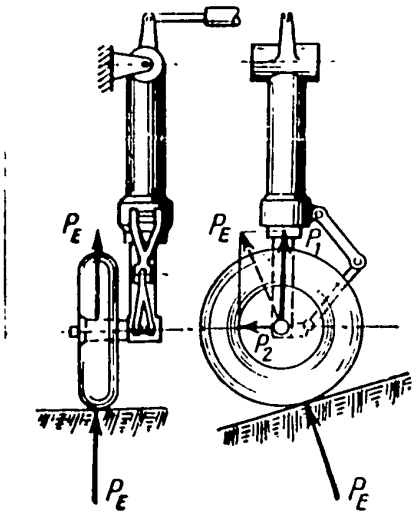

Fig.265 - Diagram of a Cantilever Landing Gear

The landing gear represents a beam, one end of which is fixed, while the external force is applied to the other end by means of the wheel.

The wheel, under the action of the external load P_E, is deformed and transfers the load to the axle over two roller bearings. We are not interested here in the strength of the wheel since the wheels are standard and their strength is guaranteed by the manufacturer which produces them.

Let us resolve the force P_E into its components (Fig.265): One of them, P_1, will act in the plane of the axle and the strut, while the other, P_2, is perpendicular to this plane.

Action of the Force P_1

Under the action of the force P_1 (Fig.266) the axle of the wheel will bend as a cantilever beam. The greatest bending moment will be at the point where the wheel is fixed to the axle, namely the strut

$$M_b = P_1 a,$$

where a is the lever arm of the force.

The force P_1 and the bending moment $M_b = P_1 a$ are transferred from the axle

STAT

the strut, so that in all the cross sections of the strut the bending moment $P_1 a$ will have a constant value. The diagram of M_b is shown in Fig.267. Through the length e of the bending moments, $M_b = P_1 a$ will be absorbed by the rod and cylinder. If we draw the diagonal CD, we will divide the diagram of M_b into parts belonging to the rod (the lower one) and the cylinder (the upper portion).

The force P_1 will compress the rod of the strut with a force of

$$\sigma_{com} = \frac{P_1}{F_{rd}},$$

where F_{rod} is the cross-sectional area of the rod.

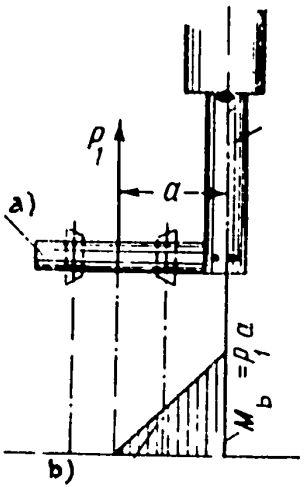

Fig.266 - Bending of the Axle

Under the action of the force P_1, the wheel axle bends with a maximum bending moment at the cross section near the strut.

a) Wheel axle; b) Strut

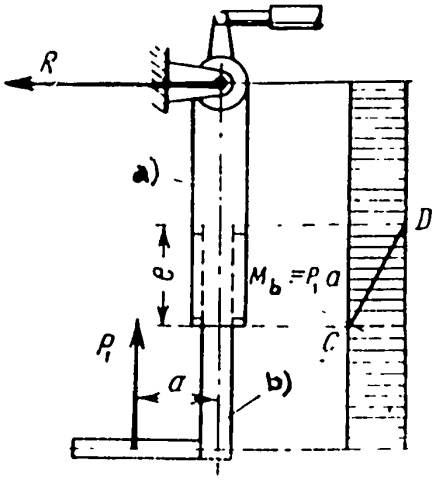

Fig.267 - Bending of the Strut

Over the entire length of the strut, the bending moment created by the force P_1 will be of the same magnitude. Through the length e, this moment will be absorbed by the rod and the cylinder simultaneously. The diagonal CD divides the diagram of the bending moments into two parts: one, referring to the rod, and the other to the cylinder.

a) Cylinder; b) Piston

From the rod, this force is transmitted to the mixture, and from the mixture to the air. Air transmits this force to the cylinder bottom, from where the load

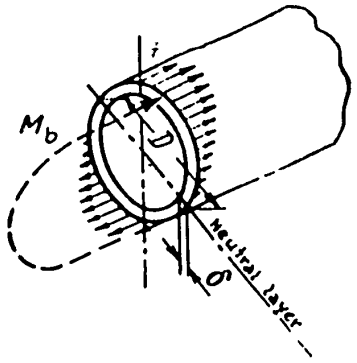

Fig.268 - Distribution of Normal Stresses through the Cross Section Under the Action of the Bending Moment

Large stresses σ occur in the fibers which are far from the neutral layer and are small near the neutral layer

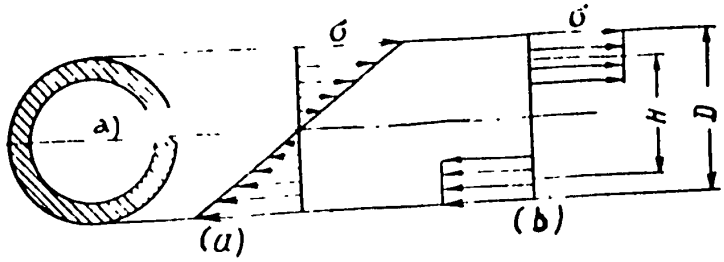

Fig.269 - Actual and Approximate Distribution of Stresses in a Tubular Girder

When determining the stresses σ in the tubular girder we consider it approximately to be a double-belt beam with a height $H \approx \frac{2}{3}D$

a) Neutral layer

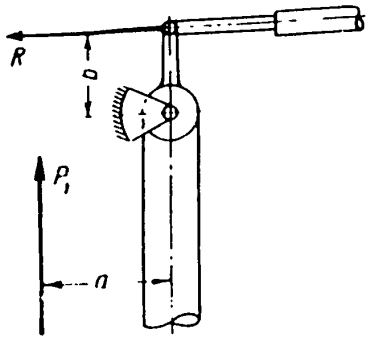

Fig.270 - Loading of the Upper Support

If we imagine the strut separated from its upper support, it will rotate under the action of the moment P_1a. Reaction in the upper support R acting on the lever arm b hinders this rotation

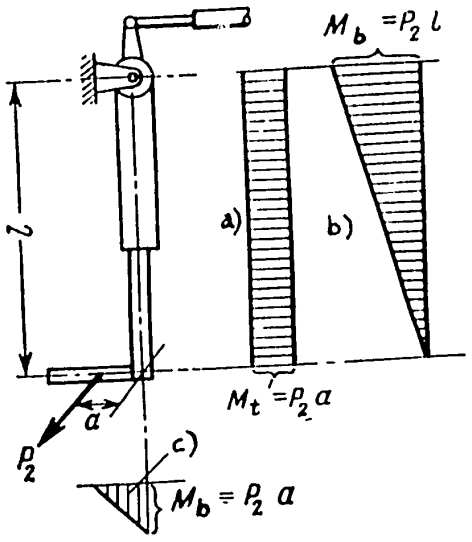

Fig.271 - Work Performed by the Landing Gear under the Component Force P_2

Under the action of the force P_2 the axle is bent, and the strut is both bent and twisted

a) Torque diagram; b) Diagram of strut bending moment; c) Diagram of axle bending moment

STAT

transmitted to the strut joint.

Due to the high pressure of the mixture and air, the cylinder will operate as a vessel, subject to an internal pressure.

Under the action of M_b the strut is bent, and the individual fibers of the strut and cylinder will be subject to normal pressures σ (Fig.268).

The true distribution of the bending stresses through the cross section of the pipe is described in Fig.269a. In determining the stresses σ, we approximately make use of the law described in Fig.269b. By this we determine the stresses σ in the tube as if it was a double-ring beam with a height H and with an area of each ring equal to F_p.

$$\sigma \approx \frac{M_b}{HF_p}, \tag{128}$$

where we approximately assume that

$$H = \frac{2}{3} D$$

and

$$F_p = \frac{1}{3} \pi D \delta.$$

Reaction in the upper support (Fig.270) is determined from the equality of the moments

$$P_1 a = Rb,$$

from where

$$R = \frac{P_1 a}{b} \tag{129}$$

Action of the Force P_2

Under the action of this force (Fig.271), the axle is bent in the plane perpen- STAT

dicular to the strut and passing through the axle. Its greatest bending moment will occur at the place where the axle is attached to the strut

$$M_b = P_2 a.$$

For the strut, this moment is the torque M_t, which retains a constant value through the entire length of the strut

$$M_t = P_2 a = \text{const.} \tag{130}$$

Moreover, other bending moments caused by the same force P_2 will act in the cross sections of the strut. The M_b of the greatest magnitude will be found in the joint

$$M_b = P_2 \ell .$$

Under the action of $M_b = P_2 a$ in the wheel axle and of $M_b = P_2 l$, normal stresses will occur in the strut. The magnitude of these stresses is determined by the same method as those caused by the force P_1, i.e.,

$$\sigma = \frac{M_b}{HF_p}. \tag{131}$$

Under the action of the torque M_t, lateral stresses will occur in the rod and cylinder, whose magnitude is determined by the formula

$$\tau = \frac{M_t}{2F}, \tag{132}$$

where $F \approx \frac{\pi D^2}{4}$ is the cross-sectional area of the tube circuit.

This eq.(132) is valid only for those sections of the strut length where there is neither a two-piece cross beam nor a regular cross beam (Fig.272). In those places where the cross beam is mounted, the torque will be transmitted by the bending of individual elements of the landing gear, in which normal stresses will occur.

STAT

Cross-Beam Performance

If we would separate the cross beam at the joint k (Fig.272), a mechanism will result, i.e., the rod will rotate inside the cylinder under the action of the torque (see the lower position of the cross beam shown in dotted lines). From this, we can conclude that the two-piece cross beam participates in the work of the strut under the action of $M_t = P_2 a$. In practice it can be assumed that both halves of the cross beam are tied together by a hinge. In this case, they can exert a mutual influence only by means of a force since it is impossible to transmit a moment through a hinge.

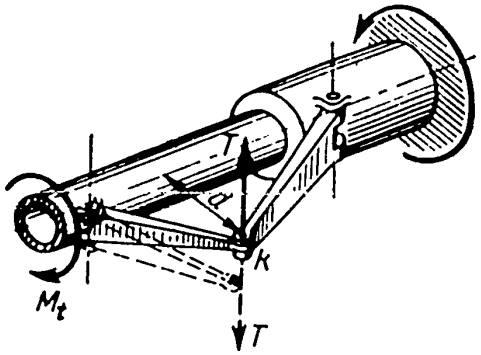

Fig.272 - Work of a Two-Piece Cross Beam When the Strut is Twisted

If we imagine the cross beam separated at the hinge k, a mechanism will be formed, which will be balanced on application of forces of interaction T of the two halves of the cross beam.

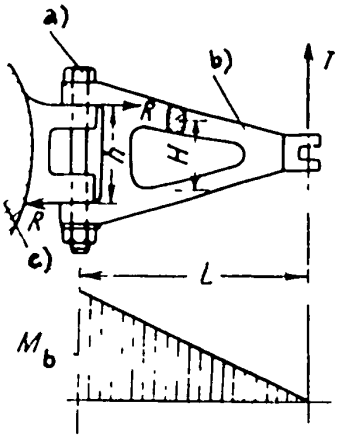

Fig.273 - Bending of the Two-Piece Cross Beam and Shear of the Connecting Bolt

The force T is transmitted to the rod (cylinder). The two-piece cross beam is bent and shearing of the connecting bolt occurs.

a) Connecting bolt; b) Fulcrum;

c) Piston

In order that the lower half of the cross beam does not move with respect to the upper one, an interacting force T with a lever arm d, with respect to the axle of the strut, must be in operation.

STAT

The magnitude of the force T is determined from the condition of absence of rotation

$$M_t = Td,$$

from which it follows that

$$T = \frac{M_t}{d}. \qquad (133)$$

Under the action of the force T, each half of the two-piece cross beam is bent like a cantilever beam, which is fixed to the rod (Fig.273) or to the cylinder.

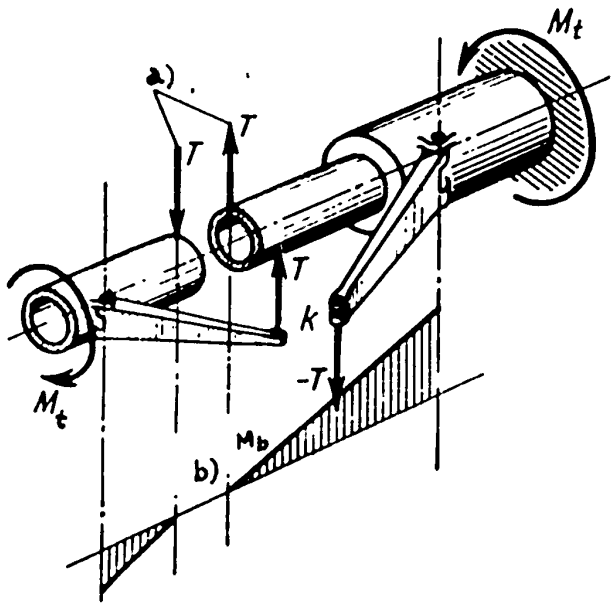

Fig.274 - Work of the Rod on the Fulcrum Section

The rod is bent under the action of the torque M_t

a) Shear forces - forces of interaction in rod; b) Rod diagrams

From the action of M_b normal stresses will occur in the rings of the two-piece cross beam.

$$\sigma = \frac{M_b}{W_T}, \qquad (134)$$

STAT

where H is the distance between cross-beam rings;

F_t is the cross-sectional area of a cross-beam ring.

The maximum bending moment of the cross beam

$$M_b = TL$$

is transmitted to the rod or cylinder by shearing of the bolt. The shearing forces R are determined from the equality of moments

$$TL = Rh,$$

from where

$$R = \frac{TL}{h}. \tag{135}$$

The lateral stresses from shearing of the bolt are determined by dividing the shearing force R by the cross-sectional area of the bolt F_b

$$\tau_{mean} = \frac{R}{F_b}. \tag{136}$$

Let us examine the work of the rod on the fulcrum section. Let the rod (Fig. 274) intersect with a plane perpendicular to its axis and passing through the joint of the cross beam k. Then, under the action of the force T, applied to the lower portion of the two-piece cross beam, the cut portion of the rod will tend to move in the direction of action of the force T. In reality there will be no such motion since the cut-off portion must be balanced. Therefore, the acting force T will be balanced by the internal force of the elasticity of the rod, which is located in the plane of the cross section and causes shear. In this manner, the cross section of the above-described rod will also be subject to interacting forces equal to T, under whose action the rod and cylinder in the section under the two-piece cross beam will be bent (see the diagram of M_b).

STAT

As a result of the analysis it can be concluded that the torque $M = P_2 a$ at the fulcrum section is transmitted by the bending of the rod, cylinder, and the fulcrum itself.

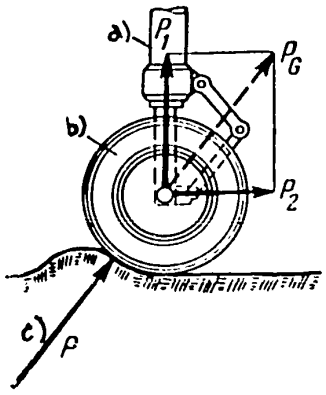

Fig.275 - Loading of the Wheel During a Front Impact

Here, unlike during a rough landing, the component force P_2 is directed backward.

a) Strut; b) Wheel; c) Force of front impact

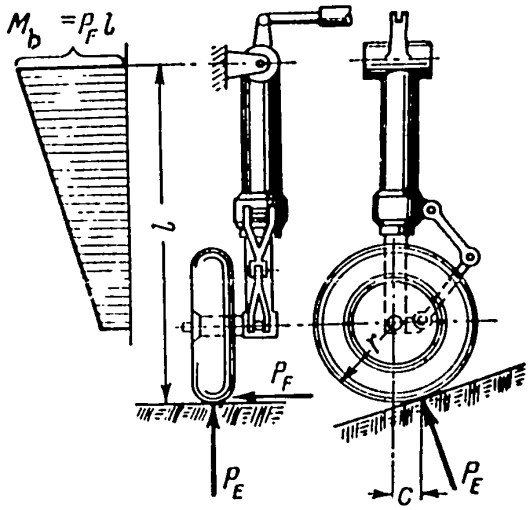

Fig.276 - Case of a Lateral Loading of the Landing Gear

In this case, the wheel is loaded with two forces: A force normal to the ground P_E, and a friction force P_F, which lies in the plane of the ground.

For a final evaluation of the strength of the landing-gear elements it is necessary to sum up the similar stresses in the dangerous points of an element under discussion, which are caused by simultaneously acting forces.

In exactly the same way must the analysis of the function of landing-gear elements in other design cases be performed, if they differ from the just discussed case only in the magnitude and direction of action of the external force. For instance, in case of the wheel striking an obstacle during forward motion (Fig.275), the component force P_2 will be directed toward the rear.

Case of Lateral Loading of the Landing Gear

Here the calculation of loads is performed separately for those caused by th

force P_E and for those caused by the action of the lateral force P_F (Fig.276). The action of the force P_E has been discussed above. But the lateral force P_F will bend the wheel axle with a moment uniform throughout the entire length of the axle

$$M_b = P_F r.$$

Under the action of the force P the entire strut will be subject to torque with a constant moment throughout the entire length of the strut

$$M_t = P_F c.$$

Moreover, the strut will be bent by the force P_F. This bending moment will vary throughout the length of the strut (see diagram of M_b).

Section 53. Semicantilever Landing Gear

Semicantilever landing gears (see Fig.258), if the cantilevers are removed, can have one or two degrees of freedom. Two degrees of freedom are created by a Cardanic joint of the landing gear.

Cantilevers are used to eliminate these degrees of freedom during touchdown and moving of the aircraft on the ground, and to make the landing gear system more rigid. To ensure retraction of the landing gear during flight, the cantilevers are of the collapsible type.

Landing gear diagrams are designed with one cantilever if, during retraction, the gear moves along the wing chord or along the wing span. If the gear moves at an angle, i.e., simultaneously along the span of the wing and along its chord, two cantilevers are used. In this case the strut can rotate around any of the two axes.

Let us examine the work performed by the elements of a semicantilever landing gear.

Let us take the case of a rough landing (Fig.277).

The external load does not depend on the diagram of the landing gear and

be determined in the same way as in a cantilever-type landing gear.

The axle and the lower portion of the strut, up to the cantilever nodal point, will work in the same manner as they do in a cantilever diagram. Only the portion of the cylinder which is above the cantilever nodal point will work in a different manner since it will be subject to the stress of that cantilever.

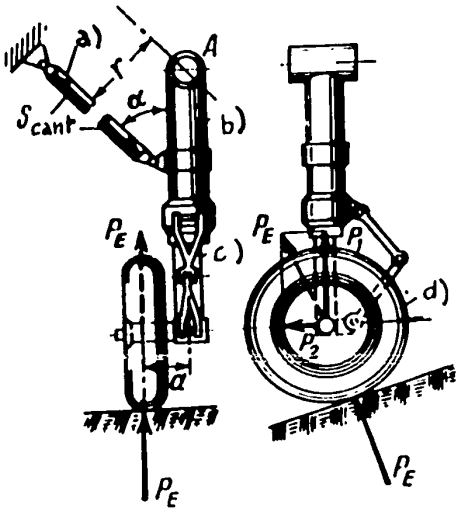

Fig.277 - Performance of a Landing Gear of the Semicantilever Type

The cantilever causes elongation of the portion of the cylinder above the cantilever nodal point

a) Cantilever; b) Cylinder; c) Piston; d) Wheel

In order to analyze the work of the landing gear, let us substitute the cantilever by the stress S_{cant} acting in it.

The design of the upper portion of the cylinder is performed in two stages:

First stage - the calculation of action of the force P_E is performed, the landing gear being assumed as a cantilever type;

Second stage - the action of the force acting through the cantilever is calculated. To do this, it is necessary to determine the stress in the cantilever.

Determination of Stress in the Cantilever

Since the cantilever is joined by a hinge, it causes only axial stresses. If we imagine the cantilever to be dissected, the rigid diagram of the landing gear will be turned into a mechanism, and the strut will rotate about the upper node under the action of the moment $M = P_1 a$. In reality, there is no such rotation since it is prevented by the cantilever. Therefore, the cantilever will be loaded with a compression stress. The magnitude of this stress is determined from the

STAT

equality of moments (see Fig.277)

$$P_1 a = S_{cant} r,$$

from where

$$S_{cant} = \frac{P_1 a}{r}. \qquad (137)$$

If there are two cantilevers, the order of determination of their stresses remains the same: it is necessary to write two equations of moments with respect to the two axes of rotation of the strut.

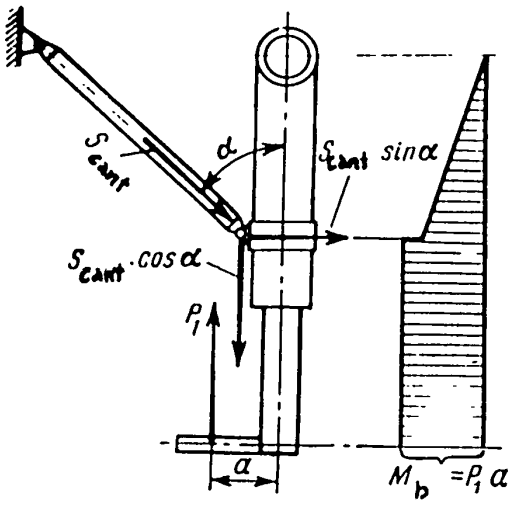

Fig.278 - Influence of a Cantilever On Bending of the Cylinder

Force P_1 bends the cylinder in one direction, and the stress S_{cant} in another. Because of this, the upper portion of the cylinder is unloaded.

When the stress in the cantilever is found, we can determine the internal strain

$$\sigma = \frac{S_{cant}}{F_{cant}}. \qquad (138)$$

The upper part of the cylinder will be unloaded of the action of the force P_1 (Fig.278, diagram M_b) due to the cantilever.

The work of the strut, over its entire length, due to the action of the force P_1 will be similar to the work of a cantilever system: the rod being compressed will transmit the force P_1 to the liquid, and the latter will pass it to the air; the air transmits the force P_1 to the nodal point of the strut through the cylinder bottom. Due to the external pressure of air, the cylinder tends to burst.

In our example, the cantilever has no influence on the work of the strut due to the force P_2 (see Fig.275), since it lies in the plane of the strut and axle.

STAT

But if the cantilever is carried beyond this plane, component forces are generated due to stresses in the cantilever, which will be perpendicular to the plane of the strut and axle; this may change the performance of the upper portion of the cylinder.

Since the cantilever is not at a right angle to the axis of the strut but at an acute angle α to it, the cylinder will be loaded with an additional axial stress due to the action of the component force $S_{cant} \cos \alpha$. In our case, the cylinder in its upper portion is also stretched.

Section 54. Landing Gear with a Lever Suspension of Wheels

The landing gear of jet aircraft has its own features. These are due primarily to the absence of a propeller. The absence of a propeller makes it possible to use shorter gear, i.e., to lower the aircraft and make it more stable during its run over the runway.

The landing gear of jet aircraft generally uses a lever suspension of wheels (Fig.279). In this diagram, the shock struts are in a more favorable position since, in this landing gear system, they are subject to compression only. This fact eliminates possible detachment of the rod and piston from the cylinder and leakage of the fluid; it allows raising the initial pressure in the strut and, therefore, decreasing the overall strut dimensions. In the case of a landing gear with a lever suspension of wheels, the shocks experienced by the latter due to the horizontal components of forces become softer, i.e., the shock strut works not only from the vertical but also from the horizontal forces acting on the wheel.

Retraction of the gear in high-speed aircraft, as already mentioned, becomes mor[redacted]difficult due to the relatively small thickness of the wings. For this reason, the landing gear is very often retracted inside the fuselage. It must be noted that the fuselage also does not have much available space for retraction of the gear. This explains why high-pressure wheels of small overall size are used in jet aircraft. Such wheels assist a shock only slightly in softening shocks at touchdown and, most important, impair the aircraft roadability. As a result, airfields wi[redacted]STAT

a more impermeable soil are required.

A landing gear with a lever suspension of wheels may be of either of the cantilever or of the semicantilever type, in analogy with the diagrams examined above. The characteristic peculiarity of this landing gear is the suspension of the wheels on a special lever, which can rotate with respect to the joint, mounted on the strut-knee. The shock absorber can be designed as a self-contained element (1 - 2) (Fig.279) or it can be mounted inside the strut column (Fig. 280). In the first case, both the rod and cylinder of the shock absorber are subject to axial stresses, without being bent. This is explained by the presence of the double joints in the assembly (1) and (2) (see Fig.279), which ensure transmission of only axial stresses. In the second case (Fig.280), because of the double hinge in the assembly (1), the rod of the shock absorber is not bent, but the cylinder, which is the strut column, is bent. For this reason, the shock absorber is in a more difficult position than in the diagram of Fig.279.

Landing Gear With Shock Absorber Outside the Strut

The diagram in question (see Fig.279) consists of a strut (column) (4 - 6) which is joined to the assembly (6) with a hinge and is free to rotate with respect to the axis x - x. This degree of freedom ensures retraction and extension of the landing gear with the help of the wheel-retraction mechanism, attached by a bolt to the assembly (7). At take-off and landing, the assembly (7) remains stationary.

A lever (4 - 3) is hinged to the lower portion of the strut at the assembly (4). This lever can rotate only in its plane with respect to the assembly (4), in which the bolt is mounted on a large base. The freedom of the lever rotation is limited by the shock absorber (1 - 2), which is double-hinged at the assemblies (1) and (2), in order to prevent bending of the shock absorber.

At the assembly point (3) a semiaxis (3 - 5) is rigidly fixed to the lever. The wheel is mounted to this semiaxis. It must be noted that instead of a semiaxis, a semifork or a fork-and-axle could be mounted on the lever. STAT

Below, as an example, we will study the work of separate landing-gear elements during a rough landing, i.e., from the force P_w.

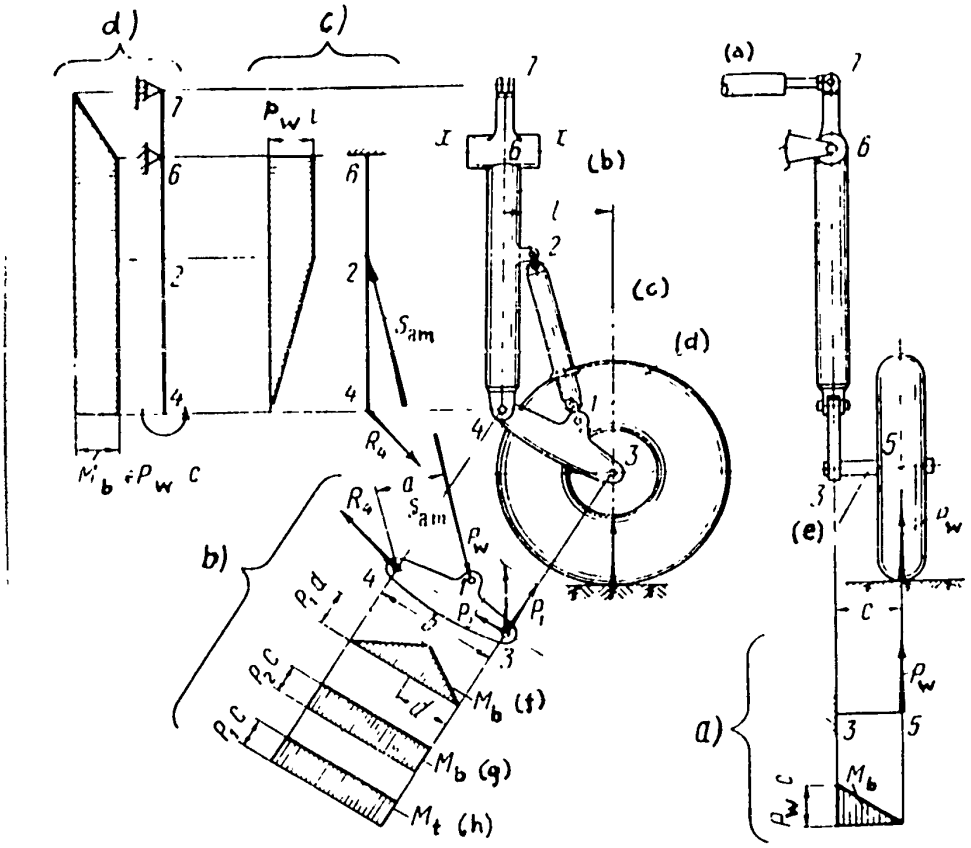

Fig.279 - A Landing Gear With Lever Lifting Mechanism of Wheels - Shock Absorber Outside the Strut

(a) Lifting cylinder; (b) Strut (main); (c) Shock absorber; (d) Fork arm; (e) Semiaxle; (f) M_b from force P_1; (g) M_b from force P_2; (h) M_t from force P_1

Work of the Semiaxis. The force of the ground reaction P_w is directly applied to the wheel and is transmitted to the semiaxis through the roller bearings. In this case, the semiaxis (3 - 5) (Fig.279a) is bent like a cantilever beam. The diagrams of the bending moments change according to a linear law with the maximum value of $P_w c$ at the point (3).

STAT

Work of the Lever. The moment $P_w c$, together with the force P_w, are transmitted to the lever (3 - 4). For convenience in calculation, let us resolve the force P_w (Fig.279b) into its components P_1 and P_2. The force P_2 acts along the axis of the lever, while the force P_1 is normal to P_2.

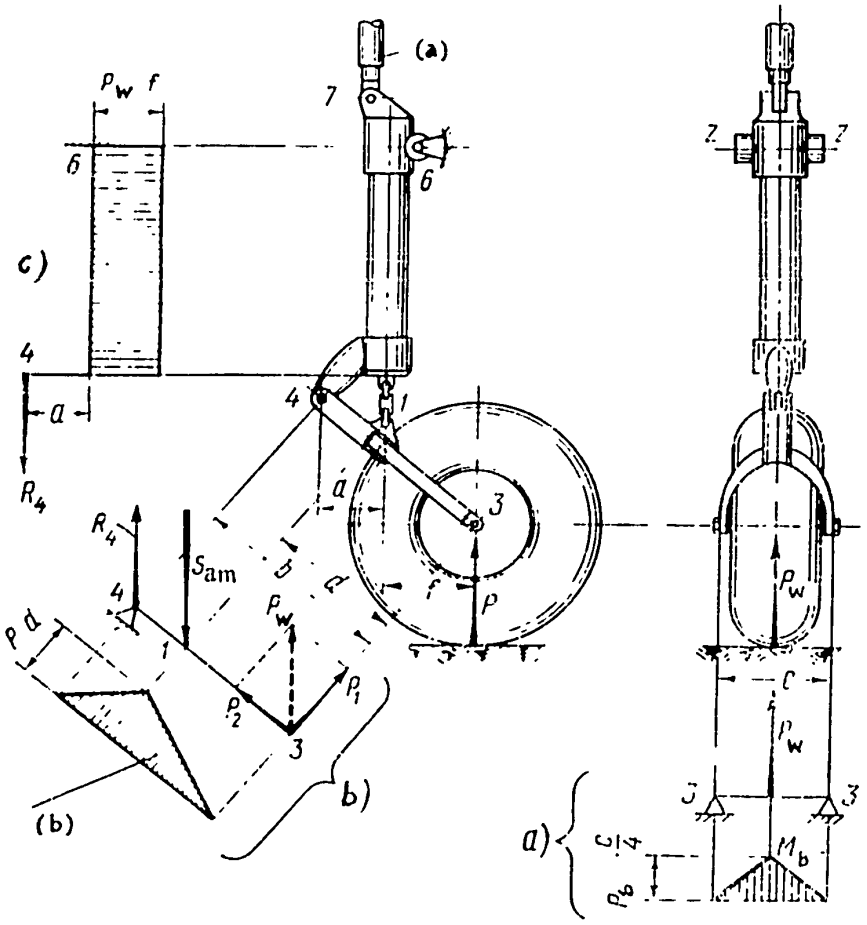

Fig.280 - Landing Gear With Lever Lifting Mechanism of Wheels - Shock Absorber Inside the Strut

(a) Lifting cylinder; (b) M_b from the force P_1

The force P_1 applied to the assembly (3) bends the lever in its plane, like a simple beam with a cantilever. The supports are: the strut (4 - 6) with a fixed assembly (4) and the shock absorber (1 - 2) with a movable assembly (1). It is not difficult to find the reactions in the supports R_4 and S_{am}. For instance, the

stress in the shock absorber (1 - 2) can be determined from the fact that the lever is hinged at the assembly point (4)

$$P_1 b = S_{am} a.$$

From this it follows that

$$S_{am} = P_1 \frac{b}{a}.$$

The diagram of the bending moments M_b for the lever, caused by the action of the force P_1, is represented by a triangle (Fig.279b). The greatest moment will occur at the point of assembly (1) of the shock absorber bracing and will correspond to the value

$$P_1 d.$$

Since the point of assembly (1) is not on the axis of the lever (4 - 3), the left portion of the lever is slightly less bent.

As the force P_1 is applied to the point (5) of the semiaxis, it will twist the lever with a constant moment

$$M_t = P_1 c,$$

which is fully transmitted to the strut through the assembly (4).

The force P_2 will cause compressive stresses in the lever, while being transmitted to the assembly (4) of the strut. Moreover, because of the lever arm c, the lever (3 - 4) will be bent in a plane perpendicular to the plane of the lever (3 - 4 - 1). The assembly (4) remains, as before, the seal. The bending moments for individual cross sections of the lever over its entire length will be constant (Fig.279b) and they will correspond to the value

$$P_2 c.$$

STAT

Strut Performance. The external loads acting on the strut (4 - 6 - 7) will be the forces transmitted through the assembly (4), and the stresses of the shock absorber S_{am}, transmitted through the assembly (2). Under the action of the loads just mentioned the strut is bent and axial deformations occur in it.

Let us examine the bend in the plane of the lever and the shock absorber (Fig.279c). Here the strut is loaded with the forces R_4 and S_{am}. The strut is attached to the aircraft by the unit (6).

Through the segment (4 - 2) the bending moments change according to a linear law. They are equal to zero at the point (4). In section (2 - 6) they are constant and equal to

$$P_w l,$$

which is clearly indicated from the general-view diagram of the landing gear.

The strut is additionally bent in the perpendicular plane (Fig.279d), being loaded at the assembly with a concentrated moment

$$M_w = P_w c.$$

This moment is the geometric sum of the magnitudes of the moments of the lever: $P_1 c$ and $P_2 c$ (Fig.279b). The value of P_w can be easily obtained from the general view of the landing gear (first projection).

The strut is bent in the perpendicular plane like a simple beam with a large cantilever (6 - 2 - 4). The supports will be found in the hinge (6) and in the unit (7) of the retraction mechanism. Therefore, throughout the length (4 - 2 - 6) the bending moments will be constant, and throughout the length (6 - 7) they will diminish until they will equal zero at the assembly (7).

This indicates that individual elements of the landing gear are deformed in different ways. For instance, the lever is bent in two planes, being twisted and compressed. In order to have any judgment as to the strength of the structure, it

STAT

is necessary to determine the stresses caused by individual kinds of deformation, to sum them up in a corresponding manner and to compare them with those which the structure is able to withstand.

Landing Gear With the Shock Absorber Inside the Strut

This landing-gear diagram has the same elements (Fig.280) as the structure in Fig.279. Here the column (4 - 6) is free to rotate with respect to the axis z - z, and the retraction mechanism is arranged somewhat differently. The lever (4 - 1 - 3) is attached to the column by means of a bracket at the assembly (4). The lever is forked on the end (1 - 3). At the end of this fork, the axle (3 - 3) of the wheel is mounted. The shock absorber is placed inside the strut, whose rod is attached to the lever at the assembly (1).

Let us examine the performance of separate elements of the landing gear under the action of the vertical force P_w. We will proceed as before.

Axle Performance. The force of the ground reaction P_w is transmitted to the axle (3 - 3) over roller bearings. In our case, the fork will be the support of the axle. For this reason, the axle will be bent like a simple beam (Fig.280a). The largest magnitude of the bending moment will occur in the middle portion of the axle and will be equal to

$$P_w \frac{c}{4}.$$

Lever Performance. Let us assume that the lever and its fork (4 - 1 - 3), consist of a single element. Then let us resolve the force P_w (Fig.280b) into its components P_1 and P_2. The force P_2 will create compressive stresses in the lever, while P_1 will bend it. The maximum bending moment will, as before, be equal to

$$P_1 d$$

which will occur near the junction (1) of the shock-absorber rod.

STAT

The reaction in the assembly (4) will equal to

$$R_4 = P_w \frac{f}{a}.$$

Since the forces P_1 and P_2 act on the lever symmetrically, no twisting of the lever occurs.

The stress in the shock absorber is determined by the previous formula

$$S_{am} = P_1 \frac{b}{a}.$$

Strut Performance. Unlike in Fig.279, only those forces will form the external load of the strut (4 - 6 - 7), which are transmitted from the lever (3 - 4) through the assembly (4); this assembly is carried somewhat toward the front. In this case, the only force (Fig.280b) will be

$$R_4 = P_w \frac{f}{a}.$$

Under the action of this force, the strut will undergo elongation and will be bent by a bending moment of constant magnitude

$$M_b = R_4 a.$$

since $R_4 = P_w \frac{f}{a}$, $M_b = P_w f$.

We would have obtained the same result if we would have examined the landing gear on the whole with the help of the general view in Fig.280.

STAT